Diffuse Nongranulomatous Lung Disorders

6

Chen Zhang and Jeffrey L. Myers

Diffuse, nonneoplastic lung diseases are a large and heterogeneous group of disorders with overlapping clinical features, usually including breathlessness and cough; diffuse radiologic abnormalities are also common. Affected patients frequently have evidence of physiologic dysfunction and defective oxygenation. High-resolution computed tomography (HRCT) scans play an increasingly important role in diagnosis of the conditions included in this category, but lung biopsy is still an essential step in the diagnostic algorithm for many of these conditions.

This chapter focuses on those diffuse lung diseases for which granulomatous inflammation is usually absent and includes both acute and chronic disorders (Fig. 6.1). Those diseases for which a subacute or chronic course is typical are separated into disorders in which air space filling is a dominant feature, as are lesions resulting from cigarette smoking, chronic idiopathic interstitial pneumonias, lung lesions in patients with systemic connective tissue diseases, and lymphangiomyomatosis.

6.1 Diffuse alveolar damage/acute interstitial pneumonia	6.2 Non-infectious air space diseases	6.3 Smoking-related interstitial lung disorders	6.4 Idiopathic chronic interstitial pneumonias	6.5 Connective tissue diseases	6.6 Lymphangioleio-myomatosis
	Organizing pneumonia Eosinophilic pneumonia Acute fibrinous & organizing pneumonia Pulmonary alveolar proteinosis	Respiratory bronchiolitis Smoking-related interstitial fibrosis Desquamative interstitial pneumonia Langerhans cell histiocytosis	Usual interstitial pneumonia Nonspecific interstitial pneumonia	Rheumatoid arthritis Systemic lupus erythematosus Scleroderma	

Fig. 6.1 Summary of entities included in this chapter, spanning a spectrum from acute to chronic diseases

C. Zhang (✉)
Department of Pathology and Laboratory Medicine, Indiana University School of Medicine, Indianapolis, IN, USA
e-mail: chenzhan@iupui.edu

J. L. Myers
Department of Pathology, Michigan Medicine, Ann Arbor, MI, USA
e-mail: myerjeff@med.umich.edu

C. Zhang, J. L. Myers (eds.), *Atlas of Lung Pathology*, Atlas of Anatomic Pathology,
https://doi.org/10.1007/978-1-4939-8689-7_6

Diffuse Alveolar Damage (DAD)

DAD (Figs. 6.2, 6.3, 6.4, 6.5, 6.6, 6.7, 6.8, 6.9, 6.10, 6.11, 6.12, 6.13, 6.14, 6.15, 6.16, 6.17 and 6.18) is a nonspecific manifestation of catastrophic acute lung injury usually seen in the context of the acute respiratory distress syndrome (ARDS). Ninety percent of patients discovered to have DAD in a surgical lung biopsy have ARDS. ARDS is defined as a syndrome of acute onset (≤1 week) characterized by diffuse radiologic abnormalities resembling pulmonary edema not explained by cardiac failure alone and hypoxemia. Mortality rates are high, ranging from 40% to over 50% depending on disease severity, the presence or absence of pre-existing lung disease, and comorbidities. DAD is seen in about half of patients with ARDS and is most common in those with severe and prolonged respiratory failure. Risk factors for developing ARDS and therefore DAD include sepsis, trauma, multiple transfusions, aspiration of gastric contents, pulmonary contusion, pneumonia, and smoke inhalation. DAD occasionally occurs in patients with no identifiable risk factors or cause for ARDS, a syndrome referred to as acute interstitial pneumonia (Hamman-Rich syndrome).

The etiology or cause for DAD is often not identifiable on the basis of histology alone, but infection should always be an important consideration and often requires special stains as well as other microbiologic assays. A specific infection accounted for about one third of diagnoses in several reports of patients with ARDS who underwent surgical lung biopsy. Viruses, especially cytomegalovirus (CMV), accounted for the majority of infectious causes; less common pathogens include bacteria, *Pneumocystis jiroveci* and other fungi, and *Mycobacterium* species. Clues to an infectious etiology include a concomitant bronchopneumonia, viral cytopathic changes, frothy exudate characteristic of *Pneumocystis* pneumonia, and granulomatous inflammation. Special stains, including a silver stain for pneumocystis and other fungi, are key to identifying many of the pathogens likely to cause DAD.

Underlying collagen fibrosis, especially when coupled with honeycomb change in a patient older than 60 years of age, is another important clue that may signify pre-existing fibrotic lung disease such as usual interstitial pneumonia (UIP). In this context, and assuming no other cause for DAD, this combination of findings is characteristic of a syndrome of rapid worsening referred to as acute exacerbation (*see* section "Usual Interstitial Pneumonia (UIP)"). Acute exacerbation is occasionally the presenting manifestation of UIP in patients with previously undiagnosed disease.

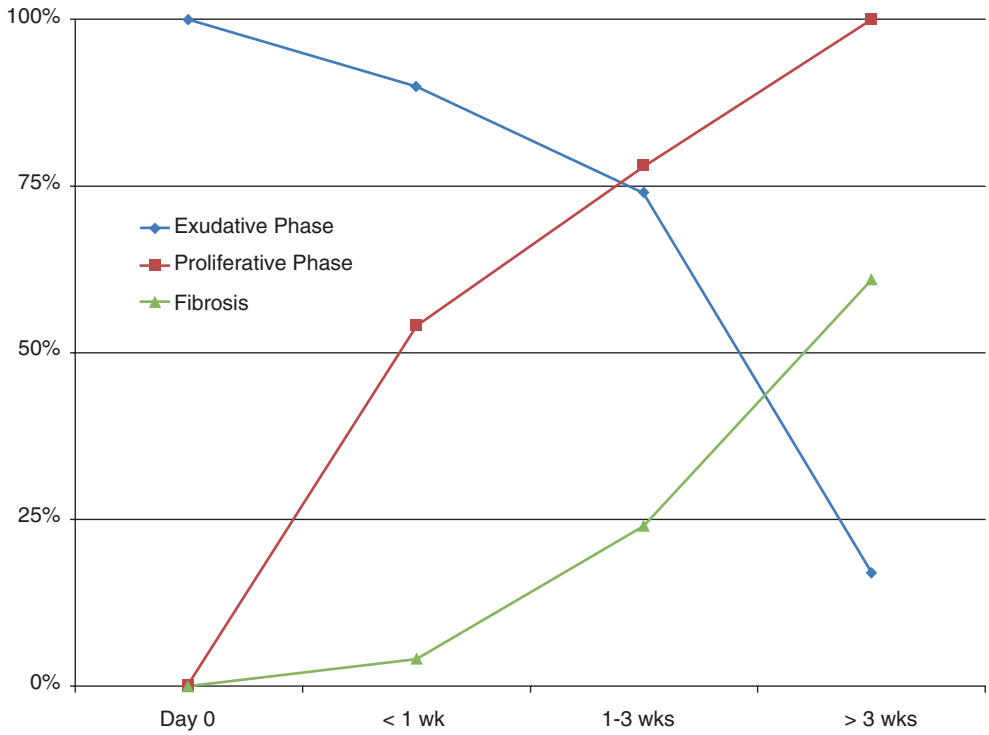

Fig. 6.2 Proportion of patients with ARDS showing exudative, proliferative, and fibrotic phase DAD at autopsy. The exudative phase is the earliest change and dominates in the first week following injury. Proliferative phase changes become more conspicuous after the first week and are the dominant finding after the first 2 weeks. Collagen fibrosis is a late-stage event that does not occur in all patients

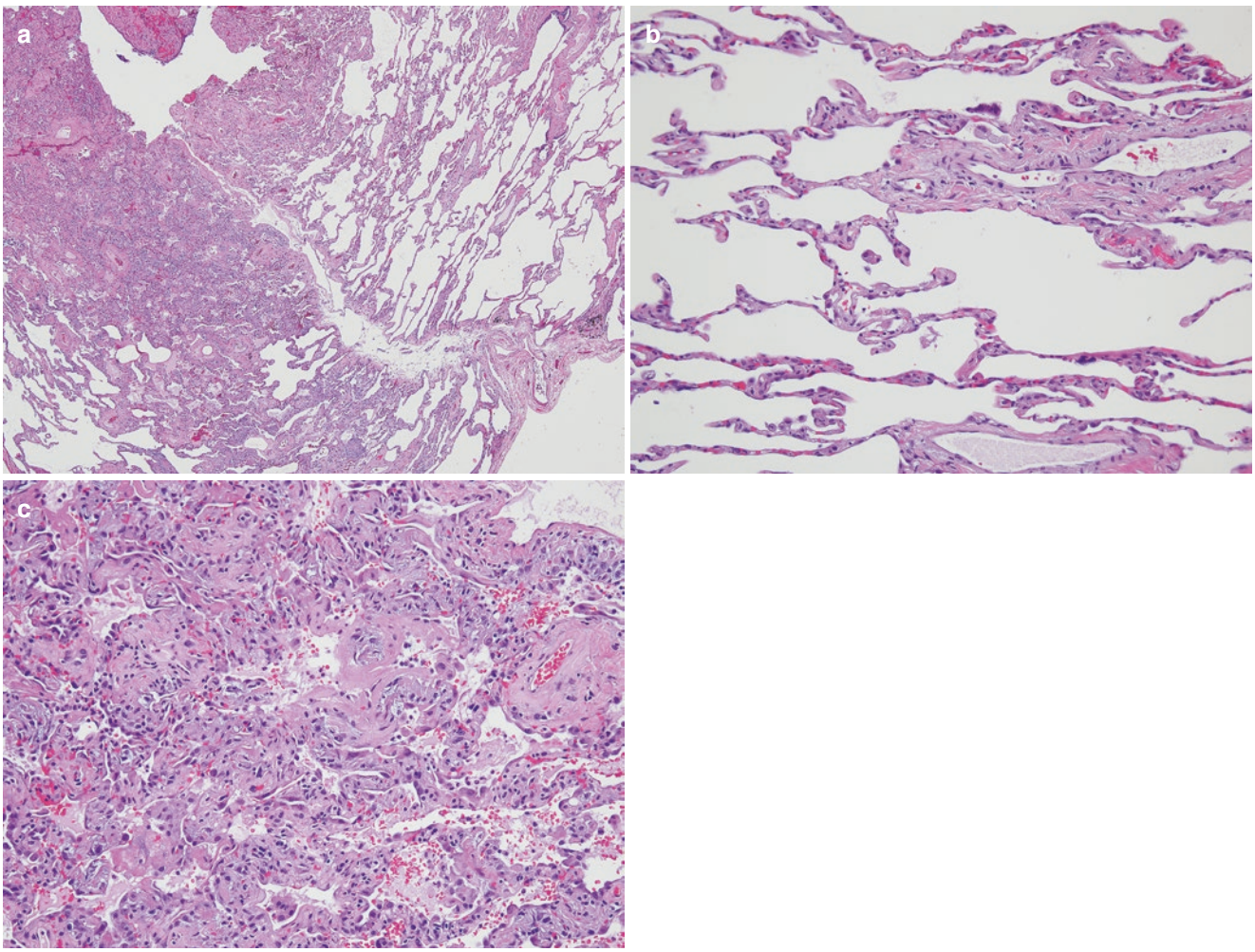

Fig. 6.3 DAD with a patchy distribution. (**a**) Low-magnification view of surgical lung biopsy from a patient with ARDS showing nearly normal lung in the upper right and DAD in the lower left portions of the field (H&E). (**b**) High-magnification photomicrograph of the nearly normal lung in the upper right portion of the field illustrated in **a** showing minimal alveolar septal thickening and congestion, which may reflect the earliest and least specific exudative phase of DAD (H&E). (**c**) High-magnification photomicrograph of DAD in the lower left portion of the field illustrated in **a** showing the early proliferative (organizing) phase with persistent hyaline membranes (H&E)

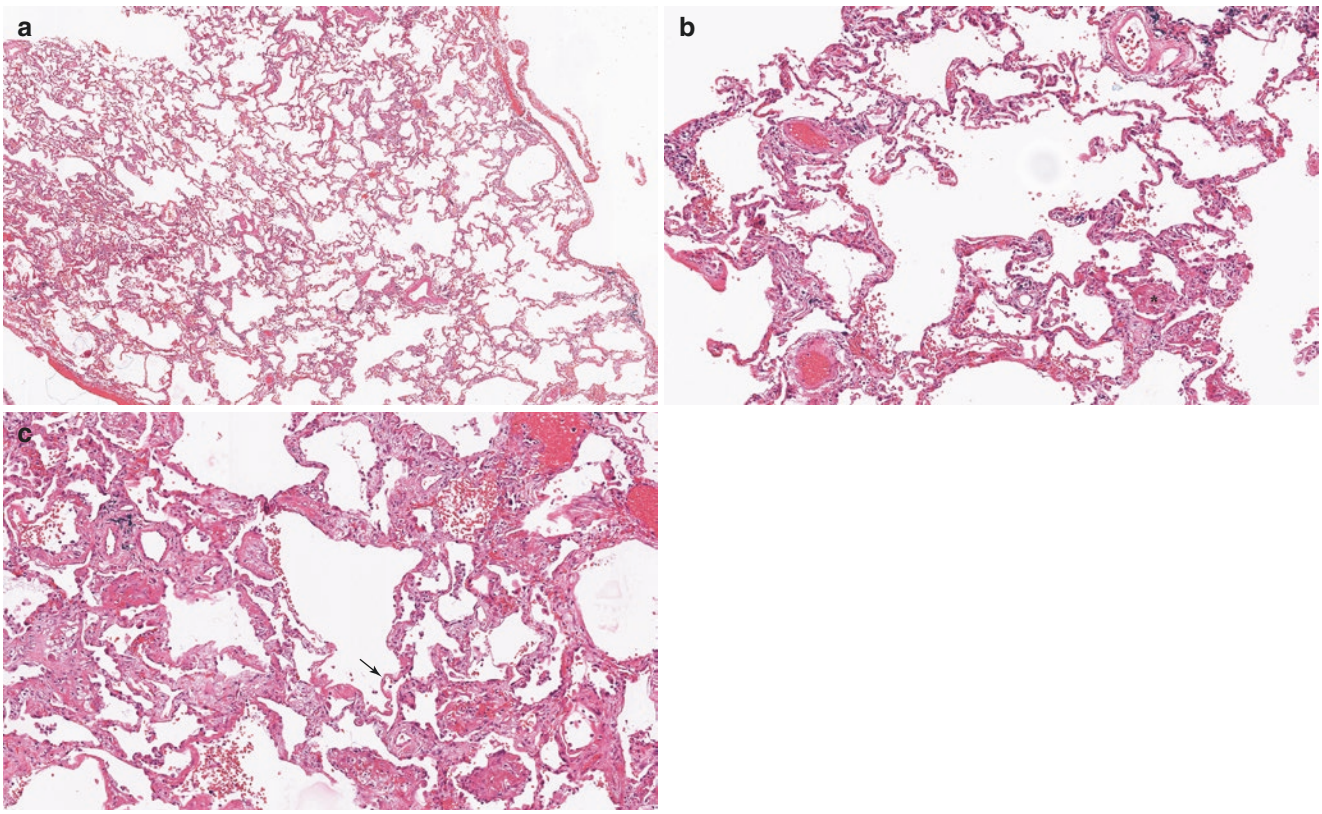

Fig. 6.4 DAD, early exudative phase. (**a**) Scanning magnification photomicrograph of the early exudative phase of DAD in a patient with ARDS (H&E). At low magnification the lung parenchyma looks nearly normal with only minimal alveolar septal thickening and overall preservation of lung architecture. (**b**) High-magnification photomicrograph of field illustrated in **a** showing alveolar septal congestion and thickening with very focal hemorrhage and fibrin in air spaces (asterisk) (H&E). In this early phase, it is very difficult and perhaps impossible to diagnose DAD on the basis of this combination of nonspecific findings alone. It is only the clinical context (i.e., ARDS) that allows more confident speculation that this is DAD in an early exudative phase. (**c**) High-magnification photomicrograph of field illustrated in **a** showing an area in which alveolar septal thickening and associated congestion and air space hemorrhage are more advanced than that seen in **b** (H&E). In addition, this field shows early hyaline membrane formations (*arrow*), which allows a more confident diagnosis of DAD

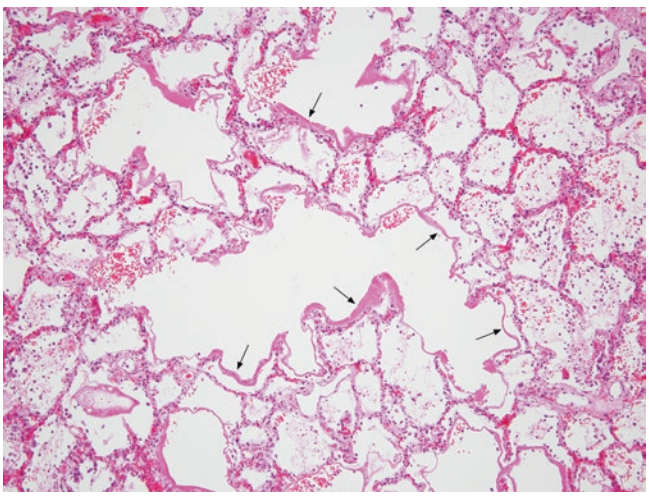

Fig. 6.5 Diffuse alveolar damage, exudative phase. Intermediate-magnification photomicrograph from patient with ARDS who had acute bronchopneumonia complicated by early DAD (H&E). Alveolar septa are mildly congested with minimal inflammation, hemorrhage, and fibrin in air spaces and hyaline membranes (arrows)

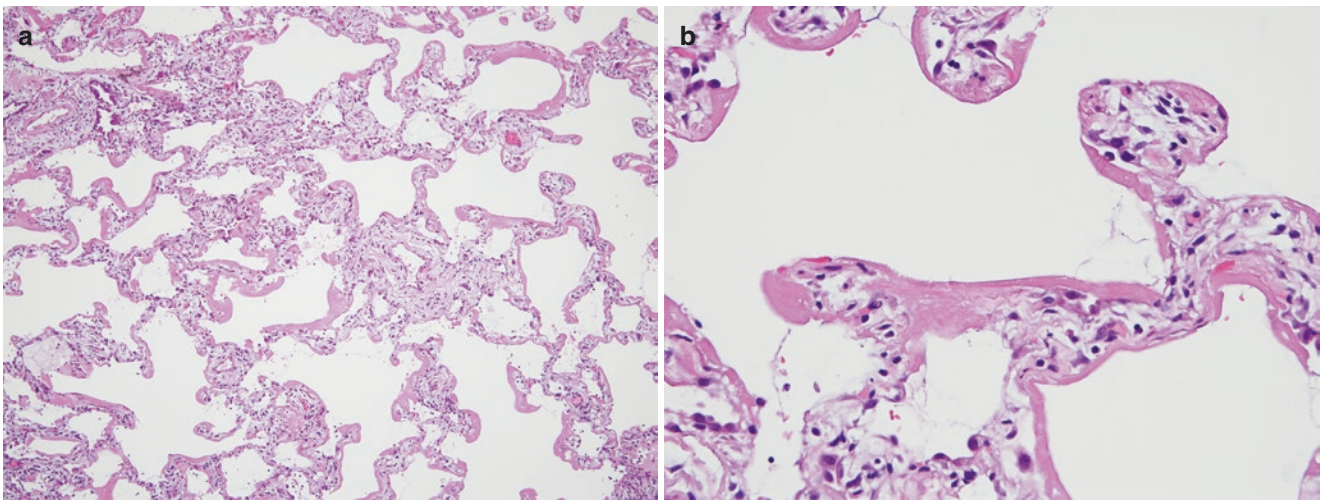

Fig. 6.6 DAD, exudative phase. (**a**) Low-magnification photomicrograph showing acute DAD (H&E). Alveolar septa are mildly thickened by a combination of interstitial edema and a relatively scant infiltrate of predominantly mononuclear cells. Acellular, brightly eosinophilic hyaline membranes are the histologic hallmark of acute DAD. (**b**) High-magnification photomicrograph showing acute DAD (H&E). Acellular, eosinophilic hyaline membranes are arranged in linear arrays along mildly thickened alveolar septa

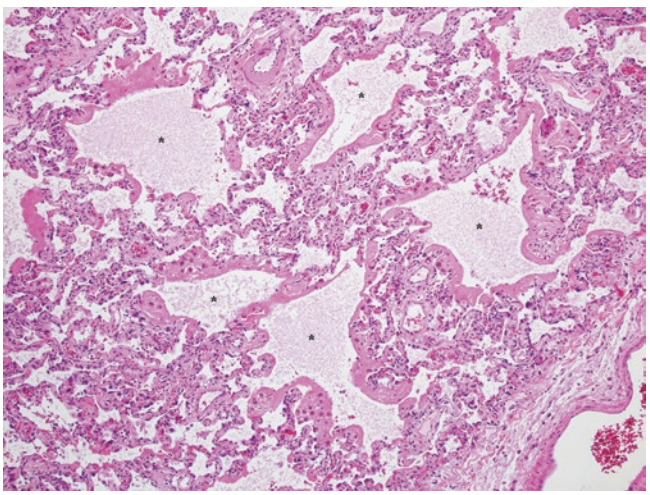

Fig. 6.7 Diffuse alveolar damage, exudative phase. Intermediate-magnification photomicrograph of surgical lung biopsy from a patient with ARDS demonstrating prominent hyaline membranes affecting mainly alveolar ducts (asterisks)

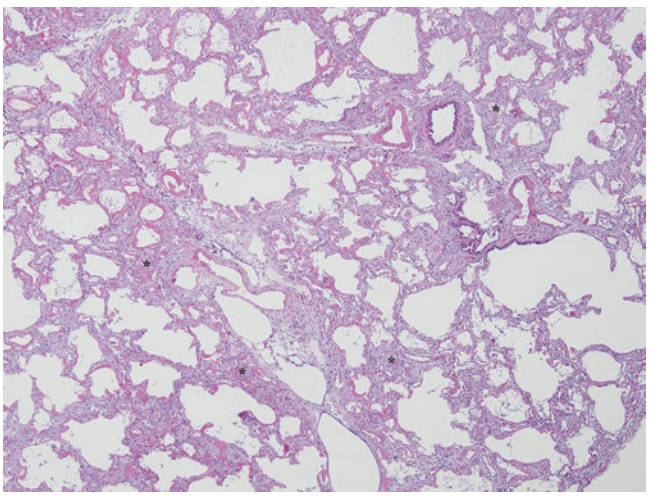

Fig. 6.8 DAD, proliferative phase. Low-magnification photomicrograph showing the early proliferative or organizing phase of DAD (H&E). Hyaline membranes remain a distinctive feature and are accompanied by expansion and distortion of the interstitium owing mainly to fibroblasts and myofibroblasts within a pale-staining basophilic matrix. In areas there is alveolar collapse (asterisks), which accounts for the increasingly distorted architecture

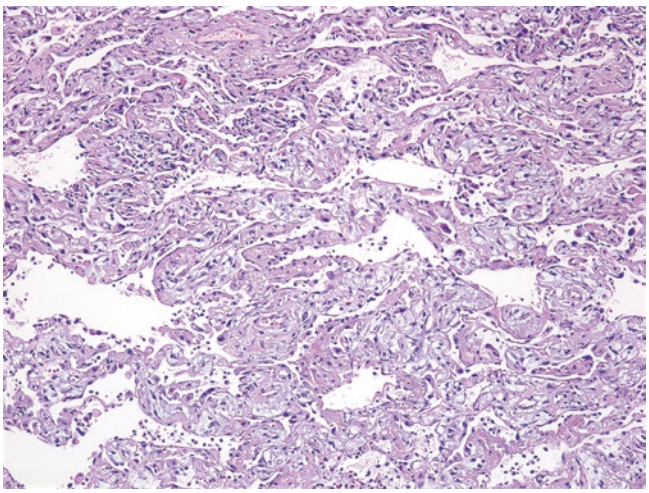

Fig. 6.9 DAD, proliferative phase. Intermediate-magnification photomicrograph showing expansion and distortion of alveolar septa by mesenchymal cells accompanied by persistent and increasingly fragmented hyaline membranes (H&E)

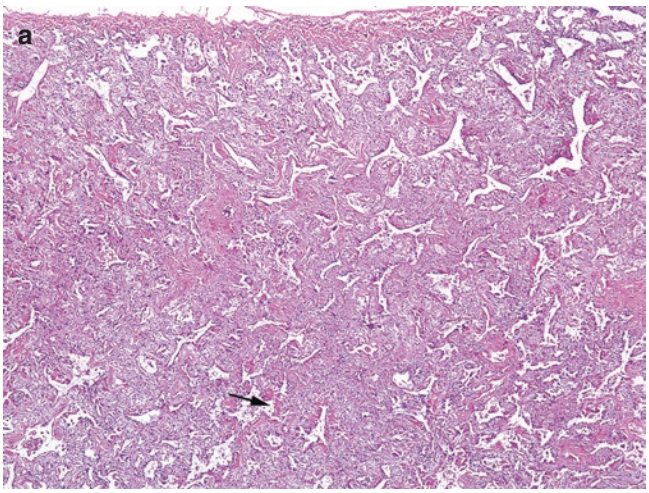

Fig. 6.10 DAD, late proliferative phase. (**a**) Low-magnification photomicrograph demonstrating the proliferative or organizing phase of DAD in a surgical lung biopsy from a patient with unexplained (idiopathic) ARDS (i.e., acute interstitial pneumonia) (H&E). There is uniform interstitial expansion and distortion resulting in markedly abnormal lung architecture with only a few widely scattered hyaline membranes (arrow). (**b**) High-magnification photomicrograph illustrating expanded, distorted, and collapsed alveolar septa in the late proliferative or organizing phase of DAD (H&E). (**c**) High-magnification photomicrograph from another patient with ARDS illustrating the proliferative phase of DAD in which collapsed alveolar septa are separated by ectatic alveolar ducts (H&E). Hyaline membrane remnants are present within the areas of collapsed and distorted interstitium

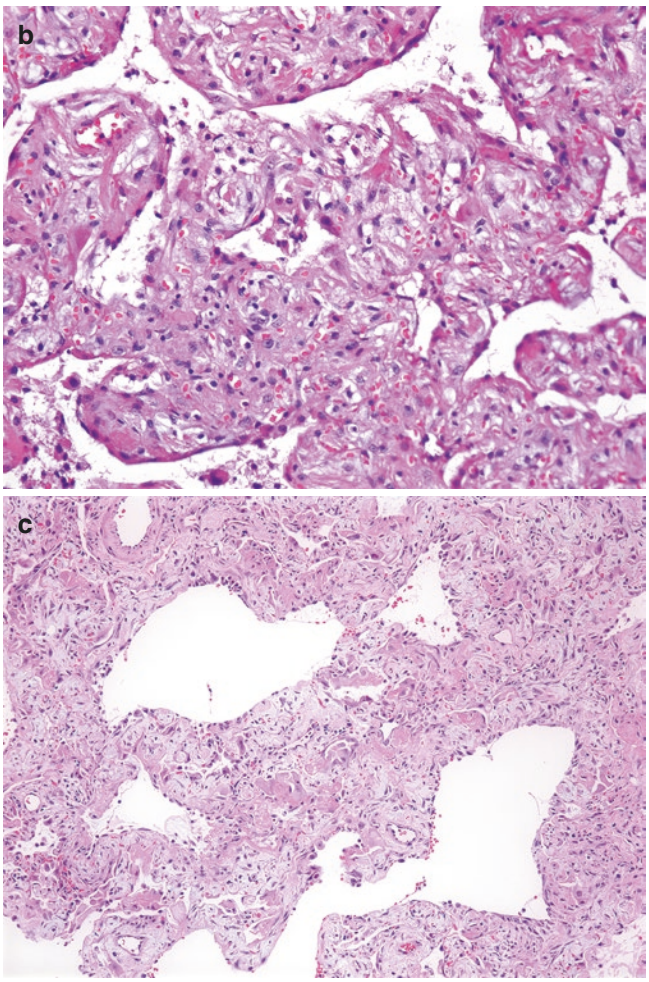

Fig. 6.10 (continued)

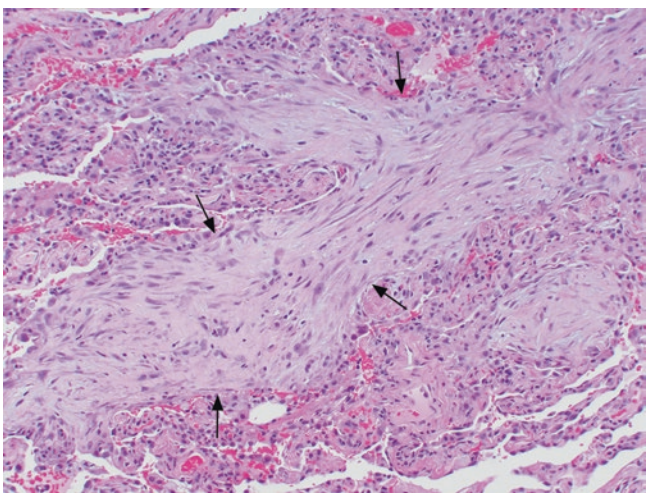

Fig. 6.11 DAD, late proliferative phase. Intermediate-magnification photomicrograph shows fibroblasts and myofibroblasts forming polypoid intraluminal structures (arrows) closely mimicking the appearance of organizing pneumonia (H&E). This demonstrates the considerable histologic overlaps between the proliferative or organizing phase of DAD and organizing pneumonia. In small biopsies organizing DAD may be indistinguishable from organizing pneumonia, but correlation with clinical and radiologic information will often resolve the diagnostic distinction

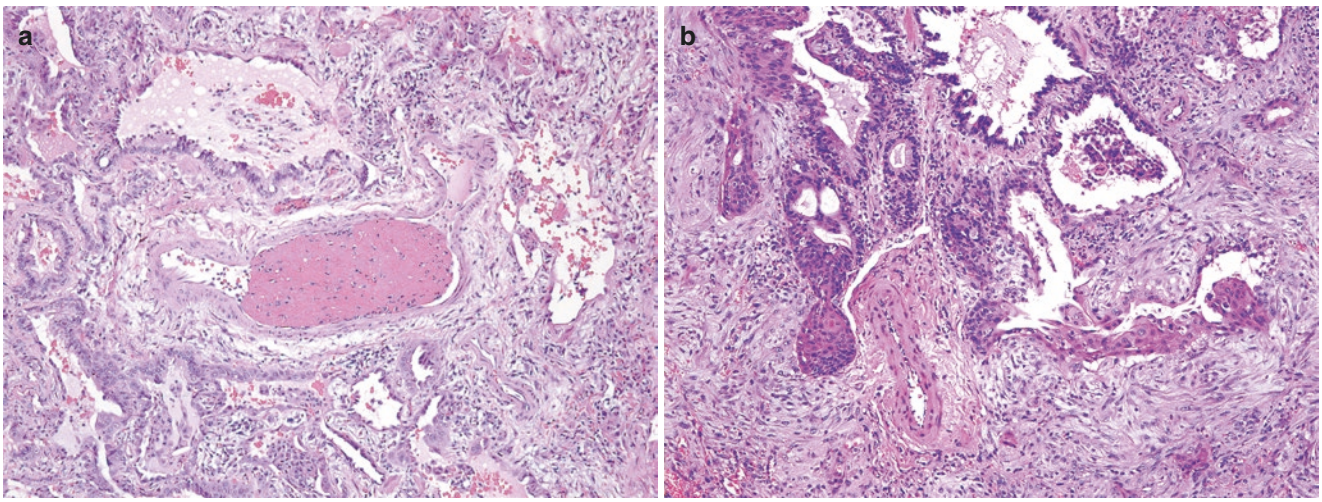

Fig. 6.12 DAD, proliferative phase. (**a**) Fibrin thrombi are a common although nonspecific finding in DAD, as illustrated in this photomicrograph of a surgical lung biopsy from a patient with ARDS (H&E). (**b**) High-magnification photomicrograph showing a distinctive pattern of squamous metaplasia involving bronchiolar epithelium in a patient with ARDS (H&E)

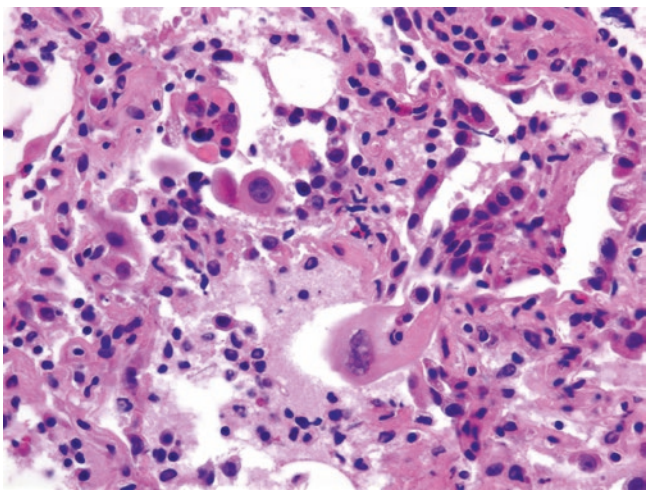

Fig. 6.13 Pneumocyte hyperplasia with reactive atypia in DAD. A high-magnification photomicrograph demonstrates hyperplastic pneumocytes in a patient with DAD (H&E). There is focal cytomegaly with nuclear enlargement and prominent nucleoli but without viral inclusions. This degree of reactive atypia is common in the organizing phase of DAD and should not be construed as either a malignancy or a marker for any specific etiology such as drug toxicity or viral infection

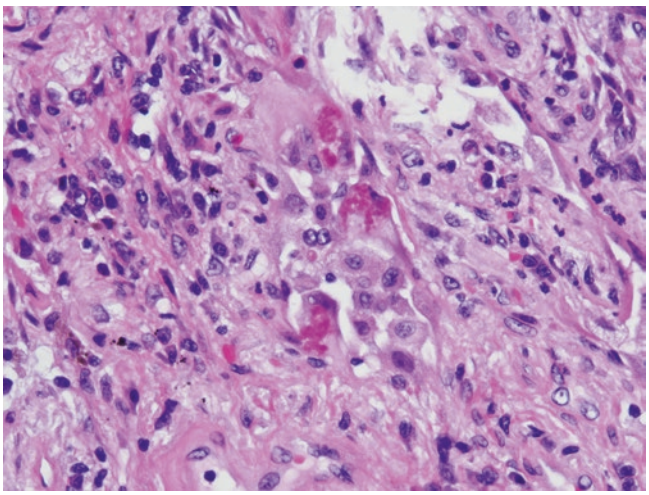

Fig. 6.14 Mallory hyaline in hyperplastic pneumocytes in DAD. This high-magnification photomicrograph illustrates densely eosinophilic cytoplasmic inclusions identical to the Mallory hyaline more commonly affiliated with hepatocytes in alcoholic hepatitis (H&E). This cytologic curiosity is not specific for DAD, occurring in other forms of diffuse lung disease including usual interstitial pneumonia

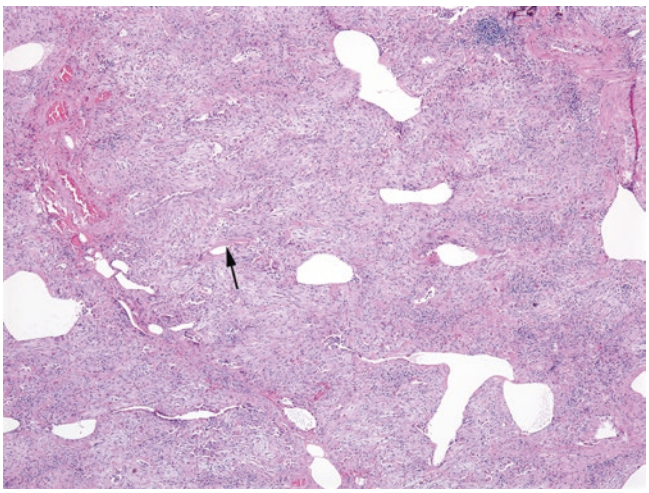

Fig. 6.15 DAD, proliferative phase. Low-magnification photomicrograph showing the proliferative phase of DAD in a patient with unexplained (idiopathic) ARDS (i.e., acute interstitial pneumonia, referred to historically as Hamman-Rich syndrome) (H&E). The lung architecture is distorted by proliferating fibroblasts and myofibroblasts and concomitant alveolar collapse. Rare hyaline membrane remnants mark some of the collapsed air spaces (arrow)

Fig. 6.16 End-stage fibrosis at autopsy in a patient with acute interstitial pneumonia. A gross photograph illustrates the cut surface of a lung from a young woman less than 35 years of age who died within 2 months of the acute onset of rapidly progressive respiratory failure. At autopsy her lung showed extensive fibrosis and honeycomb change. A surgical lung biopsy performed in the course of her hospitalization showed organizing DAD

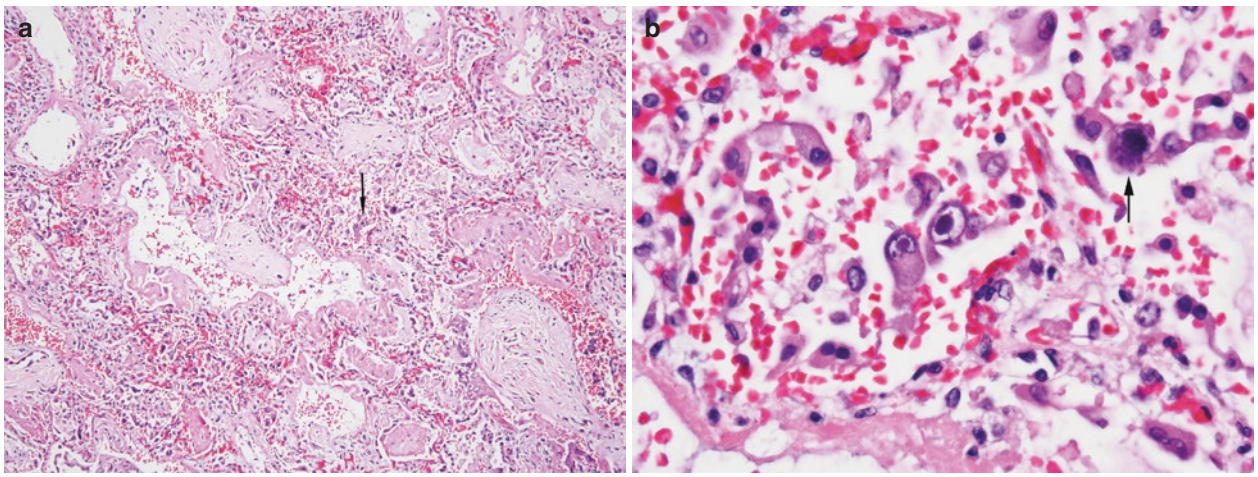

Fig. 6.17 DAD due to cytomegalovirus (CMV) infections. (**a**) Intermediate-magnification photomicrograph showing both acute and organizing DAD in which there are both well-formed hyaline membranes and organizing fibroblast/myofibroblasts; in this field, they form polypoid structures closely mimicking the appearance of organizing pneumonia (H&E). Two hyperplastic pneumocytes show nuclear inclusions typical of CMV (arrow). (**b**) High-magnification photomicrograph showing the CMV-infected cells with typical intranuclear inclusions (H&E). The cell in the upper right portion of the field shows basophilic cytoplasmic inclusions (arrow), another feature helpful in recognizing CMV (H&E)

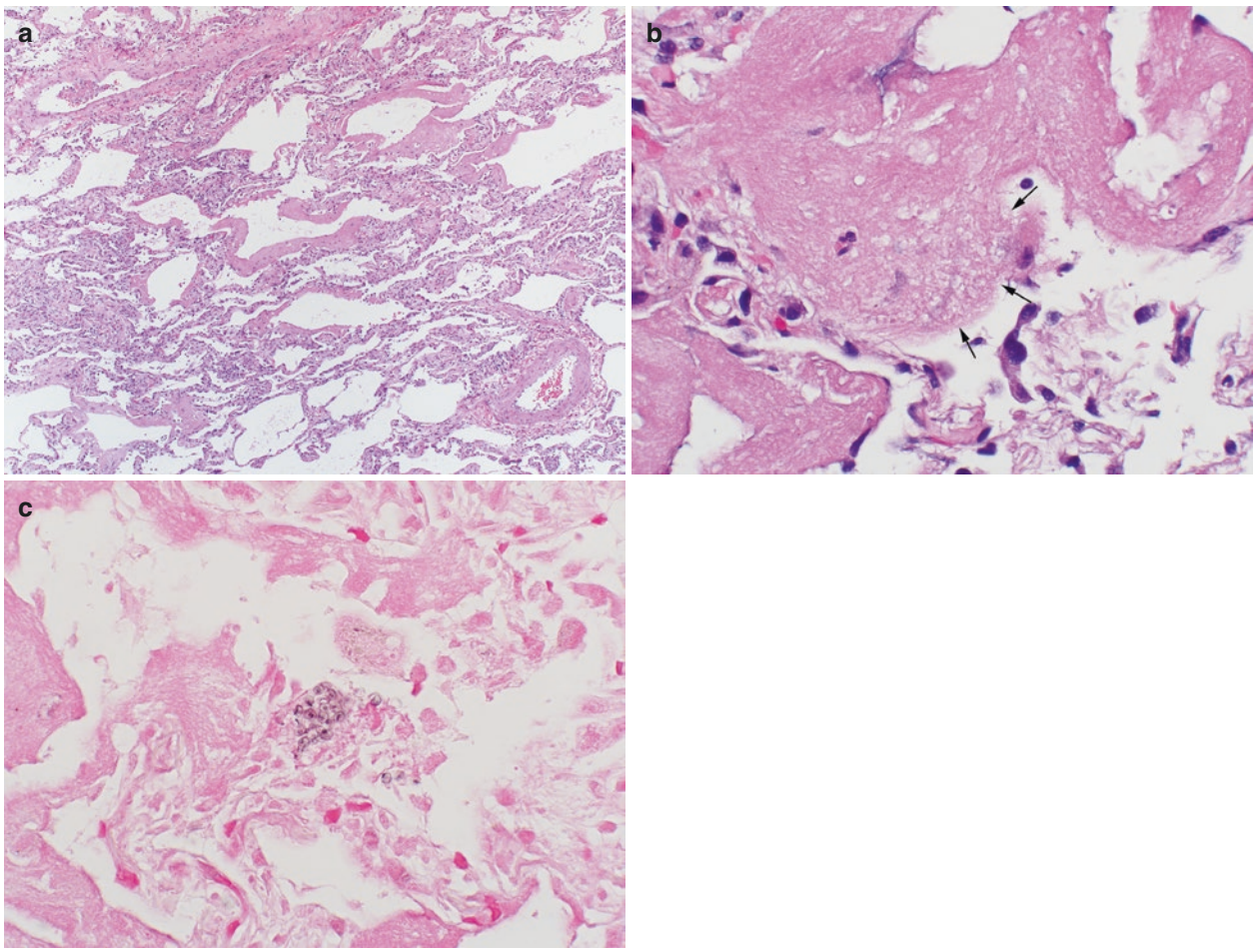

Fig. 6.18 DAD caused by infection with *Pneumocystis jiroveci* (*Pneumocystis* pneumonia). (**a**) Low-magnification photomicrograph of surgical lung biopsy from a patient with ARDS showing acute DAD with thick, lush hyaline membranes typical of those sometimes seen in patients with *Pneumocystis*-associated DAD (H&E). (**b**) High-magnification photomicrograph showing a small focus of frothy exudate (arrows) within one of the thick hyaline membranes in the same patient with *Pneumocystis*-associated DAD (H&E). (**c**) High-magnification photomicrograph illustrating organisms typical of *Pneumocystis jiroveci* in the same surgical lung biopsy showing DAD characterized by thick hyaline membranes (Gomori methenamine silver stain)

Noninfectious Air Space Diseases

A number of noninfectious, nongranulomatous lung diseases primarily affect the air spaces rather than the interstitial compartment. These conditions have overlapping clinical, radiologic, and histologic features and are therefore grouped together in this category. Symptoms in these noninfectious air space diseases tend to include some combination of cough, shortness of breath, and fever, and thus they mimic the clinical features of infection. At low magnification these lesions have in common a patchy and frequently bronchiolocentric distribution for which the differential diagnosis sometimes also includes infectious pneumonia (*see* Chap. 4). Differences are attributable primarily to differences in the histologic characteristics of the air space exudate itself.

Organizing Pneumonia

Organizing pneumonia (Figs. 6.19, 6.20, 6.21, 6.22, 6.23, 6.24, 6.25, 6.26 and 6.27) is predominantly an air space lesion that occurs in a variety of clinical and histopathologic contexts. Organizing pneumonia sometimes occurs as a secondary finding in patients with other primary pathologic processes. For example, organizing pneumonia is commonly seen distal to centrally obstructing tumors and is frequently combined with other histologic findings in patients with aspiration pneumonia, hypersensitivity pneumonia, and granulomatosis with polyangiitis (Wegener granulomatosis). Patients in whom organizing pneumonia represents the primary pathologic abnormality fall into several different clinical groups, including those with idiopathic disease (*cryptogenic* organizing pneumonia), those with underlying diseases or conditions known to cause or be associated with organizing pneumonia (*secondary* organizing pneumonia), and patients with localized PET-positive radiologic abnormalities that may mimic lung neoplasms (*focal* organizing pneumonia). Patients with cryptogenic organizing pneumonia (COP), referred to historically as bronchiolitis obliterans organizing pneumonia (BOOP), constitute the majority for whom organizing pneumonia is the primary finding in diagnostic lung biopsies. COP usually presents as a subacute respiratory illness characterized by several weeks of cough and shortness of breath, often following a viral-like prodrome. Fever is present in about half of affected patients. Pulmonary function studies show a mild to moderate ventilatory defect often accompanied by a diminished diffusion capacity for carbon monoxide (DLco). Typical radiologic findings include patchy, bilateral ground-glass attenuation with or without consolidation with preservation of lung volumes. COP usually responds favorably to oral corticosteroid therapy, although relapse occurs in as many as half of patients if steroids are tapered prematurely. The presence of collagen fibrosis has been associated with a worse prognosis and may indicate that the organizing pneumonia is a secondary rather than a primary finding in a patient with a clinically occult underlying fibrotic lung disease that is not well represented in the sampled tissue. Patients with COP, including those with localized radiologic abnormalities (*focal* organizing pneumonia), tend to have a better prognosis compared to patients with organizing pneumonia secondary to an underlying condition (e.g., connective tissue disease) or cause (e.g., drug-induced disease), although both groups of patients have high rates of treatment response and low disease-specific mortality.

Identifying organizing pneumonia in a lung biopsy is often an important preliminary step in recognizing patients with COP but requires correlation with other clinical and radiologic data to exclude other potential causes or associations (*secondary* organizing pneumonia). It is also important that biopsies be carefully evaluated for histologic clues helpful in establishing specific causes for organizing pneumonia. For example, aspiration of food and other particulates from the upper gastrointestinal tract has been highlighted as a circumstance in which organizing pneumonia may be a prominent histologic finding in surgical lung biopsies. Organizing pneumonia also may be a prominent finding in certain infections, and for that reason special stains should be performed whenever organizing pneumonia is accompanied by granulomatous and/or acute inflammation.

Organizing pneumonia that includes not only granulomatous inflammation but also necrotizing vasculitis may be a clue to the diagnosis of the BOOP-like variant of granulomatosis with polyangiitis (Wegener) and requires not only special stains to exclude infection but also correlation with clinical data to confidently establish a diagnosis of Wegener granulomatosis.

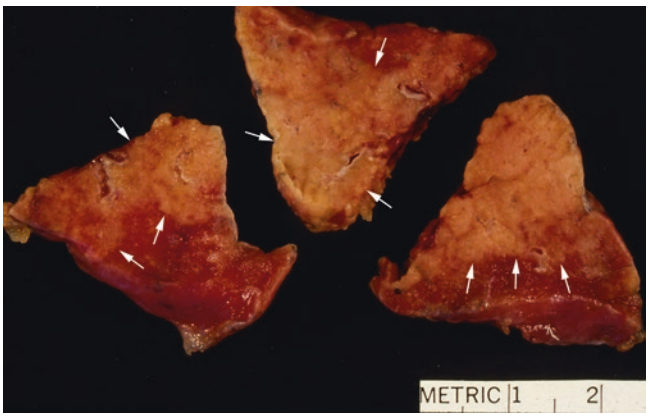

Fig. 6.19 Gross photograph of surgical lung biopsy from patient with COP. Areas of pallor were firm on palpation and corresponded to the areas of organizing pneumonia (arrows)

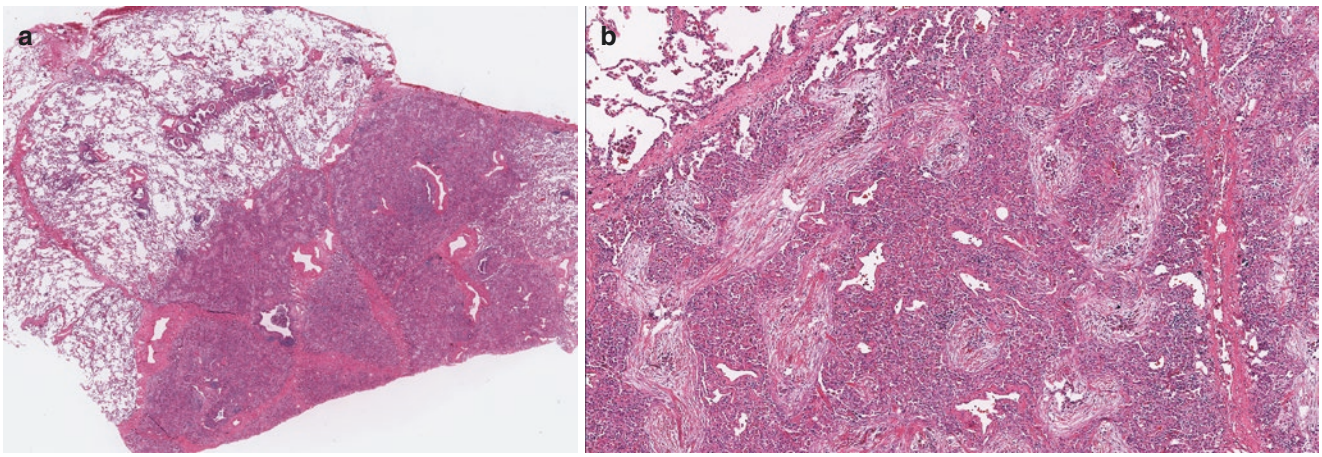

Fig. 6.20 Organizing pneumonia in a patient with COP. (**a**) This scanning magnification photomicrograph shows the sharp contrast between the area of organizing pneumonia at lower right and relatively normal lung in the upper left (H&E). Organizing pneumonia fills air spaces and therefore appears solid at lowest magnification. (**b**) Intermediate-magnification photomicrograph of organizing pneumonia illustrated in lower right portion of **a** showing to better advantage the characteristic polypoid plugs of organizing fibroblasts and myofibroblasts, in this case with an associated infiltrate of lymphocytes and plasma cells within the central areas of the plugs themselves (H&E). The configuration of the organizing fibrosis reflects the anatomy of the respiratory bronchioles and alveolar ducts in which it resides

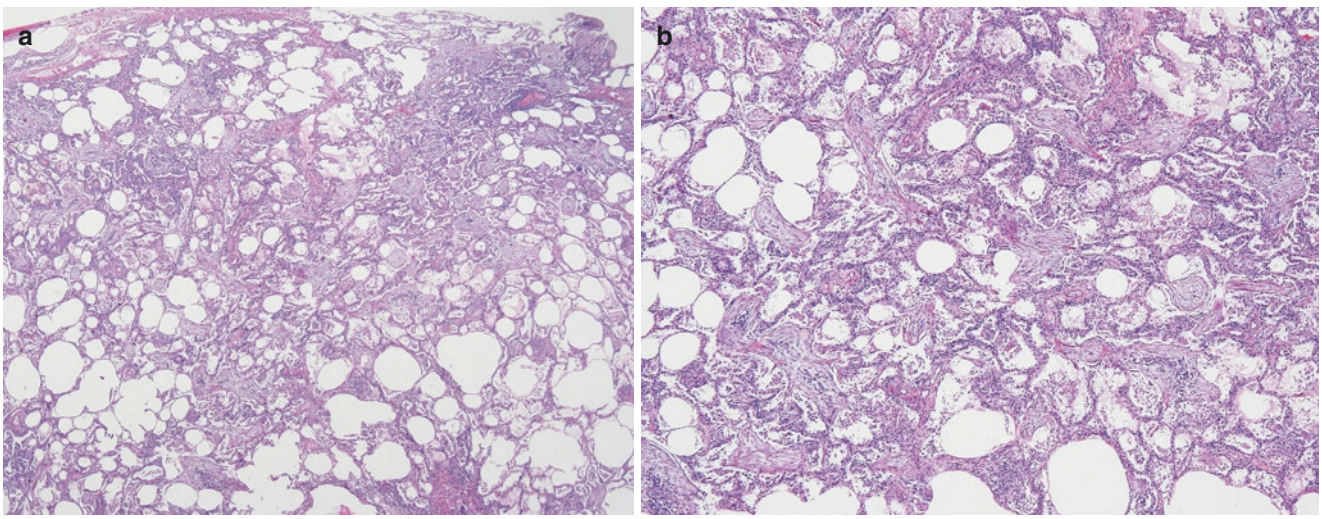

Fig. 6.21 Organizing pneumonia in a patient with COP. (**a**) Low-magnification photomicrograph showing organizing pneumonia in a well-inflated surgical lung biopsy (H&E). The patchy abnormality comprises very distinctive plugs of organizing fibroblasts and myofibroblasts situated mainly within the lumina of branching airways and alveolar ducts. (**b**) Intermediate-magnification photomicrograph from same surgical lung biopsy shows to better advantage the intraluminal plugs of organizing tissue affiliated with a scant infiltrate of mononuclear inflammatory cells (H&E). Alveolar septa show a similar infiltrate of mononuclear inflammatory cells, but the interstitial changes are limited to the areas with intraluminal fibrosis

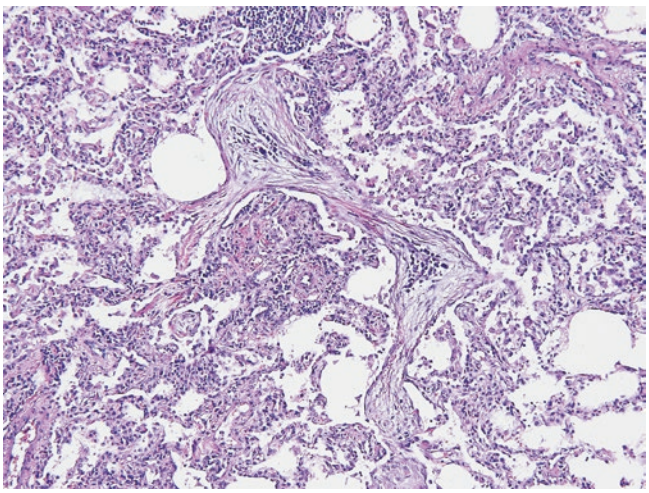

Fig. 6.22 Organizing pneumonia in a patient with COP. Higher-magnification view of the surgical lung biopsy illustrated in Fig. 6.21 showing the characteristic branching pattern of organizing pneumonia in a well-inflated lung biopsy. Note that while organizing pneumonia is centered on the airways, there are concomitant interstitial abnormalities that are limited to the areas of intraluminal fibrosis

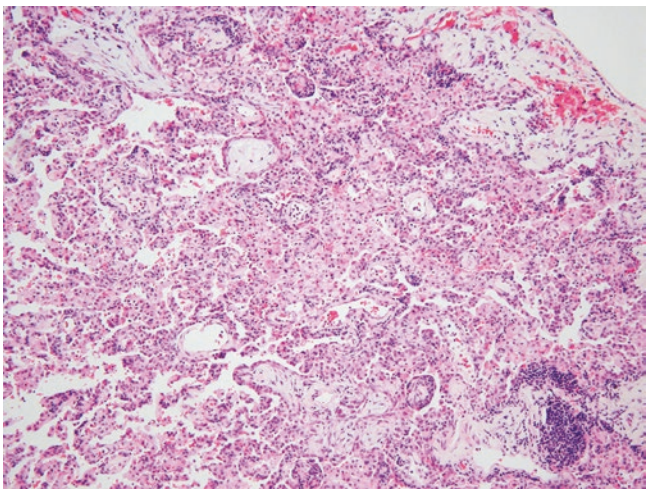

Fig. 6.24 Foamy alveolar macrophages in organizing pneumonia. Intermediate-magnification photomicrograph shows prominent foamy macrophages in the region of organizing pneumonia (H&E). This is a common although nonspecific finding in organizing pneumonia that represents microscopic obstructive pneumonia resulting from small airway dysfunction

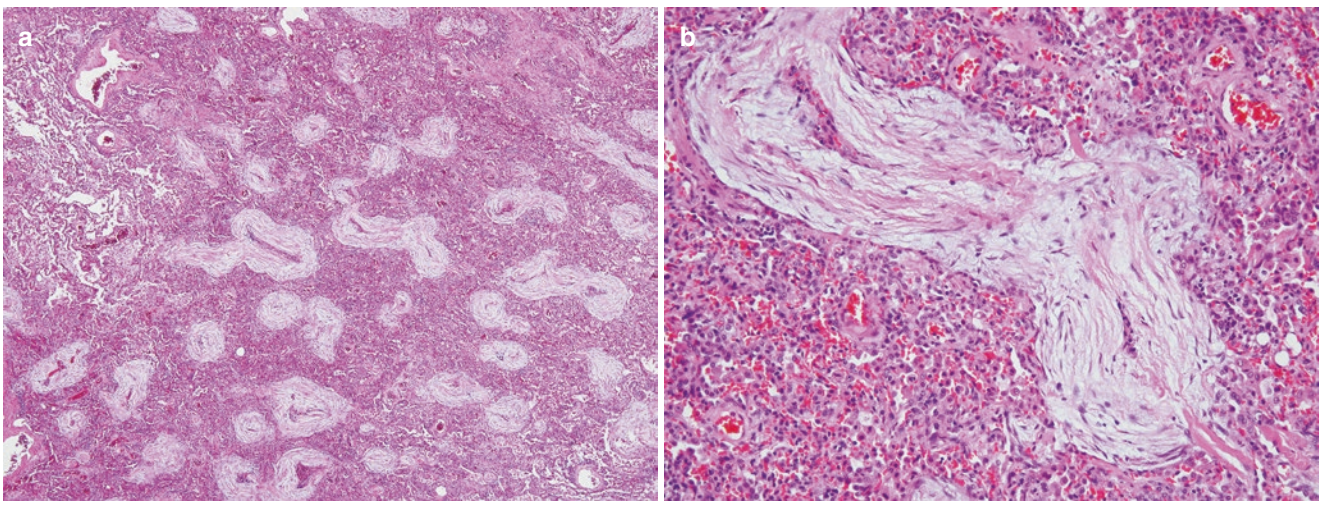

Fig. 6.23 Organizing pneumonia in a patient with COP. (**a**) Low-magnification photomicrograph showing the polypoid plugs of organizing fibroblasts and myofibroblasts outlined in sharp relief against a backdrop of collapsed intervening air spaces (H&E). The plugs of intraluminal fibroblastic tissue are centered on respiratory bronchioles and alveolar ducts, which accounts for this peculiar and distinctive low-magnification appearance. (**b**) Higher-magnification photomicrograph from low-magnification field illustrated in **a** showing bland fibroblasts and myofibroblasts arranged in a vaguely linear fashion within an edematous and focally collagenized matrix to form a cast of the affected distal airway surrounded by compressed alveolar spaces (H&E)

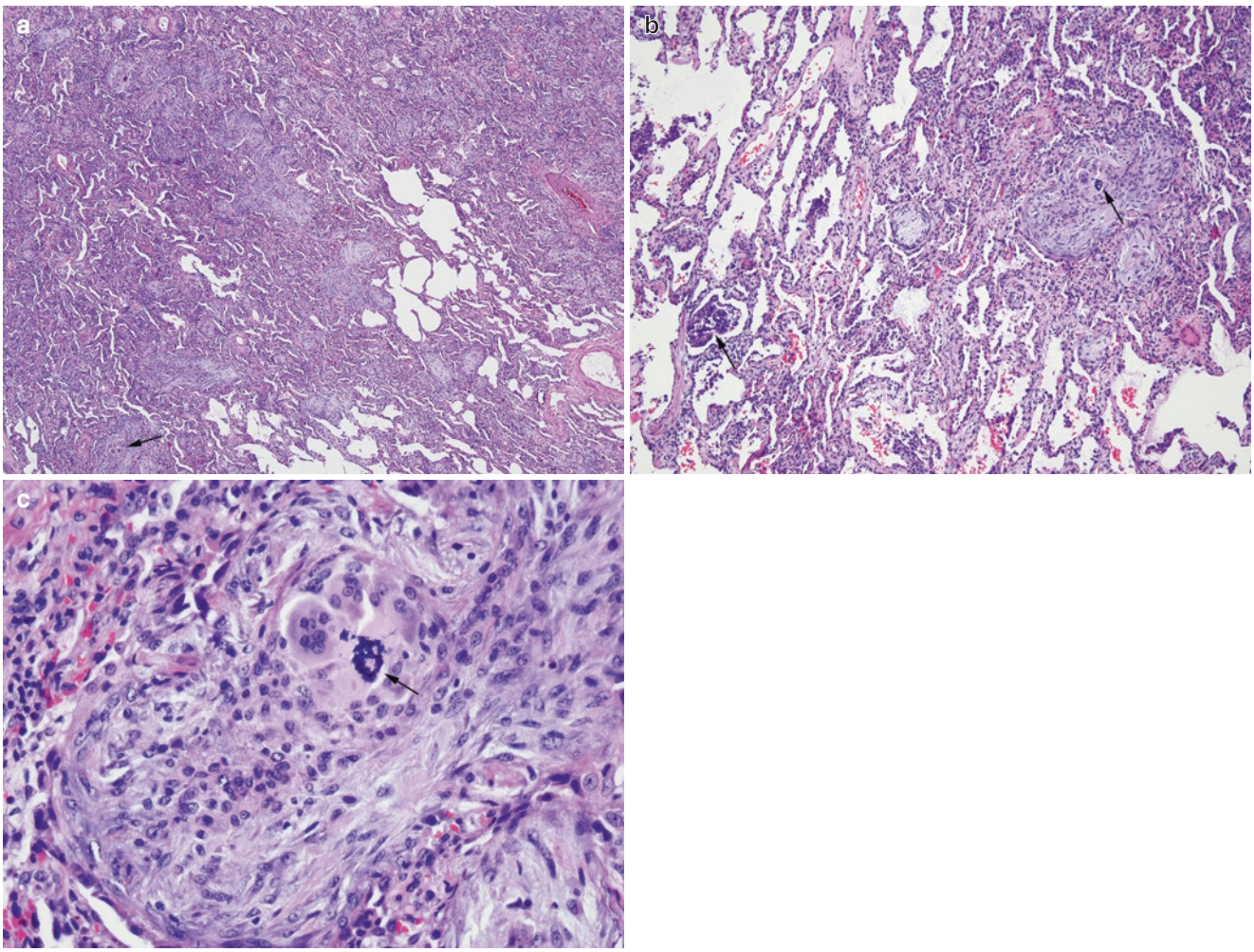

Fig. 6.25 Organizing pneumonia in a patient with aspiration of gastric particulates. (**a**) Low-magnification photomicrograph showing organizing pneumonia that might easily be construed as COP (H&E). In multiple areas throughout the biopsy, however, the organizing pneumonia is accompanied by foreign particulates with an associated giant cell reaction (arrow), as illustrated at higher magnification in **b**, **c**. (**b**) Intermediate-magnification photomicrograph from surgical lung biopsy showing extensive organizing pneumonia and associated multinucleated giant cells containing basophilic, coral-like cytoplasmic inclusions (arrows) typical of crospovidone, a chemically inactive filler (excipient) used in oral medications (H&E). (**c**) High-magnification photomicrograph showing crospovidone (arrow) affiliated with a foreign body giant cell reaction in the midst of what is otherwise typical organizing pneumonia (H&E)

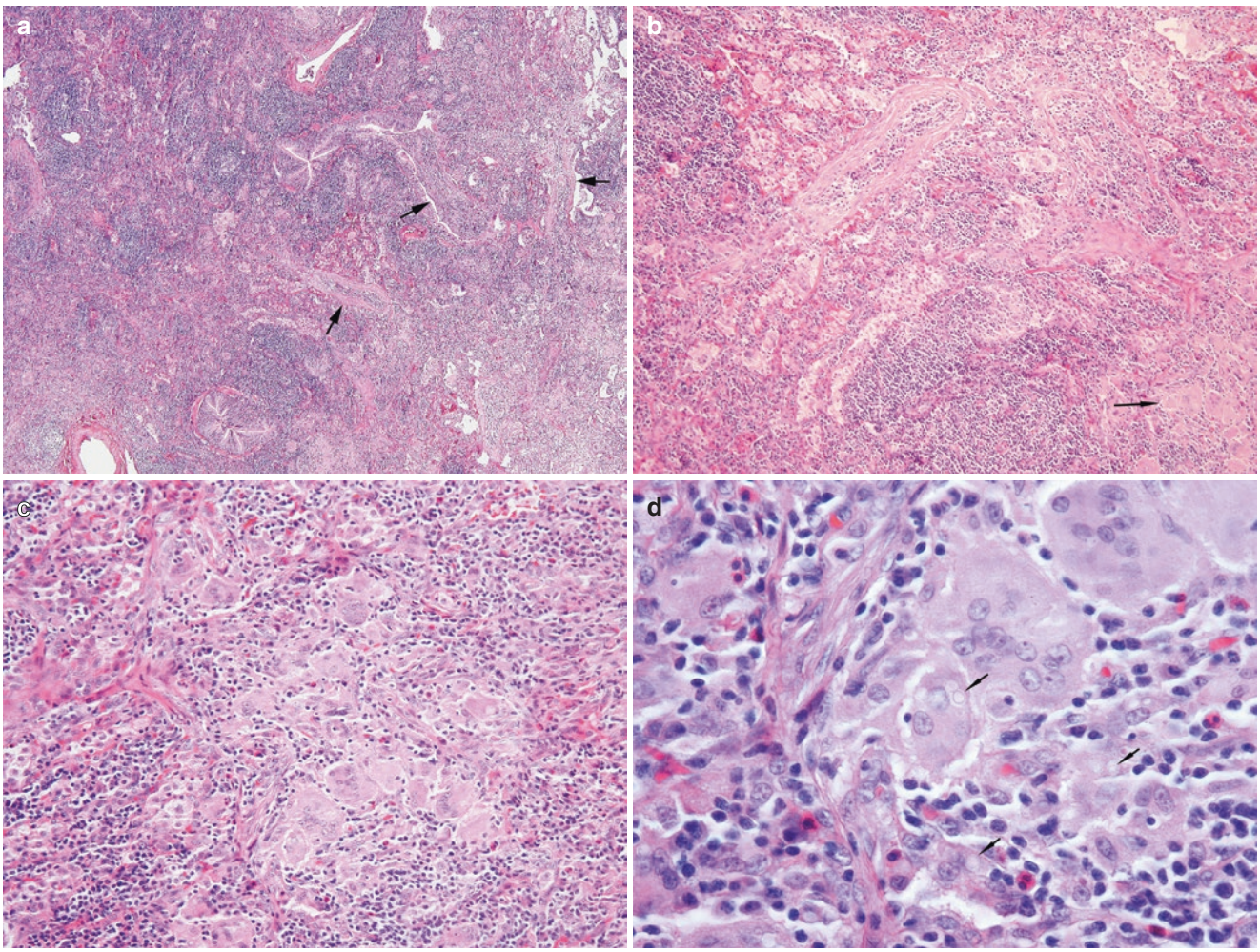

Fig. 6.26 Secondary organizing pneumonia in cryptococcosis. (**a**) Low-magnification photomicrograph showing organizing pneumonia (*arrows*) with prominent foamy macrophages and a dense inflammatory infiltrate (H&E). (**b**) Intermediate-magnification photomicrograph showing organizing pneumonia with foamy alveolar macrophages and an inflammatory background that includes loose clusters of epithelioid macrophages and giant cells (*arrow*), resulting in a vaguely granulomatous appearance (H&E). (**c**) High-magnification photomicrograph showing poorly formed granulomatous inflammation illustrated in **b** (H&E). (**d**) High-magnification photomicrograph of the granulomatous inflammation illustrated in **c** showing multiple fungal yeast forms (arrows) with clear halos, thin delicate pale-staining walls, and narrow-neck budding typical of *Cryptococcus neoformans* (H&E)

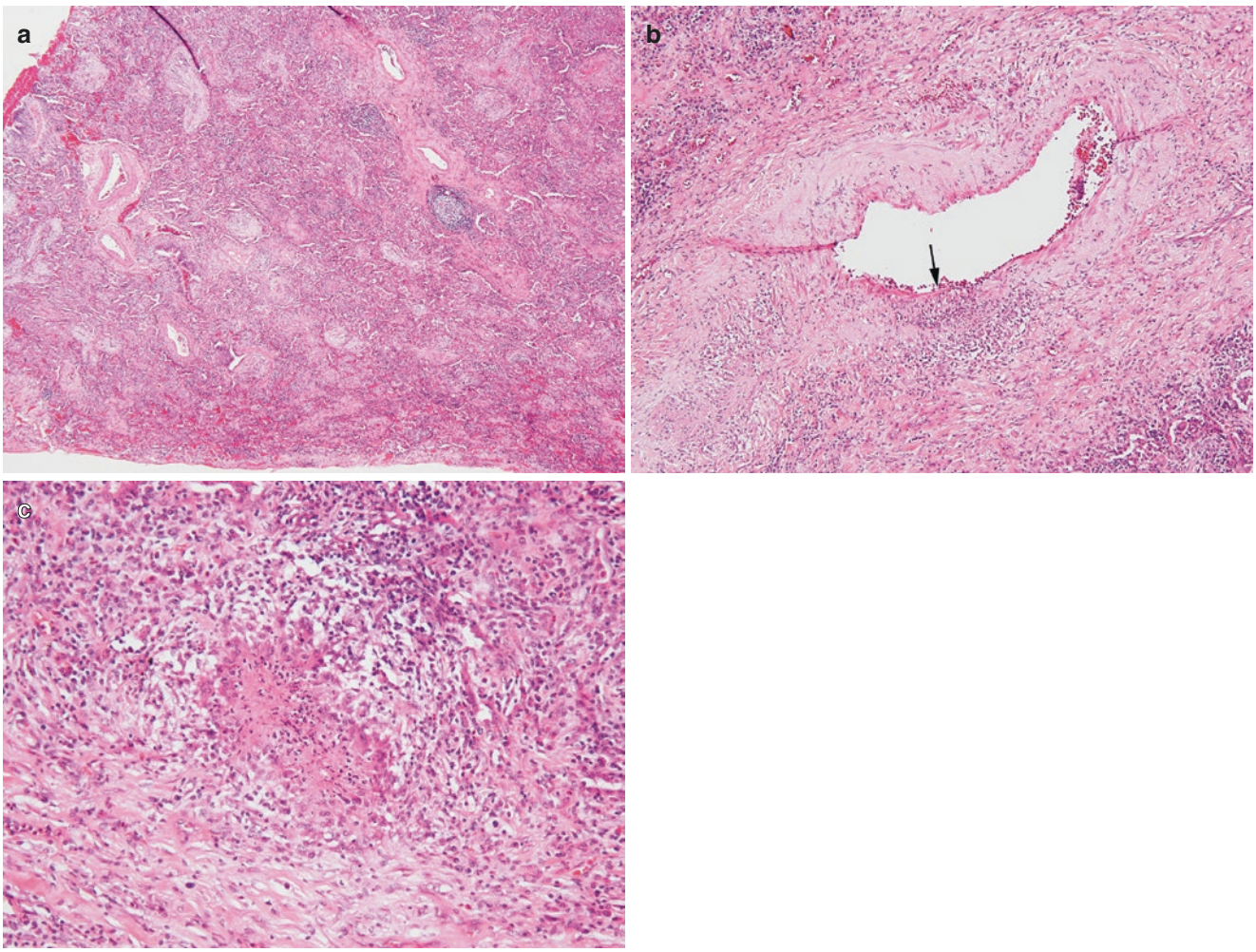

Fig. 6.27 BOOP-like variant of granulomatosis with polyangiitis (Wegener). (**a**) Low-magnification photomicrograph showing features typical of organizing pneumonia (H&E). (**b**) Intermediate-magnification photomicrograph from the same biopsy showing a necrotizing vasculitis characterized by a focal, transmural infiltrate of predominantly neutrophils with associated karyorrhexis (H&E). (**c**) Intermediate-magnification photomicrograph showing a palisaded granuloma typical of granulomatosis with polyangiitis (Wegener) in the same lung biopsy in which organizing pneumonia was the dominant feature (H&E). This combination of findings has been described in patients with the BOOP-like variant of Wegener granulomatosis

Eosinophilic Pneumonia

Eosinophilic pneumonia (Figs. 6.28, 6.29, 6.30, 6.31, 6.32, 6.33 and 6.34), like organizing pneumonia, refers to an air space-filling process that occurs as both a primary and a secondary finding in various clinical and histologic contexts. Löffler syndrome, also termed simple pulmonary eosinophilia, has distinctive clinical and radiologic findings and therefore rarely requires lung biopsy for diagnosis. The histologic findings are presumed to overlap with those seen in chronic eosinophilic pneumonia (CEP), a syndrome of unknown etiology characterized by a subacute or chronic course that likely accounts for most patients in whom surgical lung biopsy is required for diagnosis. Acute eosinophilic pneumonia differs in that patients present with rapidly progressive respiratory failure and experience equally rapid recovery either spontaneously or with corticosteroid therapy.

CEP accounts for the majority of patients with eosinophilic pneumonia diagnosed on the basis of surgical lung biopsies. Chronic eosinophilic pneumonia is characterized by a subacute or chronic course in which symptoms persist for weeks or months. Some patients experience a waxing and waning course that may persist for years. Women in their fourth or fifth decades of life account for the majority of patients, and nearly half have underlying asthma. Cough is the most common presenting complaint and may be accompanied by systemic symptoms, including fever, weight loss, and night sweats. Peripheral eosinophilia occurs in nearly 90% of patients. Like COP, most patients with CEP experience complete recovery with corticosteroid therapy. Relapses are common if treatment is withdrawn prematurely.

Acute eosinophilic pneumonia (AEP) is a febrile illness associated with rapidly progressive hypoxemic respiratory failure, diffuse radiologic abnormalities, bronchoalveolar lavage eosinophilia of greater than 25%, absence of an identifiable etiology (i.e., infection, parasitic infestation, drug exposure), and either spontaneous recovery or rapid response to corticosteroid therapy. A subset of patients with AEP develop ARDS and therefore resemble patients for whom DAD is a more common biopsy finding. Peripheral eosinophilia occurs in about half of patients with AEP. A syndrome identical to idiopathic AEP has been described in first-time cigarette smokers and less commonly in those who resume smoking after a period of smoking cessation. AEP is frequently diagnosed on the basis of clinical, radiographic, and bronchoalveolar lavage findings without resorting to lung biopsy. By definition, AEP is associated with an excellent prognosis, with all patients recovering either spontaneously or after corticosteroid therapy.

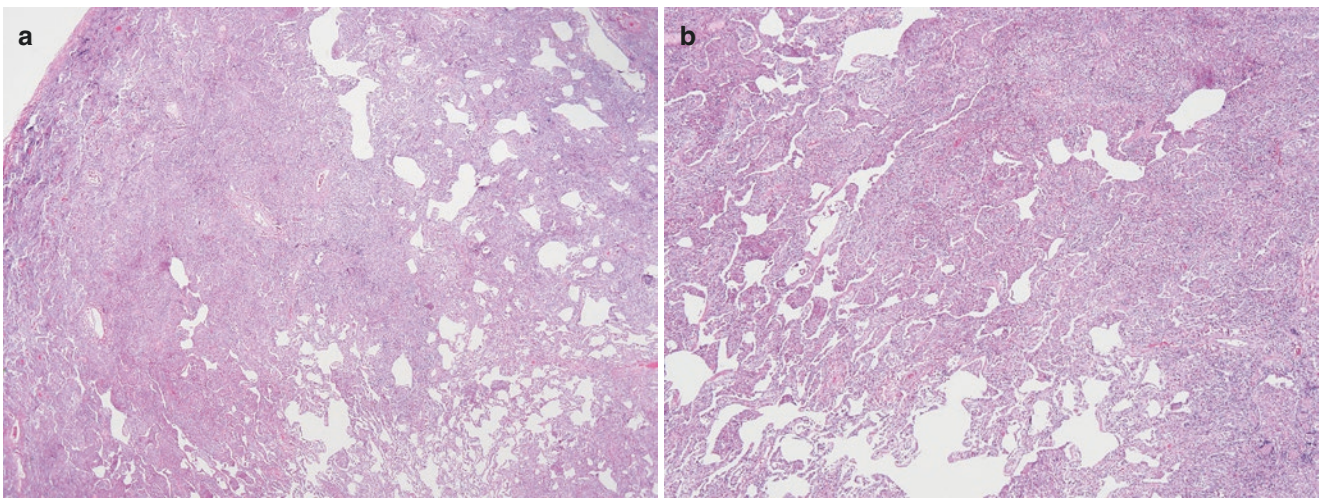

Fig. 6.28 Eosinophilic pneumonia in a patient with CEP. (**a**) Low-magnification photomicrograph of CEP showing patchy air space-filling process (H&E). (**b**) Intermediate-magnification photomicrograph showing a combination of inflammatory cells and fibrin in air spaces accompanied by expansion of the interstitium by a similar inflammatory infiltrate (H&E)

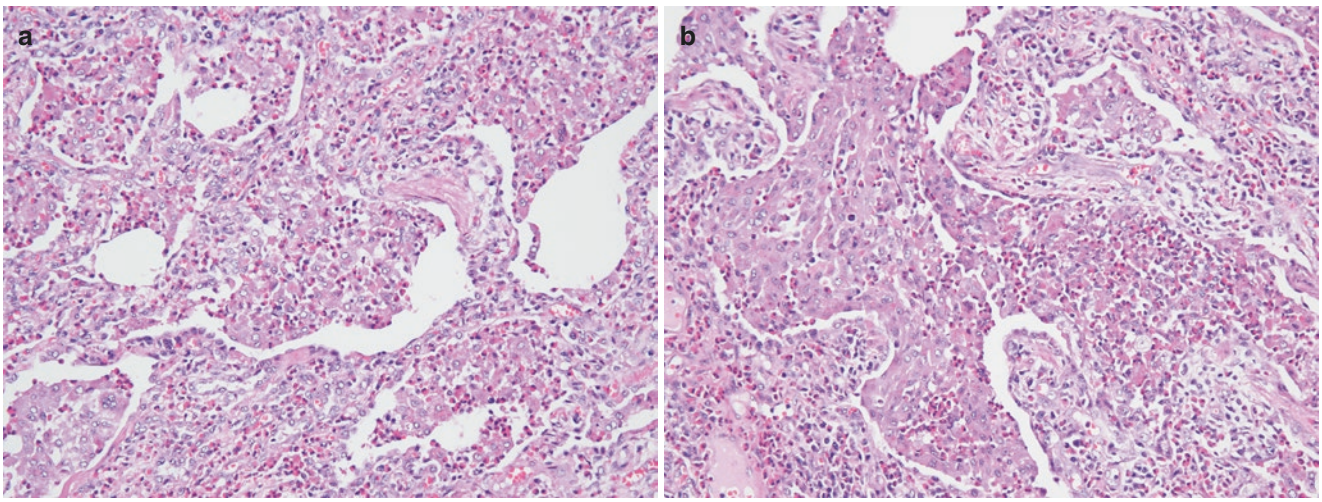

Fig. 6.29 Eosinophilic pneumonia in a patient with CEP. (**a**) High-magnification photomicrograph from patient with CEP whose biopsy is also illustrated in Fig. 6.28 showing air space and interstitial chronic inflammatory infiltrate in which eosinophils predominate (H&E). (**b**) High-magnification photomicrograph of a different field in the same biopsy showing both eosinophils and alveolar macrophages (H&E). Macrophages are often a prominent component of the air space exudate in eosinophilic pneumonia and sometimes overshadow the eosinophils

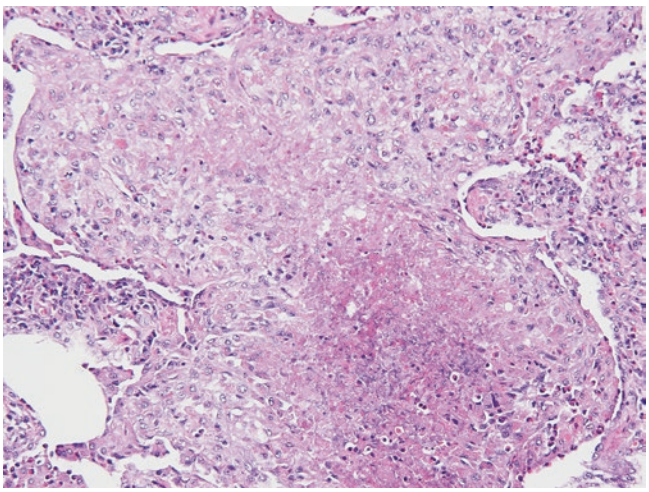

Fig. 6.30 Eosinophilic pneumonia in a patient with CEP. This high-magnification photomicrograph of a surgical lung biopsy from a patient with CEP shows focal necrosis in an air space exudate made up mainly of macrophages with eosinophils clustered at the periphery and within an expanded interstitial structure (H&E)

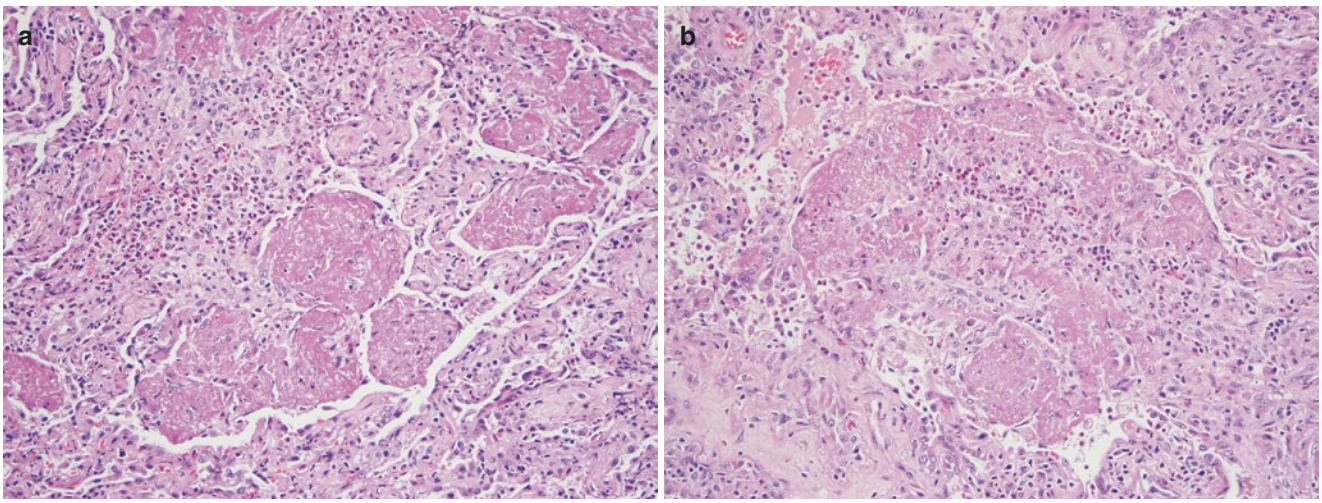

Fig. 6.31 Eosinophilic pneumonia in a patient with CEP. (**a**, **b**) Two high-magnification photomicrographs show a prominent fibrinous air space exudate that was a focal finding in a patient with biopsy findings that were otherwise typical of CEP (H&E). Fibrin predominates in the air spaces, but clusters of eosinophils are present within the air spaces as well as the interstitium and are key to distinguishing eosinophilic pneumonia from acute fibrinous and organizing pneumonia (AFOP)

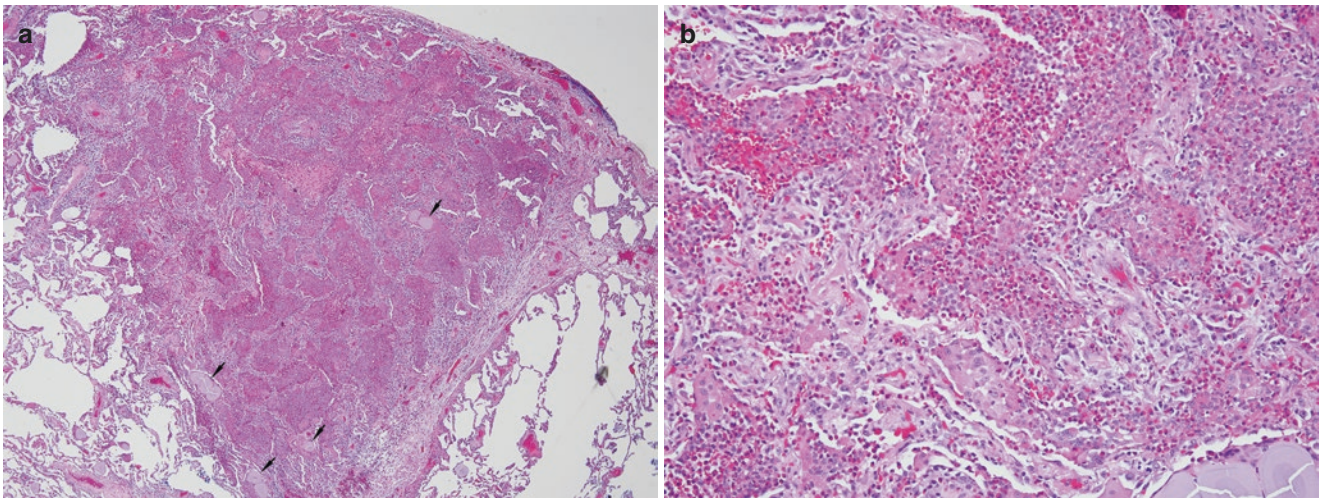

Fig. 6.32 Eosinophilic pneumonia in a patient with chronic eosinophilic pneumonia. (**a**) Low-magnification photomicrograph showing a very patchy air space-filling process in which fibrin is a prominent feature (H&E). Note multiple corpora amylacea (arrows) embedded in the fibrinous inflammatory infiltrate, an incidental finding of no special significance. (**b**) High-magnification photomicrograph of eosinophilic pneumonia showing a combination of fibrin, eosinophils, and macrophages in eosinophilic pneumonia (H&E). Note portion of corpora amylacea at lower right, an incidental finding

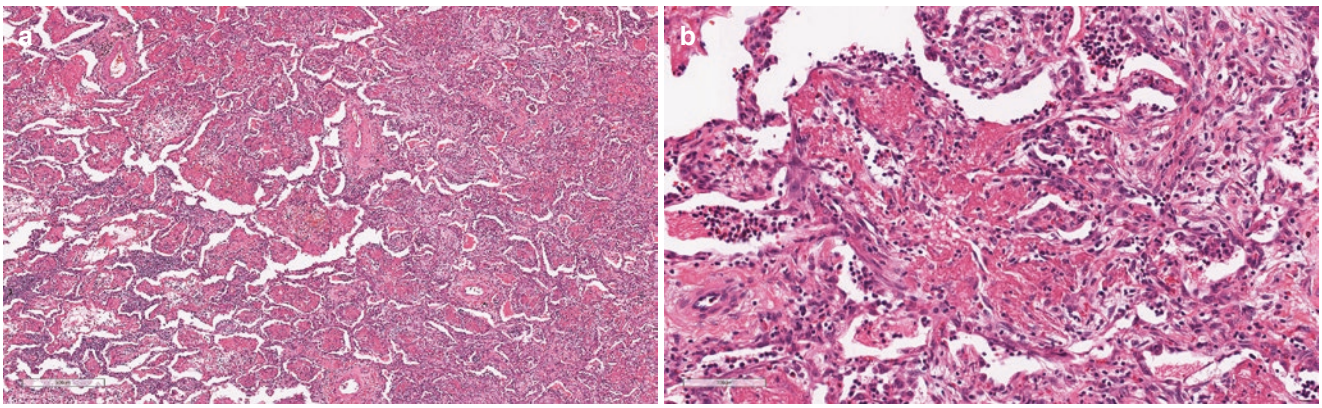

Fig. 6.33 Organizing eosinophilic pneumonia in a patient with chronic eosinophilic pneumonia. (**a**) Low-magnification photomicrograph showing a combination of air space fibrin, interstitial and air space inflammation, and organizing intraluminal fibrosis resembling organizing pneumonia (H&E). (**b**) High-magnification photomicrograph showing air space fibrin associated with a mixed inflammatory infiltrate that includes clusters of eosinophils, organizing fibroblasts, and myofibroblasts, resulting in a pattern of intraluminal fibrosis resembling organizing pneumonia (H&E)

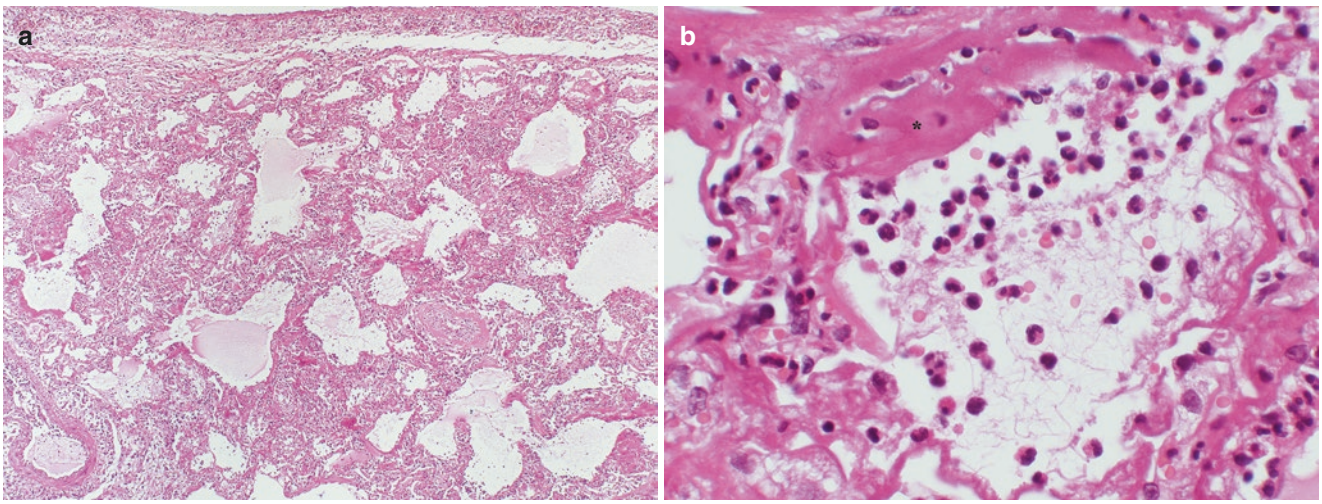

Fig. 6.34 AEP. (**a**) Low-magnification photomicrograph of a surgical lung biopsy from a patient with AEP showing a combination of interstitial thickening and a variably cellular fibrinous air space exudate with associated hyaline membranes (H&E). (**b**) High-magnification photomicrograph from same biopsy showing well-formed hyaline membrane (asterisk) and a cellular air space exudate that includes eosinophils and neutrophils (H&E). Some of the eosinophils are degranulated and recognizable only on the basis of a characteristic bilobed nucleus

Acute Fibrinous and Organizing Pneumonia (AFOP)

AFOP (Figs. 6.35 and 6.36) is a descriptive term intended from the outset to describe a fibrin-rich air space-filling lesion with features resembling those seen in DAD, organizing pneumonia, and eosinophilic pneumonia. Indeed, the original description suggested that in at least some patients, AFOP might be a histologic variant of DAD, given that just over half had a fulminant and fatal course that included mechanical ventilation. A fulminant clinical course linking AFOP with ARDS has now been documented in multiple reports. In other patients AFOP overlaps both clinical and histologic features of COP, a syndrome in which prominent fibrin may signify greater risk of relapse depending on the radiologic distribution of disease. In patients without more specific histologic findings such as hyaline membranes, classic organizing pneumonia, or eosinophilia, AFOP has been associated with various etiologies, including bacterial and viral infections, *Pneumocystis* pneumonia in HIV-infected patients, connective tissue diseases, and acute hypersensitivity pneumonia. AFOP, like the other lesions in the category of air space- filling diseases, should not be considered a specific diagnosis but rather a distinctive histology sometimes seen in other conditions (e.g., diffuse alveolar damage, organizing pneumonia, eosinophilic pneumonia). In patients without clinical or histologic features to suggest an alternative, AFOP occurs in a broad range of clinical contexts requiring not only special stains for organisms but also careful correlation with other data, including the results of microbiologic assays, to fully understand the significance of this finding.

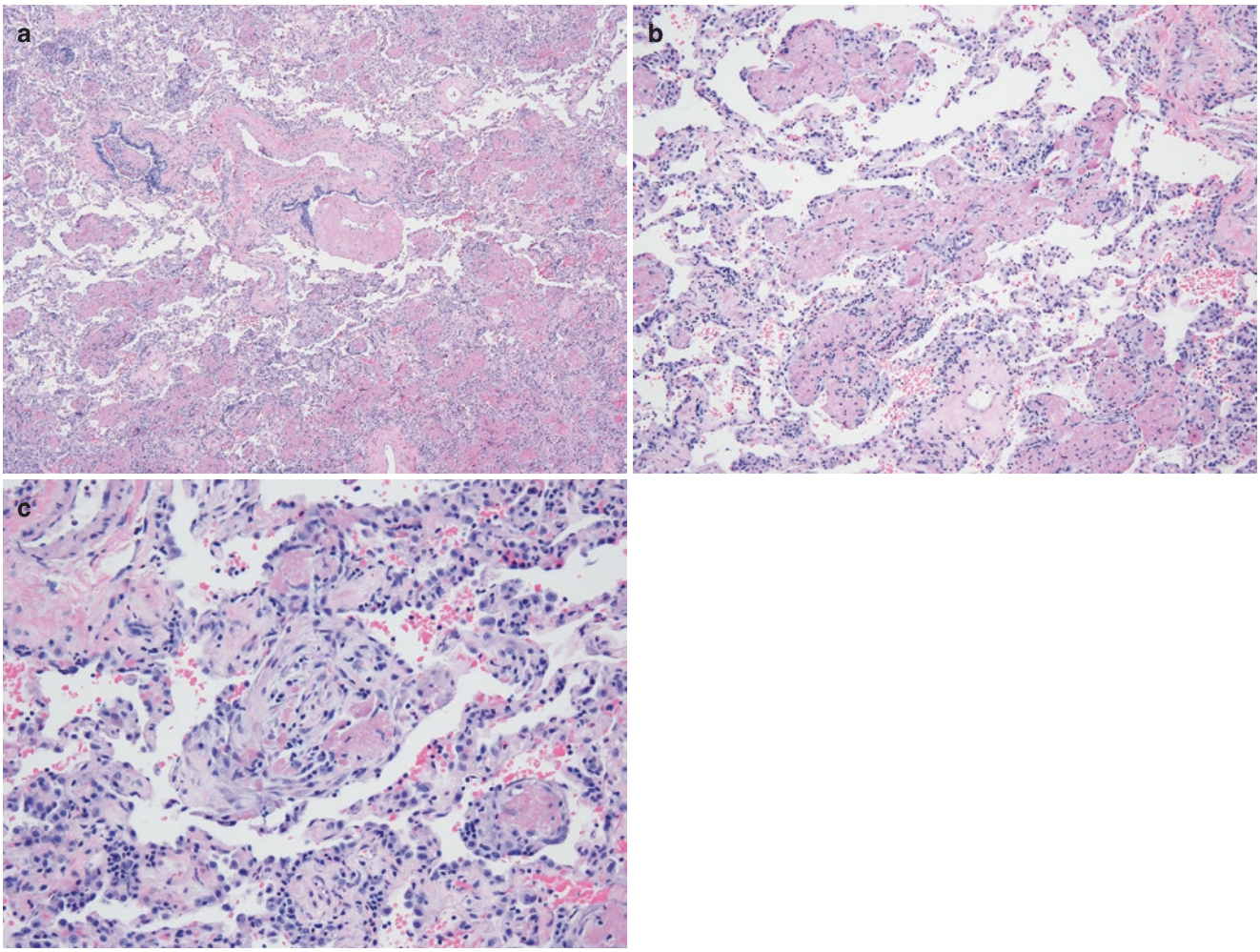

Fig. 6.35 Acute fibrinous and organizing pneumonia (AFOP). (**a**) Low-magnification photomicrograph of AFOP in a patient with unexplained bilateral opacities on CT scan (H&E). There is a patchy air space-filling process in which fibrin predominates and is accompanied by a very mild air space and interstitial infiltrate of mononuclear cells. In this field there is minimal organization of the fibrinous air space exudate. (**b**) Higher-magnification photomicrograph showing a fibrinous air space exudate with minimal association inflammation (H&E). Special stains and cultures were negative, and there was minimal eosinophilia to suggest eosinophilic pneumonia as an alternative to AFOP. (**c**) High-magnification photomicrograph from same surgical lung biopsy showing an area in which the fibrinous air space exudate illustrated in **a**, **b** is affiliated with ingrowth of organizing fibroblasts (H&E). This feature, common in AFOP, results in considerable histologic overlaps with organizing pneumonia. Indeed, some patients with lesions resembling AFOP almost certainly have a variant of organizing pneumonia (COP)

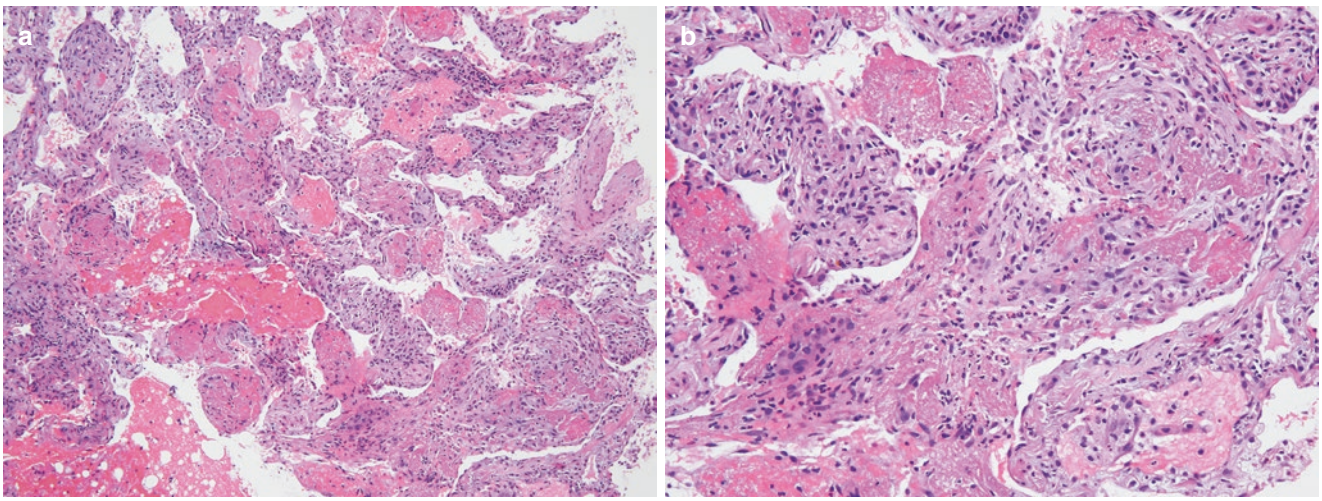

Fig. 6.36 AFOP. (**a**) Intermediate-magnification photomicrograph of core needle biopsy from patient with unexplained localized opacities on a chest CT scan (H&E). All special stains and cultures were negative for organisms, and there were no other histologic features (such as eosinophilia) to suggest a specific etiology. (**b**) Higher-magnification photomicrograph of area in lower right of field illustrated in **a** showing an organizing fibrinous air space exudate. This associated acute inflammation in this focus should at least raise the possibility of an infectious etiology (H&E)

Pulmonary Alveolar Proteinosis (PAP)

PAP (Figs. 6.37, 6.38, 6.39, 6.40 and 6.41), also called pulmonary alveolar lipoproteinosis or phospholipoproteinosis, is a distinctive lesion characterized by the presence of amorphous granular eosinophilic debris within alveolar spaces. Primary acquired PAP accounts for over 90% of patients and in most is a form of autoimmune disease driven by autoantibodies directed against granulocyte-macrophage colony-stimulating factor (GM-CSF). Secondary PAP refers to patients with certain underlying illnesses or associated conditions and has been reported most commonly in patients with hematologic malignancies and other forms of immunodeficiency. Associated opportunistic infections are common in immunocompromised patients. Less common causes of secondary PAP include occupational dust exposures and mutations in various genes that affect surfactant homeostasis in patients with congenital disease.

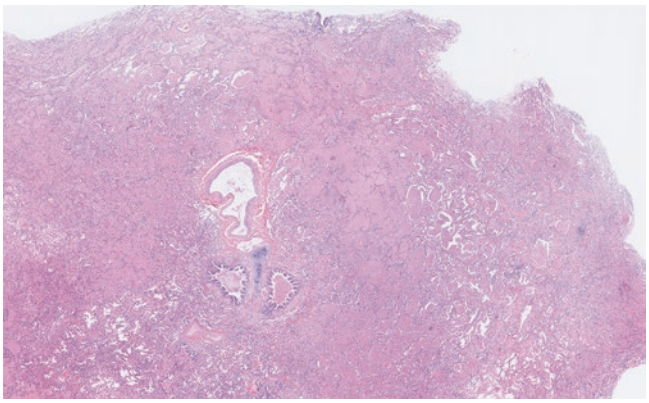

Fig. 6.37 PAP. Scanning magnification photomicrograph of surgical lung biopsy from a patient with primary acquired (autoimmune) PAP (H&E). Most of the air spaces in this sample are filled with eosinophilic debris that at first blush resembles pulmonary edema. Alveolar septa are nearly normal, showing only a mild, patchy infiltrate of chronic inflammatory cells without significant fibrosis

Primary acquired (autoimmune) PAP most commonly presents in the fourth decade of life. Nearly three fourths of patients are smokers at disease onset. Men are affected more commonly than women by a ratio of about 3:1, a disparity that may reflect historical smoking patterns. The most common symptoms at presentation are dyspnea and dry cough. Low-grade fever is seen in some, but the combination of an acute onset and fever should raise the possibility of superimposed infection. Pulmonary function studies usually show a mild restrictive ventilatory defect with a disproportionately severe reduction in the diffusing capacity for carbon monoxide (DLco). PAP is a disease with a generally good prognosis with 90% survival at 5 years. Whole lung lavage is the mainstay of therapy. PAP is an increasingly uncommon finding in surgical lung biopsies because many patients are now diagnosed on the basis of clinical and radiologic findings coupled with findings in bronchoalveolar lavage (BAL) fluid and/or transbronchial lung biopsy.

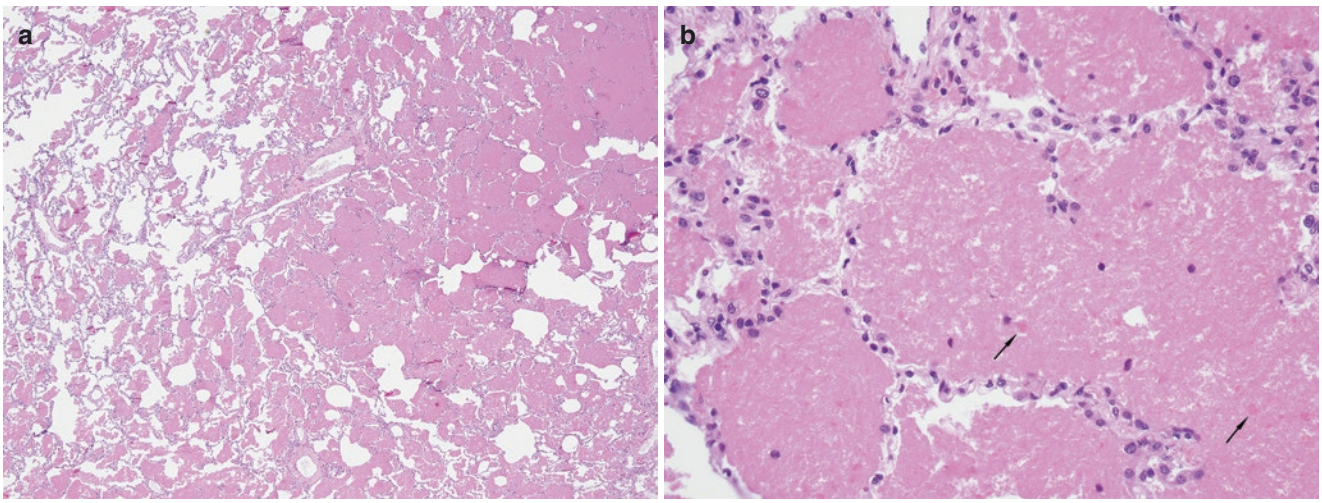

Fig. 6.38 PAP. (**a**) Low-magnification photomicrograph showing characteristic patchy distribution of a granular air space exudate in a patient with primary acquired (autoimmune) PAP (H&E). In many areas the air space exudate retracts from alveolar septa in a manner that is sometimes helpful in separating PAP from pulmonary edema. (**b**) High-magnification photomicrograph showing to better advantage the granular texture of the alveolar exudate with occasional coarse eosinophilic aggregates (*arrows*), rare mononuclear inflammatory cells, and degenerating erythrocytes (H&E). The granular nature of the exudate and associated cellular detritus is key to separating PAP from pulmonary edema

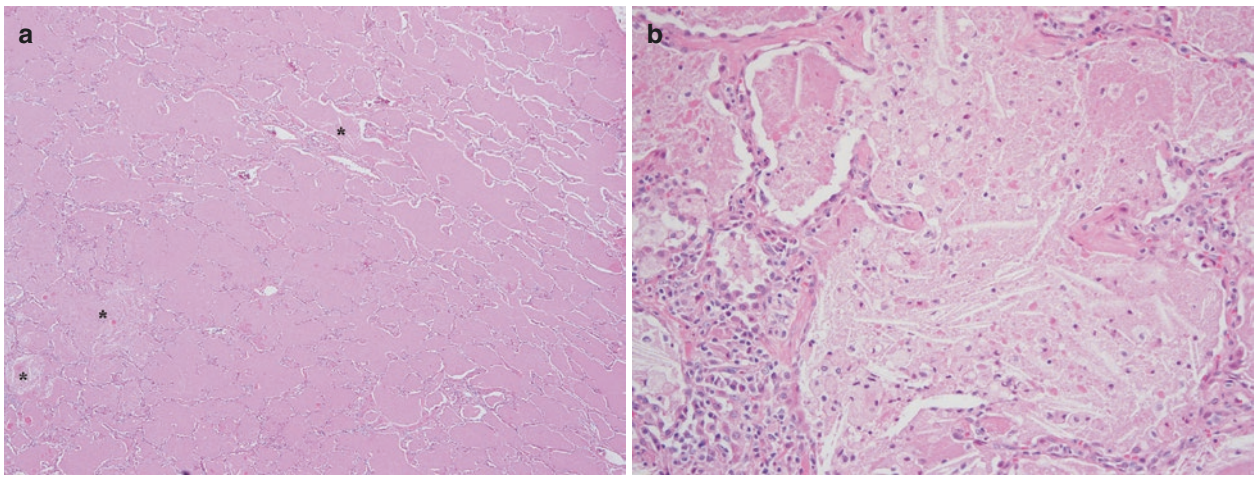

Fig. 6.39 PAP. (**a**) Low-magnification photomicrograph from another patient with primary acquired (autoimmune) PAP showing pulmonary edema-like eosinophilic air space exudate (H&E). Focal cholesterol-like clefts and granular debris with cell ghosts (asterisk) are important clues to the diagnosis of PAP. (**b**) High-magnification view of the same lung biopsy showing granular eosinophilic background, cholesterol-like clefts, macrophages, and cell ghost characteristic of PAP (H&E). Staining for periodic acid-Schiff stain, while characteristic, is relatively nonspecific. Diagnosis hinges instead on recognizing the distinctive histologic and cytologic characteristics that separate alveolar exudates of PAP from edema fluid

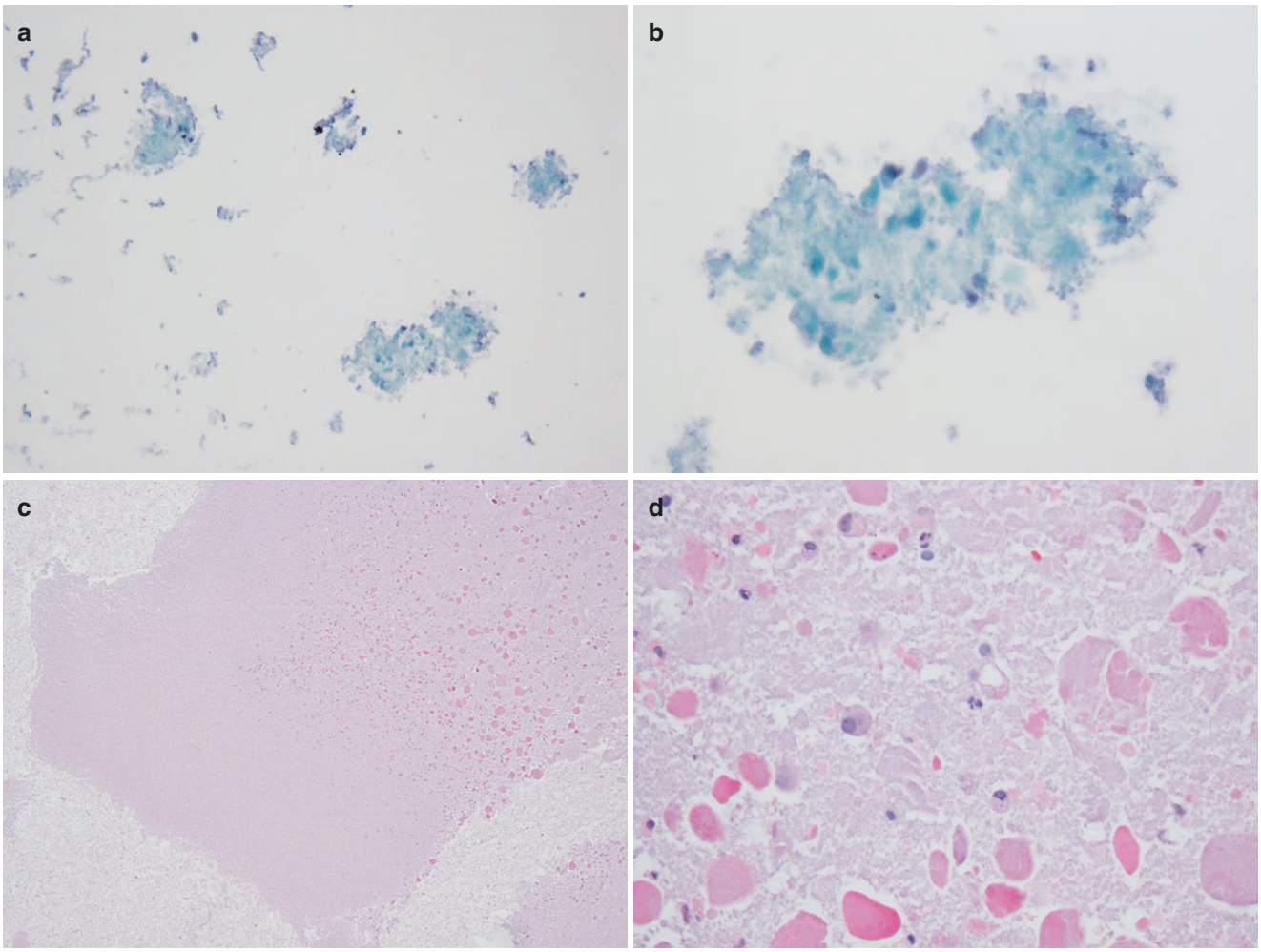

Fig. 6.40 PAP. (**a**) Intermediate magnification of ThinPrep preparation demonstrating bronchoalveolar lavage fluid from patient with PAP. Irregularly shaped fragments of a paucicellular granular exudate with coalescent globules and cell ghosts are characteristic of PAP. (**b**) High-magnification photomicrograph of one of the fragments illustrated in **a** showing PAP characterized by granular, paucicellular debris containing cell ghosts. (**c**) Low-magnification photomicrograph of cell block from a different patient using PAP (H&E). A paucicellular granular exudate shows larger aggregates or clumps of eosinophilic debris, a common finding in PAP. (**d**) High-magnification photomicrograph of cell block from same patient with PAP illustrated in **c**. A granular exudate is associated with rare macrophages, cell ghosts, and characteristic large eosinophilic aggregates (H&E)

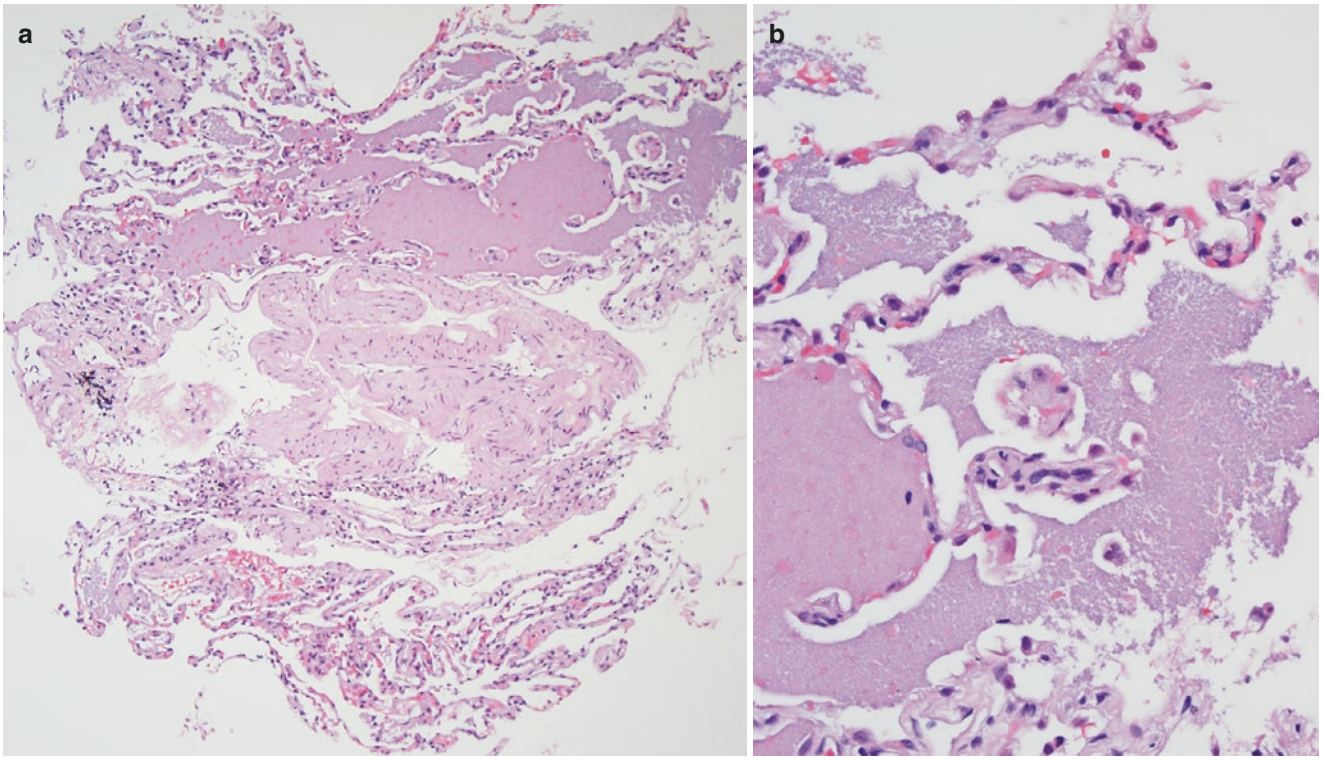

Fig. 6.41 PAP. (**a**) Low-magnification photomicrograph of transbronchial lung biopsy from a patient with primary acquired (autoimmune) PAP (H&E). The upper third of the photomicrograph shows alveolated lung parenchyma with a distinctive, paucicellular, granular air space exudate. Alveolated lung parenchyma at the bottom is unremarkable, attesting to the often patchy distribution of PAP. (**b**) High-magnification photomicrograph of the same transbronchial biopsy showing granular, eosinophilic, air space exudate typical of PAP (H&E)

Smoking–Related Lung Disorders

Cigarette smoking is associated with a range of overlapping histologic findings other than those traditionally attributed to chronic obstructive pulmonary disease (COPD). With the exception of Langerhans cell histiocytosis (LCH), the other smoking-related lesions (respiratory bronchiolitis, smoking-related interstitial fibrosis, and desquamative interstitial pneumonia) covered in this section are frequently seen in surgical specimens as incidental findings in patients who lack evidence of physiologically significant diffuse lung disease other than perhaps COPD. In asymptomatic patients without significant ventilatory defects other than those related to COPD, these frequently overlapping histologic findings serve only to corroborate a smoking history and should not by themselves be construed as evidence of diffuse restrictive lung disease. Similarly, any one or combination of these findings may be seen in smokers who have other forms of diffuse lung disease, most importantly UIP (*see* section "Usual Interstitial Pneumonia (UIP)"). On the other hand, these smoking-related lesions occasionally account for symptomatic diffuse lung disease in a highly select population of patients. In any individual patient, determining whether these lesions should be viewed as incidental, a cause of diffuse lung disease, or a confounding finding in a patient with something else altogether requires careful correlation with clinical and radiologic information.

Respiratory Bronchiolitis (RB)

Respiratory bronchiolitis (RB) is a common incidental finding in current or ex-smokers. While rare cases of RB are associated with clinical interstitial disease, the majority of the cases of RB are of no clinical significance. Histologically, RB is characterized by pigmented macrophages filling up respiratory bronchioles, alveolar ducts, and adjacent alveoli (Figs. 6.42 and 6.43).

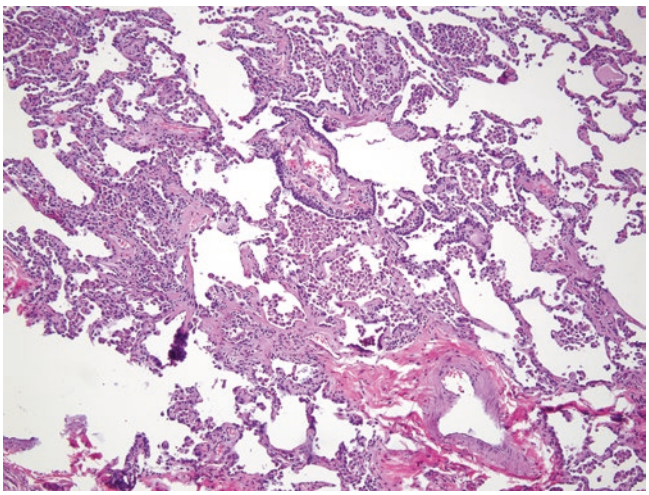

Fig. 6.42 RB. Intermediate-magnification photomicrograph showing a respiratory bronchiole and its adjacent alveoli filled with lightly pigmented macrophages typical of those seen in cigarette smokers. The air spaces away from the respiratory bronchiole are less involved

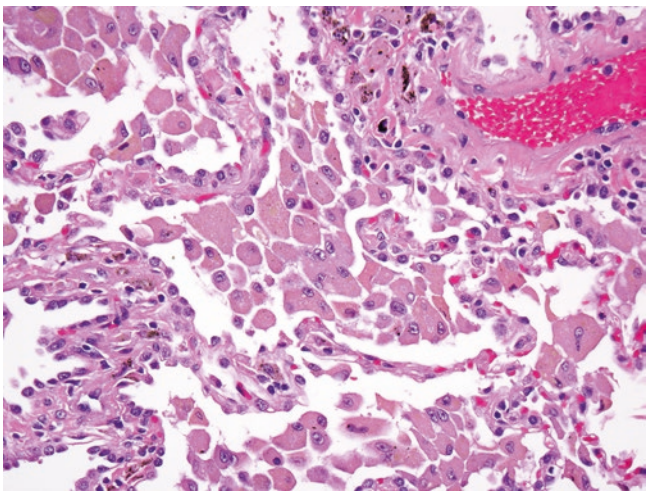

Fig. 6.43 RB. High-magnification photomicrograph showing smokers' macrophages within the air spaces that contained finely granular light brown pigment in the cytoplasm. The pigment is faintly positive on a Prussian-blue iron stain but lacks the coarse, refractile granules and bright blue staining characteristics of bleeding-related hemosiderin

Smoking-Related Interstitial Fibrosis (SRIF)

SRIF is a recently described entity that is characterized by marked alveolar septal fibrosis with distinct hyalinized collagen and minimal inflammation (Figs. 6.44 and 6.45). SRIF is most often encountered as an incidental finding in autopsy or lobectomy specimens from smokers. Rarely, SRIF causes symptoms and radiologic findings of interstitial lung disease, leading to lung biopsy.

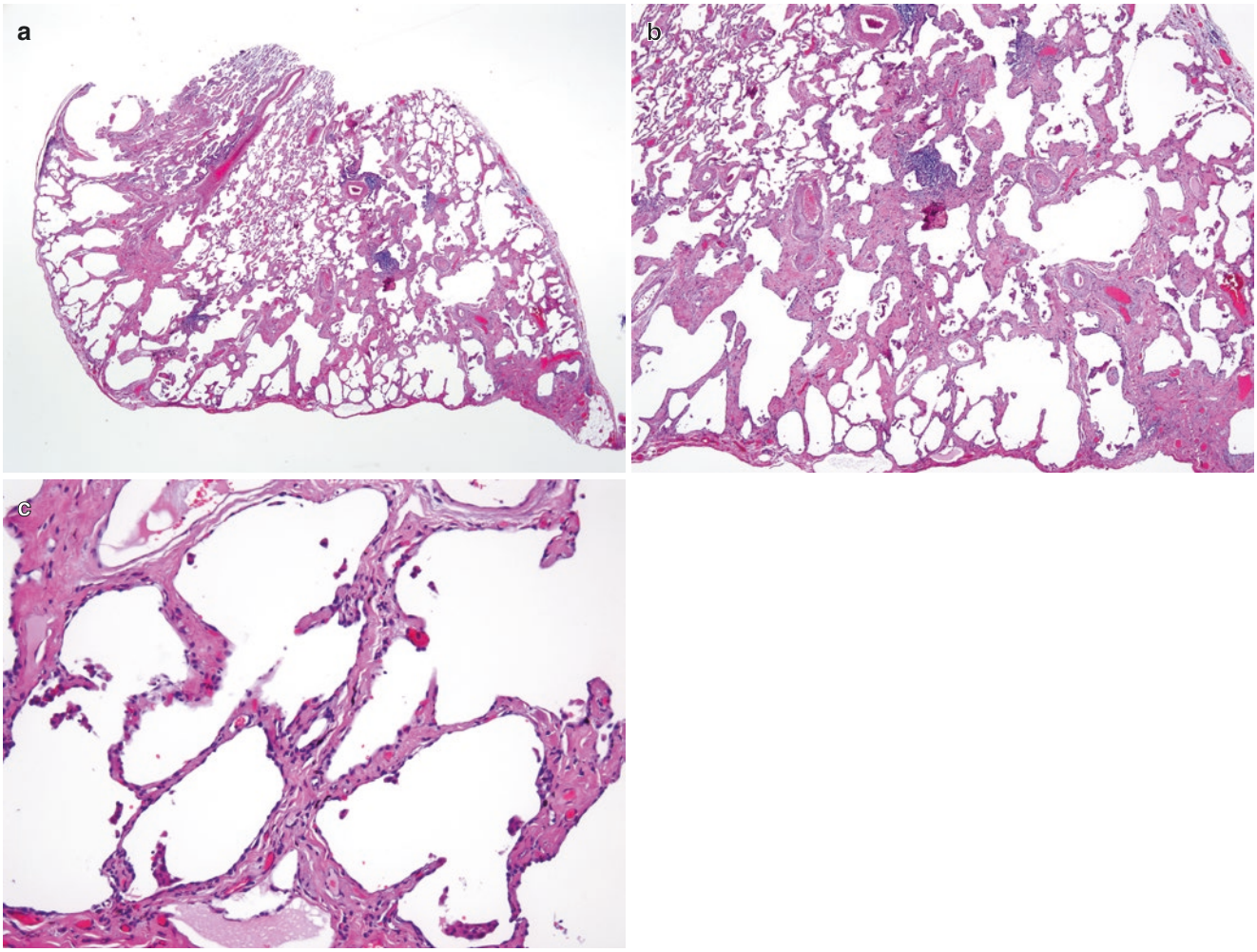

Fig. 6.44 Smoking-related interstitial fibrosis (SRIF). (**a**) Low-magnification photomicrograph showing patchy areas of lung parenchyma with thickened septa. The fibrosis involves the subpleural and centrilobular parenchyma with abrupt demarcation from uninvolved lung parenchyma. (**b**) At intermediate magnification, the involved areas show interstitial thickening by hyalinized collagen fibrosis with minimal inflammation. The alveolar spaces are enlarged and distorted. (**c**) High-magnification view of the thickened alveolar septa with hyalinized collagen bundles. No significant inflammation is present

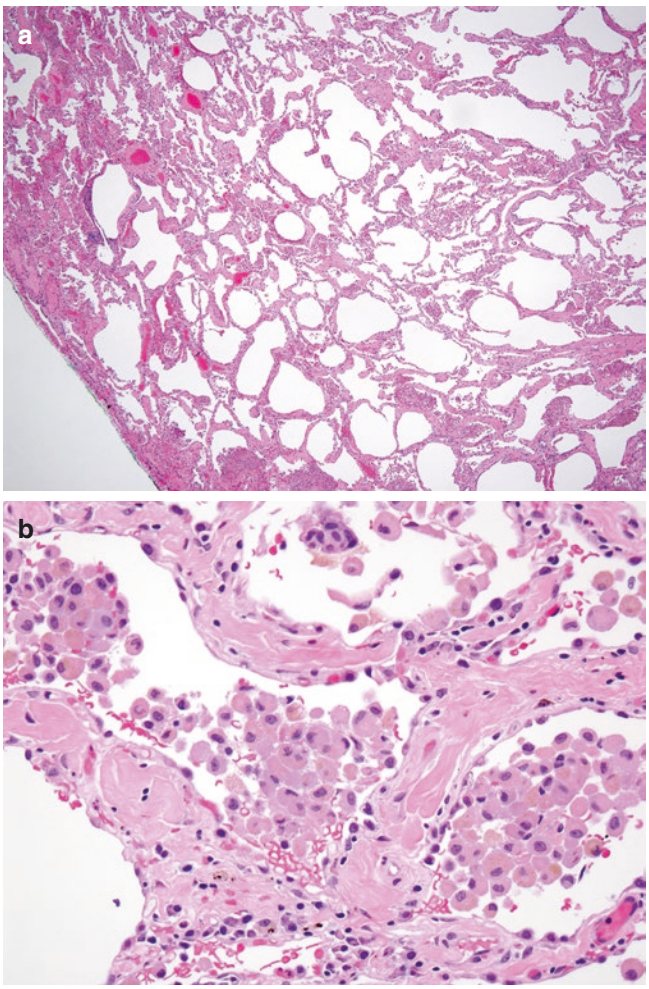

Fig. 6.45 SRIF with respiratory bronchiolitis. (**a**) At low magnification, alveolar septa are thickened, and some alveolar spaces are filled with pigmented macrophages. (**b**) High-magnification view showing alveolar septa thickened with hyalinized collagen bundles. Note the pigmented smokers' macrophages within the alveolar spaces

Desquamative Interstitial Pneumonia (DIP)

DIP, similar to RB, is also characterized by accumulation of pigmented smoker's macrophages within air spaces. Unlike RB, the changes are not limited to peribronchiolar parenchyma but instead diffusely affect air spaces with an associated interstitial pneumonia (Figs. 6.46, 6.47, 6.48 and 6.49). Ground-glass opacities and centrilobular nodules are common findings on chest CT scan. The prognosis is good in most cases.

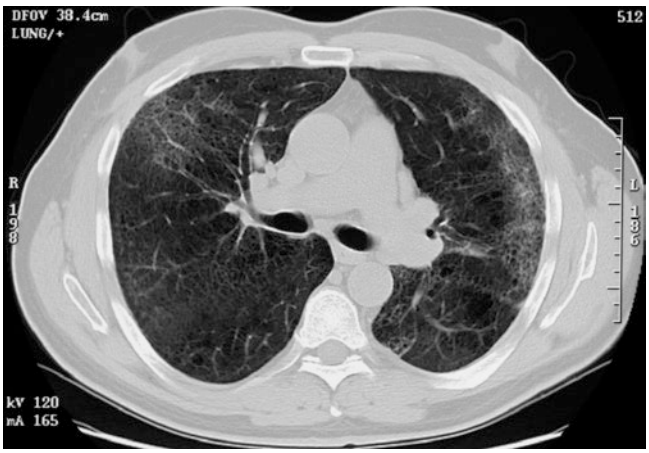

Fig. 6.46 Chest CT scan image of a patient with desquamative interstitial pneumonia (DIP). Patchy ground-glass opacities and emphysematous changes are commonly described. No significant fibrosis is noted, as evidenced by traction bronchiectasis and/or honeycomb change

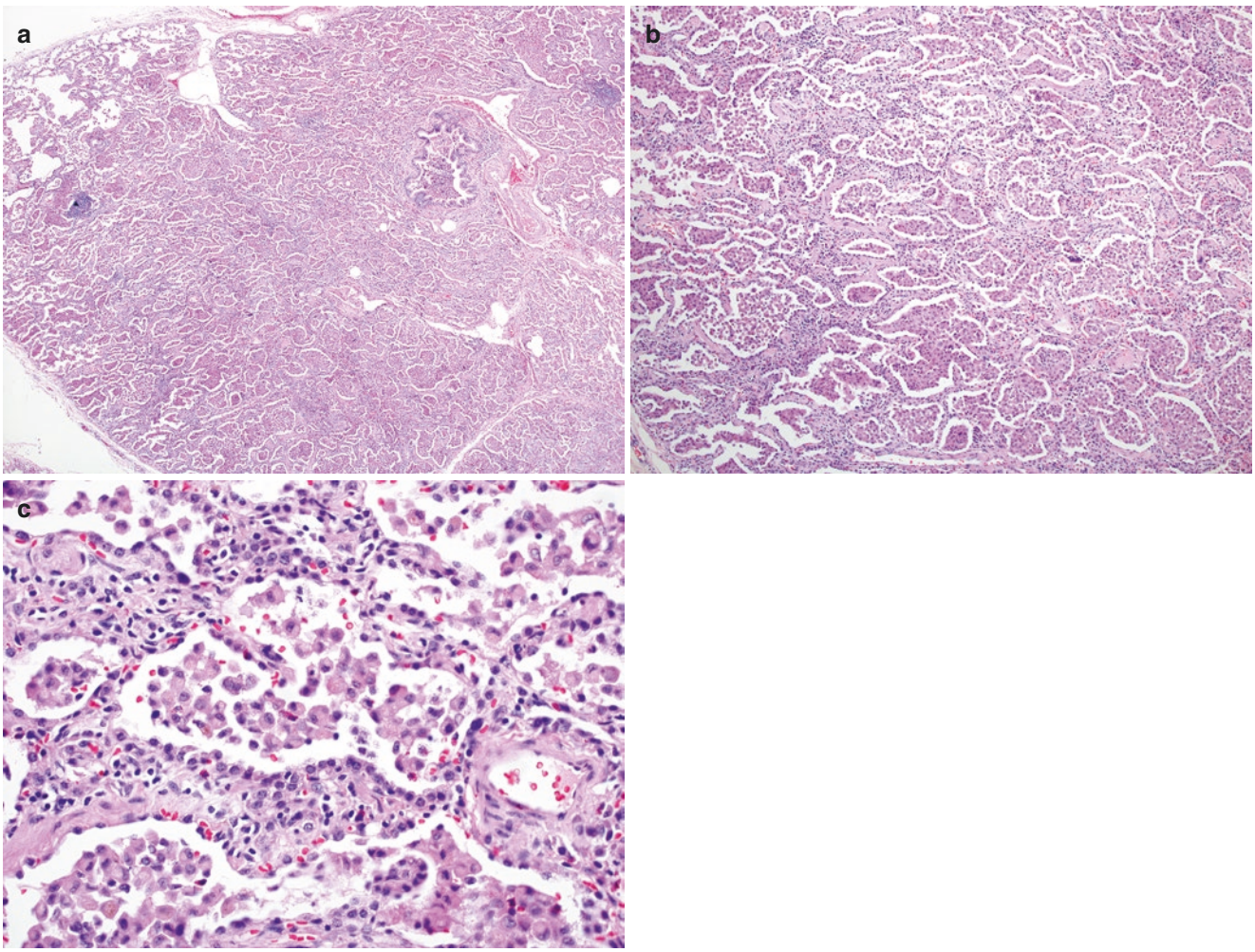

Fig. 6.47 DIP. (**a**) At low magnification, air spaces are diffusely filled by numerous pigmented macrophages. (**b**) Intermediate-magnification view showing intra-alveolar accumulation of pigmented macrophages with preserved alveolar structure and mildly thickened alveolar septa. (**c**) High-magnification photomicrograph demonstrating macrophages with light brown cytoplasmic pigment within the air spaces. The alveolar septa are expanded by chronic inflammation without the paucicellular hyalinized collagen typical of SRIF, and they are lined by reactive pneumocytes

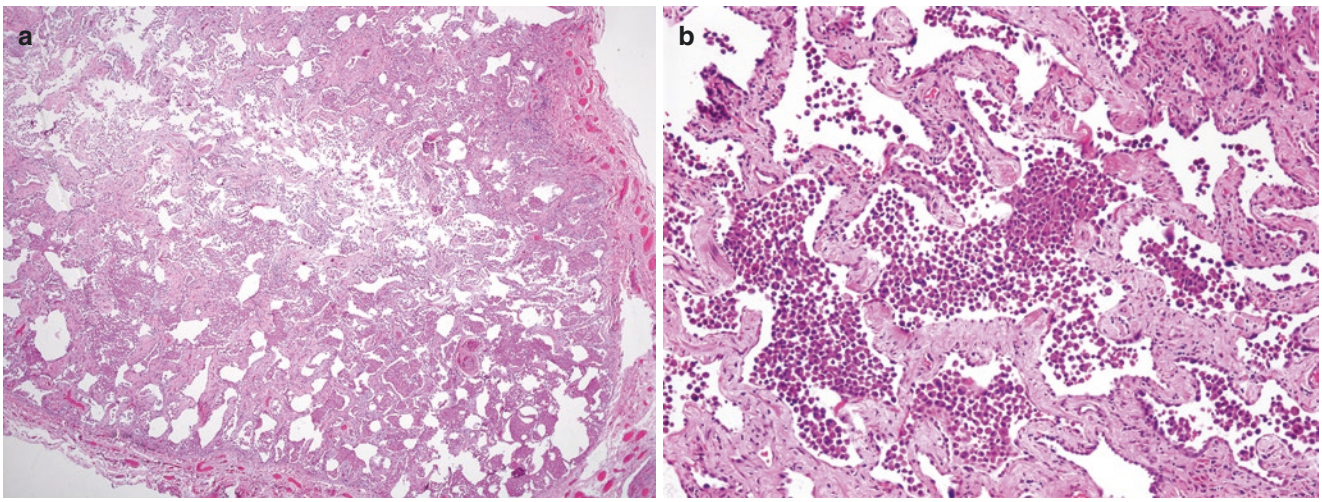

Fig. 6.48 Changes resembling DIP in smoking-related interstitial fibrosis (SRIF). (**a**) At low magnification, there is diffuse air space filling of pigmented macrophages. The alveolar architecture is preserved, but the alveolar septa are markedly thickened. (**b**) High-magnification view showing the typical pigmented macrophages filling up the air spaces and alveolar septa thickened with hyalinized collagen fibrosis

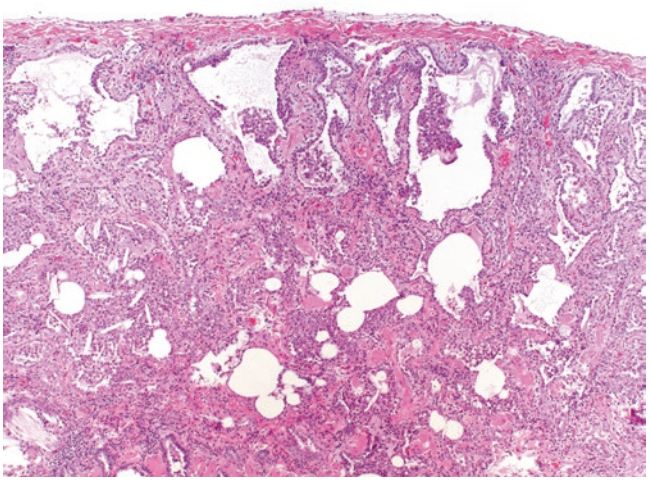

Fig. 6.49 DIP with emphysema. In addition to the typical pigmented macrophages filling up air spaces, there are also air space enlargement and concomitant interstitial pneumonia that include mild fibrosis

Langerhans Cell Histiocytosis (LCH)

LCH, formerly known as eosinophilic granuloma, is characterized by nodular bronchiolocentric infiltrates of Langerhans cells admixed with variable numbers of eosinophils and pigmented macrophages (Figs. 6.50, 6.51, 6.52, 6.53, 6.54, 6.55, 6.56 and 6.57). Some nodules may undergo central cystic changes. More commonly a distinctive pattern of paracicatricial air space enlargement (scar emphysema) accounts for the upper lobe predominant cysts and spiculated nodules that characterize radiologic findings on thoracic CT scans. In some patients fibrosis replaces the cellular infiltrate, forming a stellate-shaped scar as the only clue to the diagnosis of LCH. Definitive diagnosis of LCH requires identification of the Langerhans cell clusters and can often be made after careful examination of the rest of the specimen. LCH occurs exclusively in smokers. Coexisting smoking-related conditions such as RB, SRIF, and DIP-like changes are commonly present. Increased peribronchiolar Langerhans cells are commonly seen in smokers and are not indicative of LCH in the absence of expansile nodules. The prognosis of LCH is generally good. Many patients recover completely after quitting smoking. Identification of v-raf murine sarcoma viral oncogene homolog B1 (BRAF) mutations in a subset of patients has sparked interest in targeted therapies for those patients in whom smoking cessation alone may be insufficient. Pulmonary hypertension can occur in patients with fibrotic disease. Smoking-related comorbidities such as emphysema may also negatively impact overall prognosis.

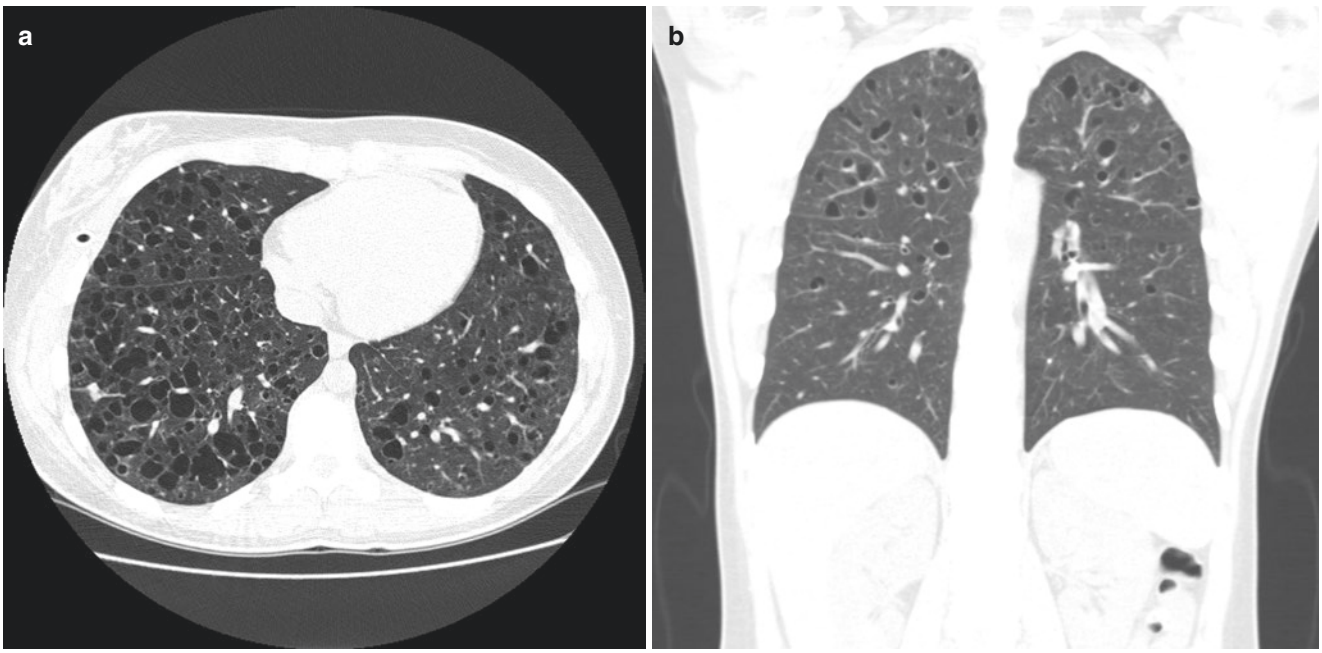

Fig. 6.50 Chest CT scan images of a patient with Langerhans cell histiocytosis (LCH). (**a**) A horizontal cross section of the chest showing numerous cysts and nodular densities. (**b**) A coronal cross section showing that the cystic and nodular lesions are predominantly within the upper lobes of the lung

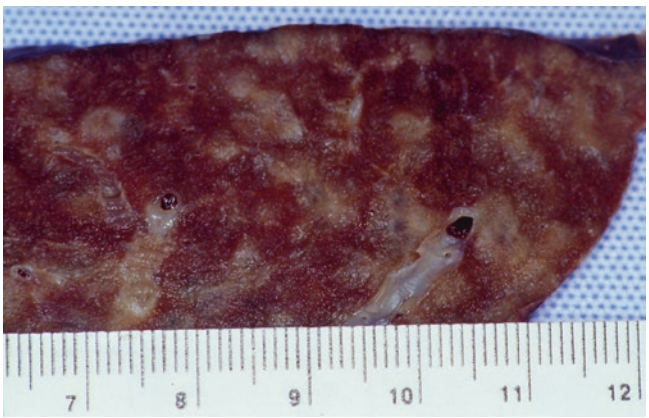

Fig. 6.51 LCH. Gross image of a lung wedge biopsy from a patient with early-stage LCH showing multiple tan-white centrilobular nodules on the cut surface

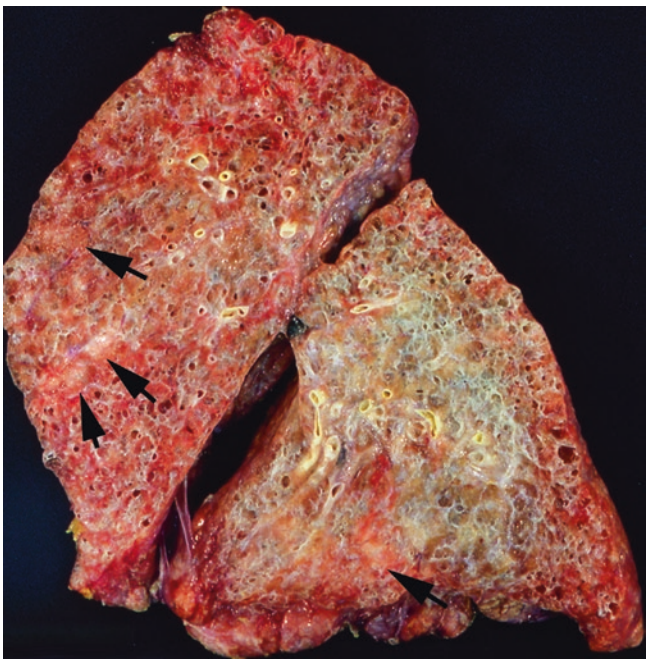

Fig. 6.52 LCH. Gross image of an explanted lung from a patient with late-stage LCH. Numerous cysts and tan-white nodules (arrows) are seen on the cut surface

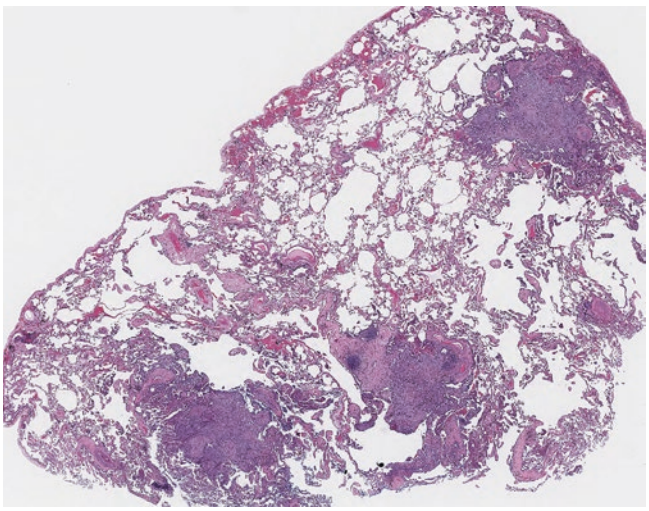

Fig. 6.53 LCH. Low-magnification photomicrograph showing multiple cellular, stellate nodules within the lung. Note the background lung parenchyma with emphysematous change and respiratory bronchiolitis

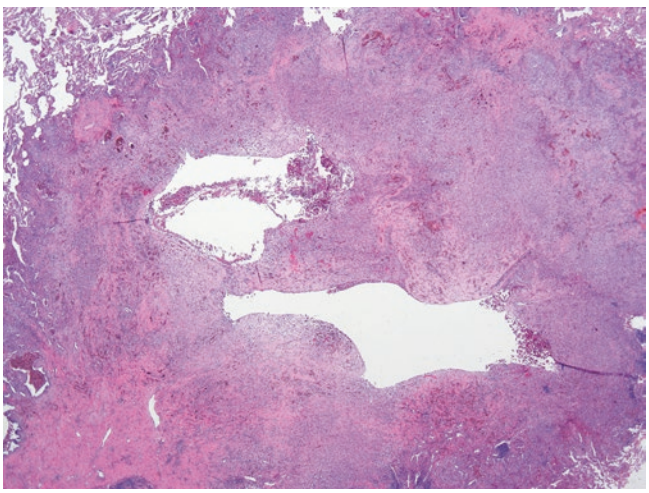

Fig. 6.54 LCH. Low-magnification view of a centrally cystic nodule from a patient with LCH. The central cyst represents the ectatic lumen of the affected airway, which is surrounded by a polymorphic infiltrate in which there are numerous Langerhans cells resulting in a vaguely granulomatous appearance

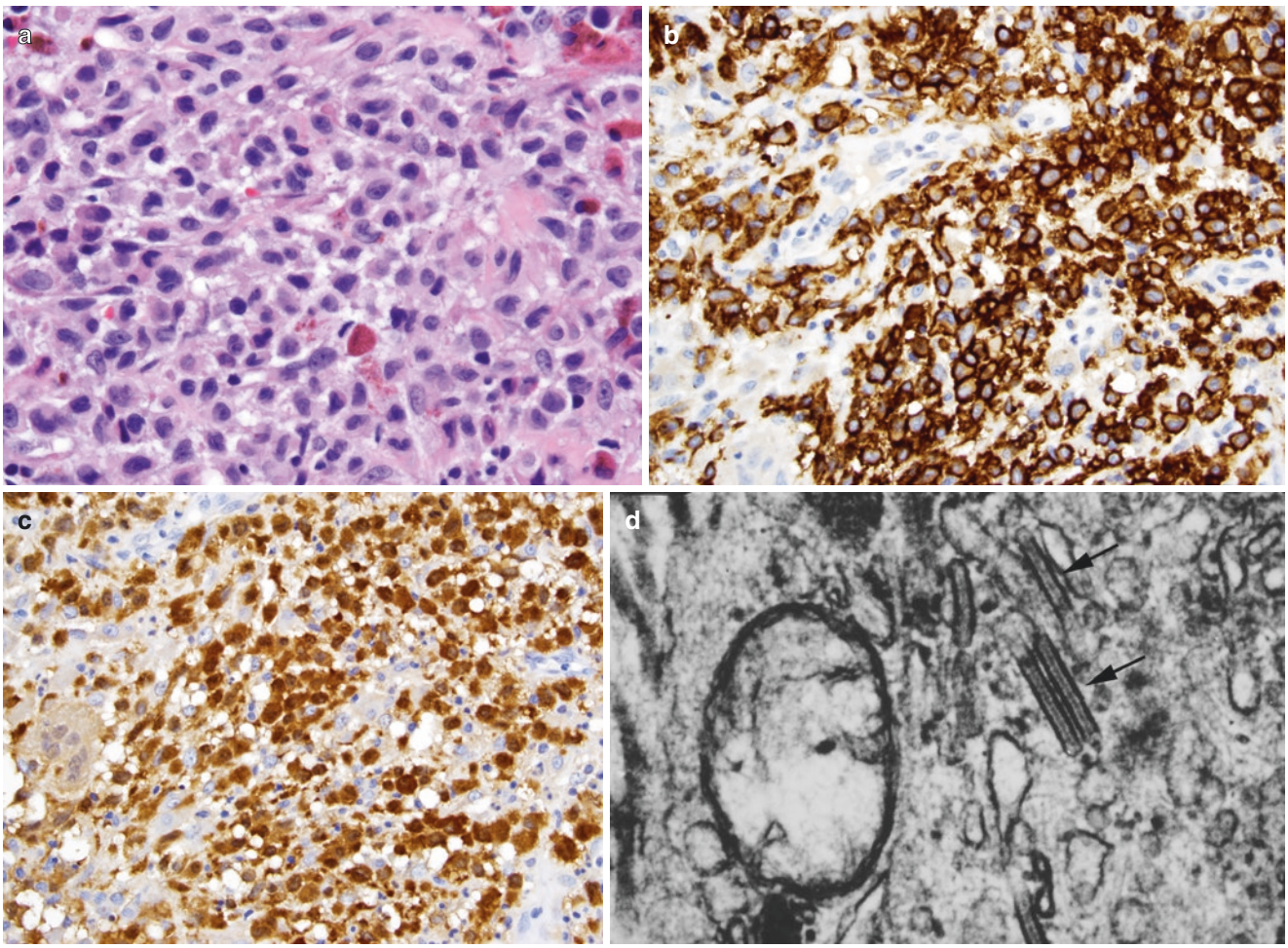

Fig. 6.55 LCH. (**a**) High-magnification view of Langerhans cells within the nodule illustrated in Fig. 6.54, mononuclear cells with folded or kidney bean-shaped nuclei, and abundant eosinophilic cytoplasm. (**b**) Immunohistochemical stain for CD1a shows positive membranous staining in Langerhans cells. (**c**) Immunohistochemical stain for S-100 shows positive nuclear and cytoplasmic staining in Langerhans cells. (**d**) Electron microscopy image of a Langerhans cell with intracytoplasmic rod-shaped Birbeck granules (*arrows*)

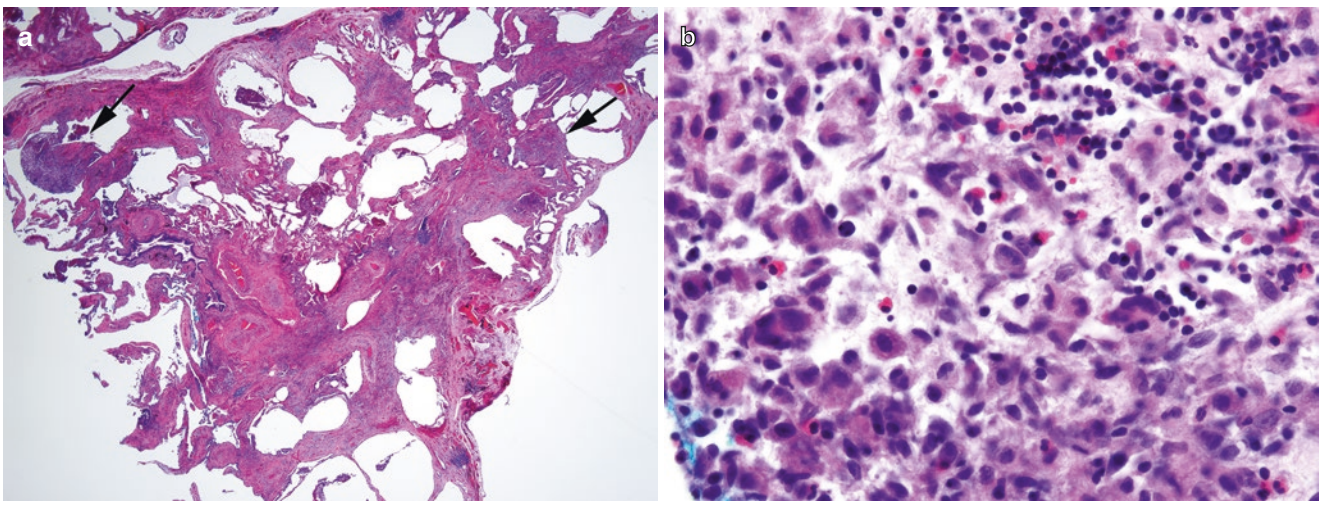

Fig. 6.56 LCH. (**a**) In this example, the lesion is almost completely replaced by fibrosis, forming a stellate-shaped scar with scar emphysema. At the periphery of the lesion, there are smaller clusters of cellular infiltrates (*arrows*). (**b**) High-magnification view of the cellular focus demonstrating typical Langerhans cells with folded or kidney bean-shaped nuclei and admixed eosinophils and lymphocytes

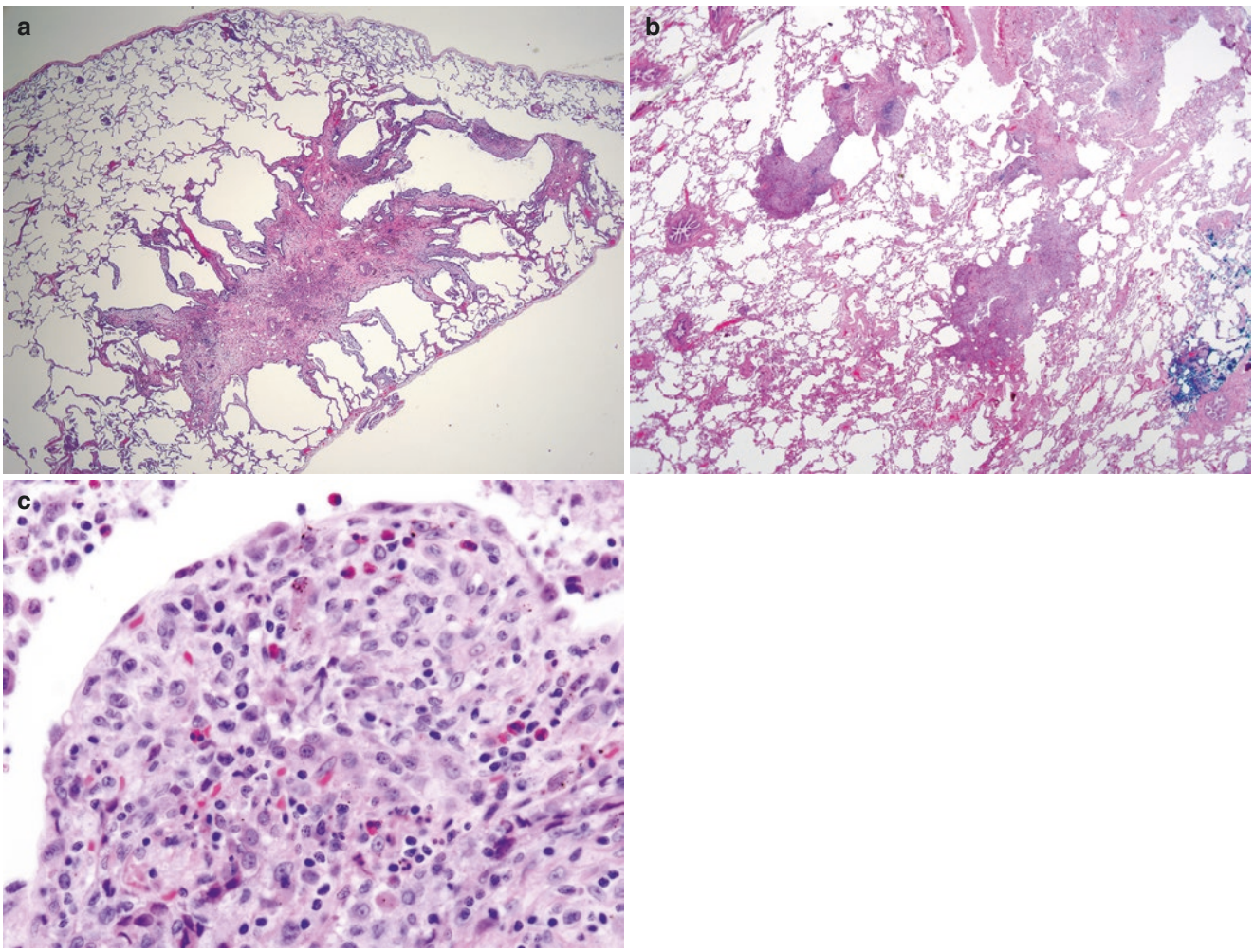

Fig. 6.57 LCH. (**a**) A stellate-shaped scar with the characteristic pattern of associated scar emphysema. Nonspecific chronic inflammatory cells and pigmented macrophages are present. This finding suggests LCH and should trigger careful examination for cellular lesion diagnostic of LCH. (**b**) Another low-magnification field from the same specimen shows two cellular nodules. (**c**) High-magnification view of one of the nodules illustrated in part **b** demonstrating numerous Langerhans cells admixed with scattered eosinophils and pigmented macrophages

Idiopathic Interstitial Pneumonias

Histopathologic classification of idiopathic interstitial pneumonias is useful in separating them into distinct clinical categories. In 2002 and again in 2013, an international committee, supported by the American Thoracic Society and the European Respiratory Society, proposed a classification scheme based primarily on expert opinion and influenced management strategies, study design for clinical trials, and research opportunities to challenge areas in which evidence was weak.

Usual Interstitial Pneumonia (UIP)

UIP (Figs. 6.58, 6.59, 6.60, 6.61, 6.62, 6.63, 6.64, 6.65, 6.66, 6.67, 6.68, 6.69, 6.70, 6.71, 6.72, 6.73, 6.74 and 6.75) is the most common of the idiopathic interstitial pneumonias, accounting for about two thirds of biopsied patients. An American Thoracic Society (ATS) consensus statement published in 2000 linked UIP to idiopathic pulmonary fibrosis (IPF) by defining the latter as a specific form of chronic fibrosing interstitial pneumonia limited to the lung and associated with the histologic appearance of UIP on surgical (thoracoscopic or open) lung biopsy. This definition was revised in 2011 to include HRCT as an important diagnostic tool capable of identifying UIP in a minority of patients, thus obviating the need for lung biopsy. As this definition implies, UIP and IPF are roughly interchangeable terms, the exceptions being those patients with underlying systemic illnesses or occupational exposures that may suggest an etiology for their lung disease (e.g., asbestosis). IPF is a disease of middle-aged to older adults and is more common in men than in women. It is a progressive disease, with an average survival of 2–6 years after diagnosis. Some antifibrotic agents have been shown to slow disease progression; lung transplantation is the only viable treatment for patients with late-stage disease. Clinical diagnosis of IPF is often made based on typical clinical and radiologic findings; however, in patients with atypical clinical and radiologic presentations, lung biopsy is the only way to establish the diagnosis and to qualify the patients for transplantation and/or clinical trials. Atypical clinical presentations of UIP/IPF are sometimes caused by coexisting air space or interstitial diseases such as emphysema, smoking-related diseases, eosinophilic pneumonia, and malignancies.

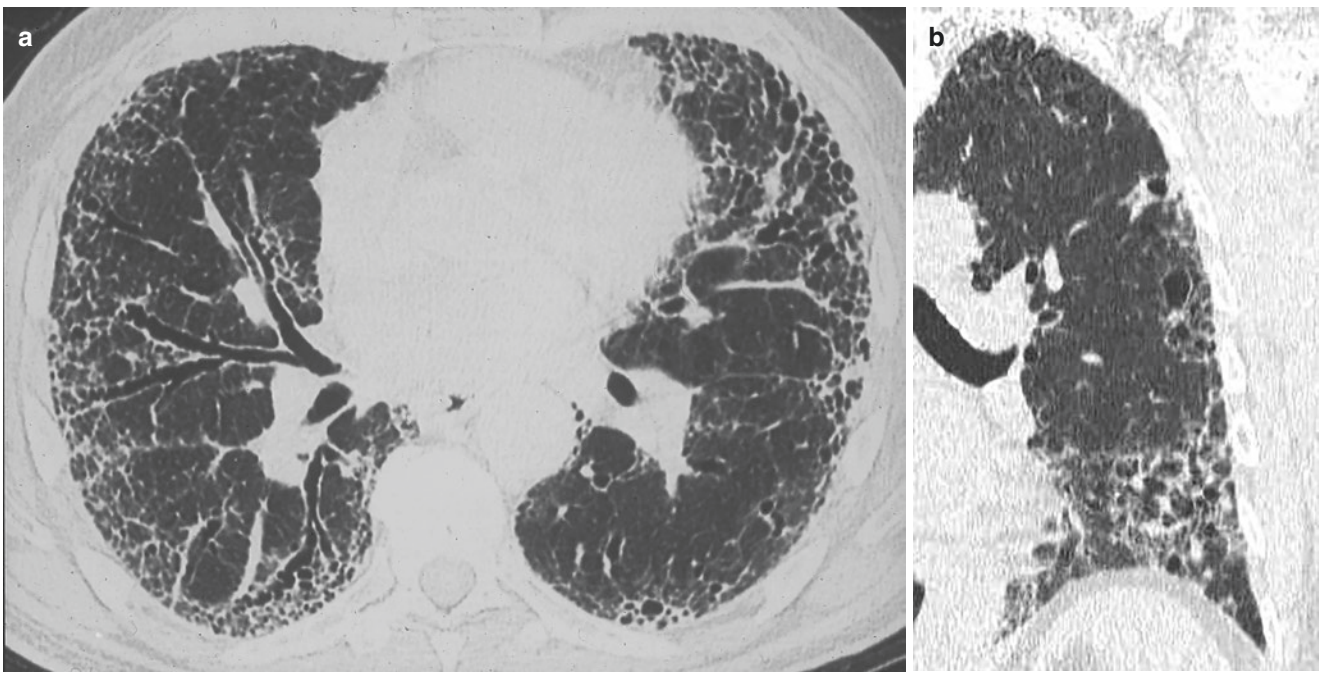

Fig. 6.58 UIP. High-resolution CT scan of the chest of a patient with UIP. (**a**) A horizontal cross-sectional image showing the typical findings of UIP: bilateral reticular marking with traction bronchiectasis and honeycomb change, more severe in the periphery. (**b**) A coronal cross-sectional image demonstrating the basilar predominant distribution of the lesions

Fig. 6.59 UIP. Gross photograph of an autopsy showing the right lung from a patient with end-stage UIP. The entire lung is smaller than normal, with diffuse scarring and subpleural honeycomb change that is more severe in the base

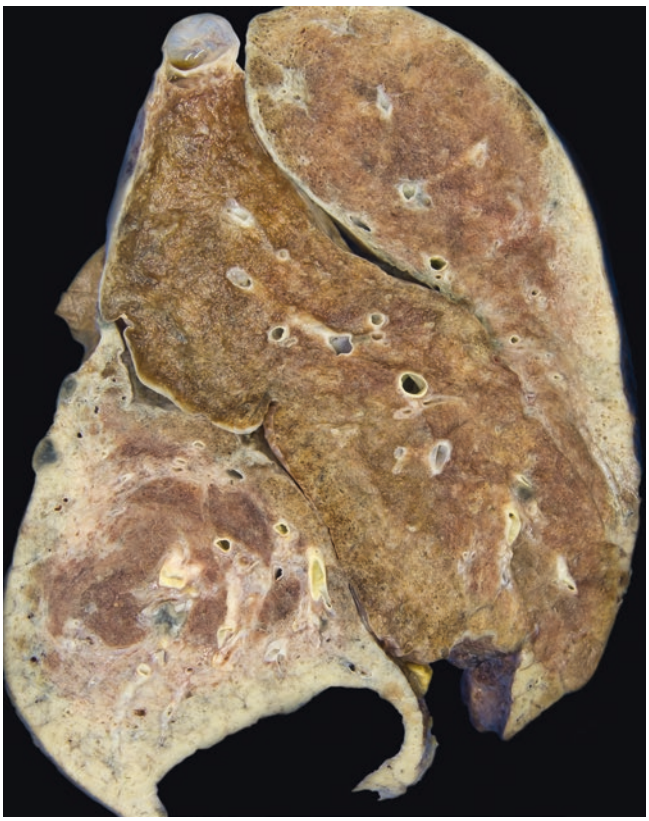

Fig. 6.60 UIP. In this explanted right lung, dense scarring and honeycomb changes are mainly seen in the shrunken lower lobe and the periphery of upper lobe

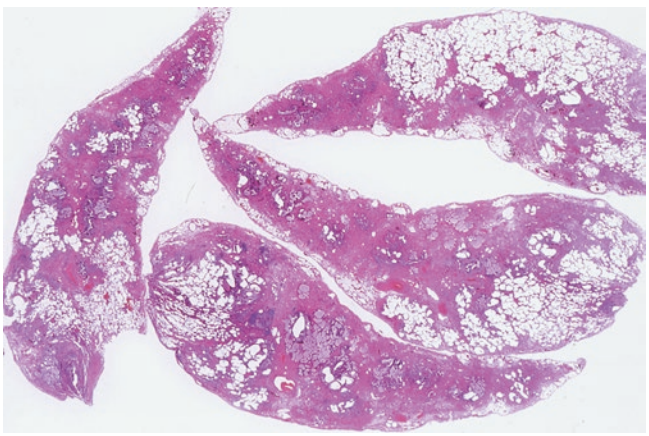

Fig. 6.61 UIP. Whole-mount sections of a lung wedge biopsy showing dense scarring and cystic changes are distributed in a patchwork pattern with peripheral accentuation (geographic or spatial heterogeneity). Areas of fibrosis completely efface the alveolar lung architecture and are juxtaposed with less affected or nearly normal lung parenchyma

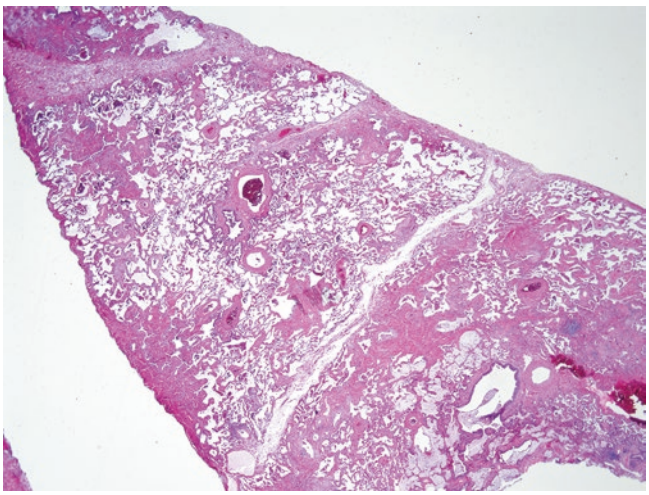

Fig. 6.62 UIP. Low-magnification photomicrograph of a surgical lung biopsy showing the typical patchwork and random distribution of collagen fibrosis that effaces the alveolar structure (architectural distortion). Less affected and nearly normal lung parenchyma is present between the areas of more severe fibrosis. Honeycomb change, architectural distortion in the form of cystic spaces containing mucus, is present at the upper left and lower right

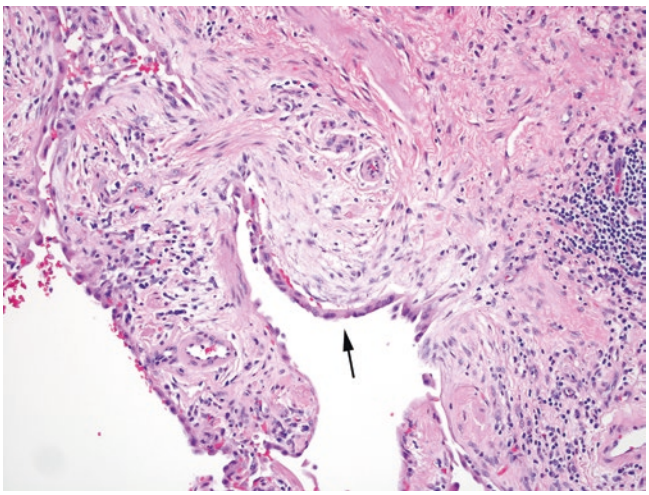

Fig. 6.64 UIP. Temporal heterogeneity, an important feature that is necessary for the diagnosis of UIP, is demonstrated in this intermediate-magnification photomicrograph. The fibrosis is composed of a mixture of newer active fibrosis in the form of a fibroblast focus (arrow) and older collagenous scar (right upper)

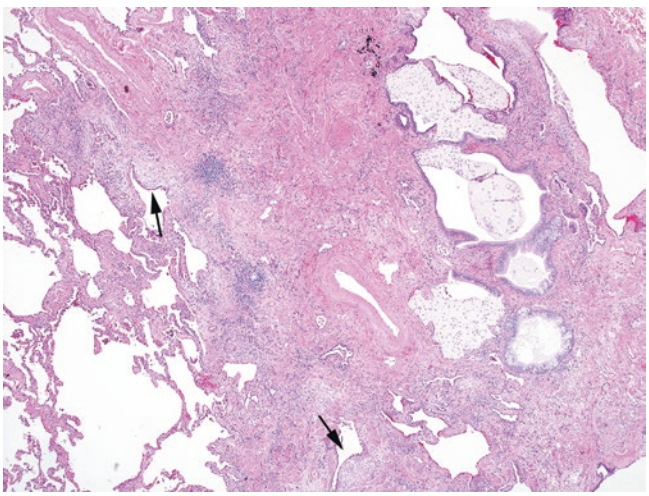

Fig. 6.63 UIP. Intermediate-magnification view of an area with significant architectural distortion caused by a dense collage scar (middle) and honeycomb change (right). A small amount of nearly normal lung parenchyma is seen in the lower left. Fibroblast foci (arrows) are visible at this magnification

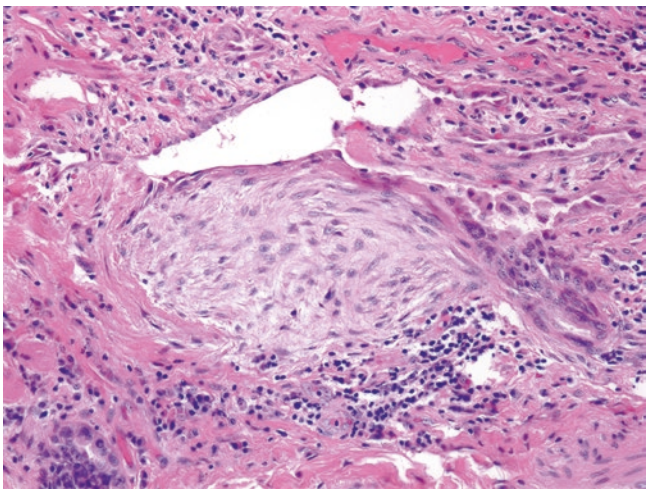

Fig. 6.65 UIP. High-magnification view of a fibroblast focus that is composed of plump spindle-shaped fibroblasts and myofibroblasts arranged in parallel within a lightly stained myxoid stroma. The luminal surface is covered with a layer of flattened pneumocytes and is sitting immediately on a bed of dense collagen fibrosis

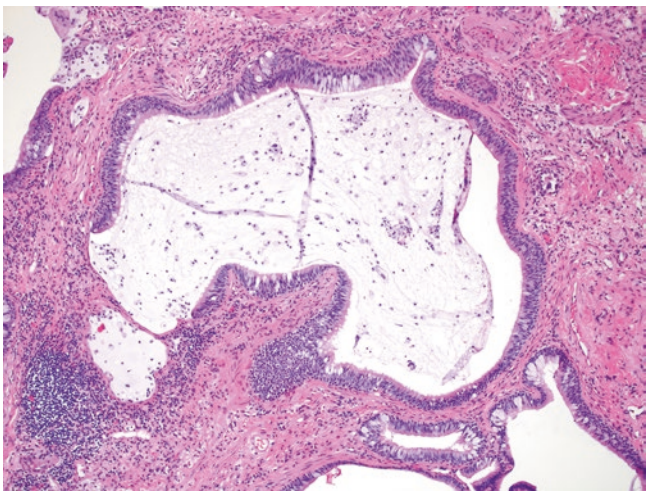

Fig. 6.66 UIP. High-magnification view of an area with honeycomb change. Multiple enlarged air spaces lined by ciliated respiratory epithelium are seen within a background of dense collagen fibrosis and chronic inflammation. There are mucin and mucin-containing macrophages within the enlarged air spaces

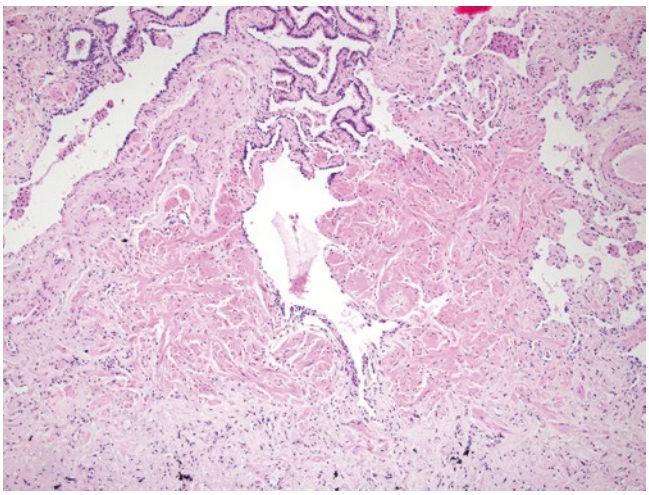

Fig. 6.68 UIP. Bundles of hyperplastic smooth muscles are admixed with collagen scars in an area of honeycomb change. The term muscular cirrhosis was used historically to convey prominent smooth muscle hyperplasia often affiliated with cobble stoning of the pleural surface

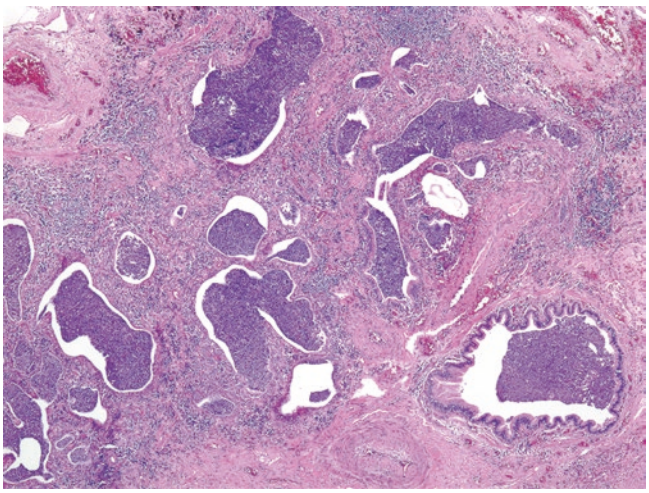

Fig. 6.67 UIP. Honeycomb areas are commonly associated with acute and chronic inflammation. Dense inflammatory infiltrates are present in the enlarged air spaces as well as the interstitium and an adjacent bronchiolar lumen (lower right)

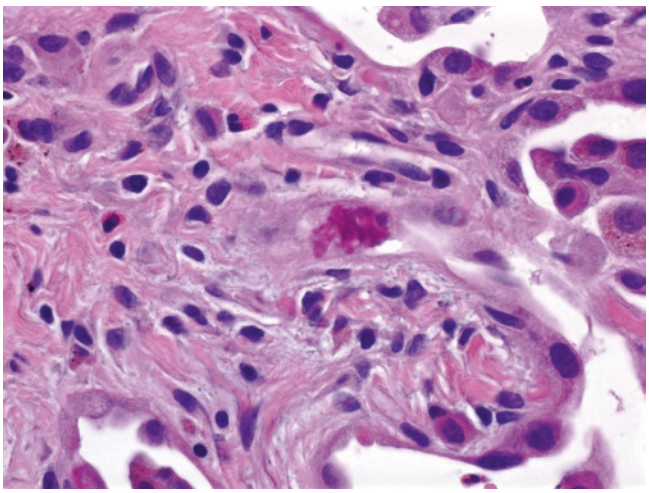

Fig. 6.69 UIP. High-magnification photomicrograph showing alveolar pneumocyte hyperplasia and amorphous eosinophilic material (Mallory hyaline) within the cytoplasm of a hyperplastic pneumocyte. Mallory hyaline is a common finding in UIP, but it is not specific and has no known clinical significance

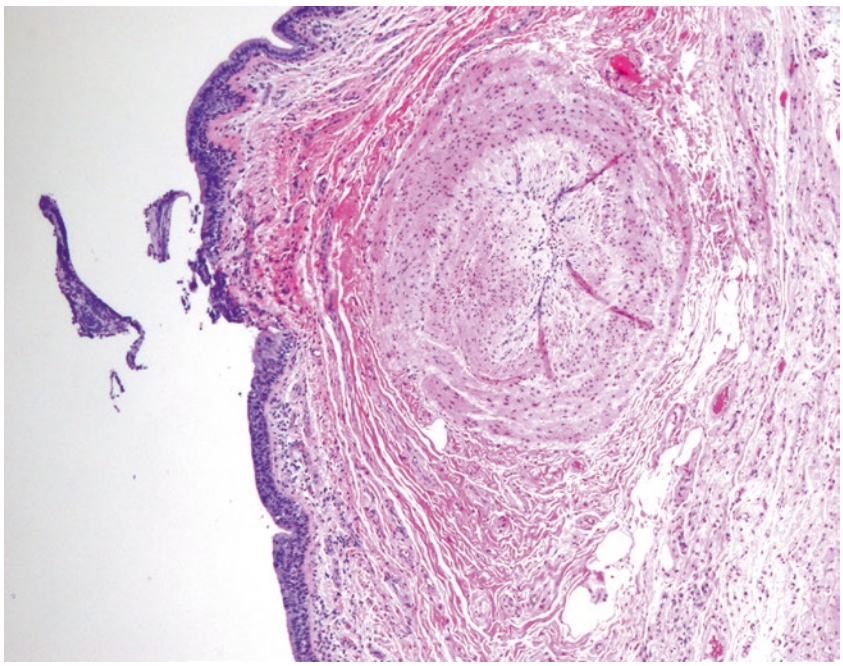

Fig. 6.70 Vascular changes in UIP. Hypertensive changes of small muscular pulmonary arteries characterized by intimal and medial hypertrophy are commonly seen associated with honeycomb changes. If the vascular hypertensive changes are prominent away from the honeycombing area, underlying collagen vascular disease such as scleroderma should be considered

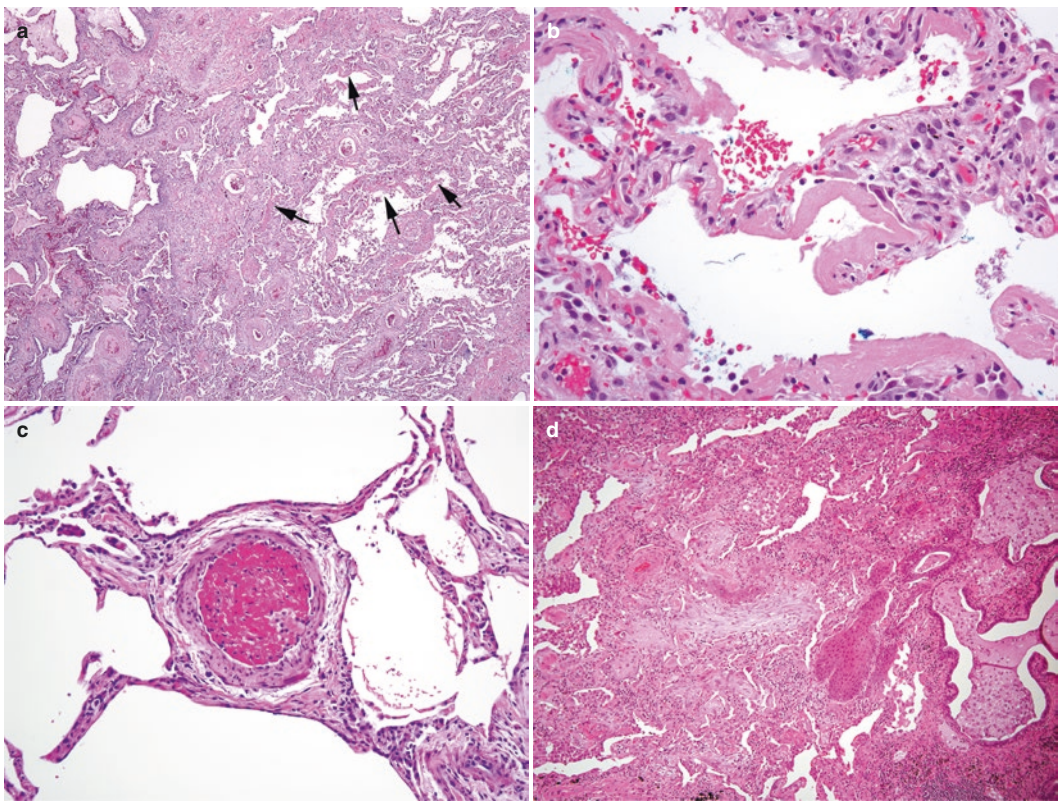

Fig. 6.71 UIP with diffuse alveolar damage (DAD) (acute exacerbation of idiopathic pulmonary fibrosis). (**a**) Low-magnification view showing patchy fibrosis and honeycomb change in the upper left. The nonfibrotic lung parenchyma on the right shows frequent hyaline membranes (arrows). (**b**) High-magnification view of the hyaline membranes, an eosinophilic membranous material lining alveolar septa. Pneumocyte hyperplasia with prominent reactive atypia is also present. (**c**) Fibrin thrombi within small arteries and arterioles are a common but nonspecific finding in DAD. (**d**) Bronchiolar squamous metaplasia is another common but nonspecific finding in DAD. Also present are changes of late organizing DAD, polypoid intraluminal proliferation of fibroblasts, and myofibroblasts mimicking organizing pneumonia

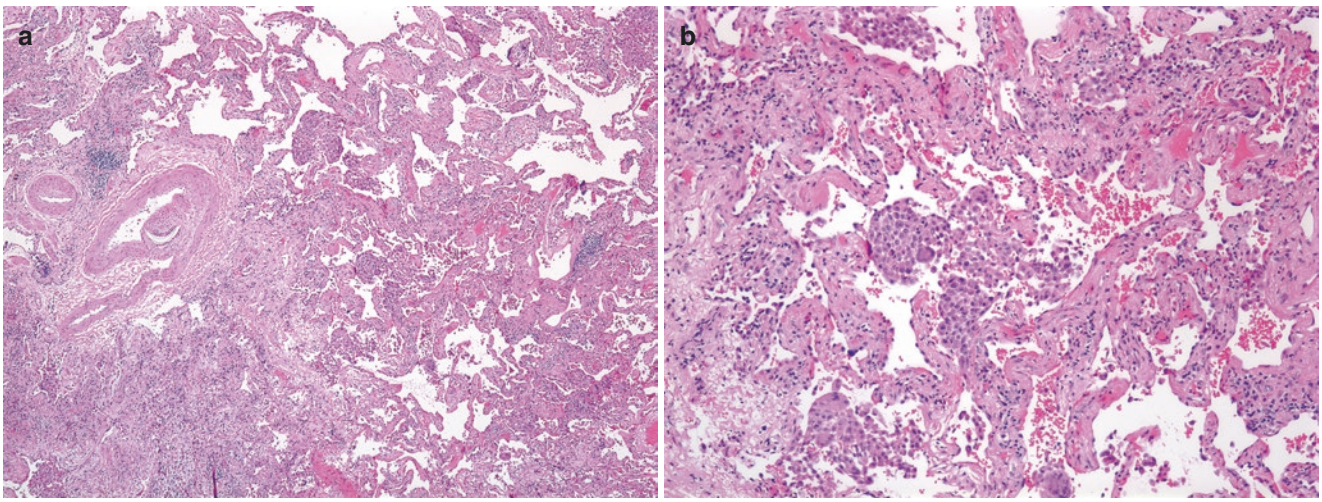

Fig. 6.72 UIP with DIP-like changes. (**a**) Low-magnification photomicrograph showing the patchwork fibrosis typical of UIP. Note the dense scarring on the lower left and relatively nonfibrotic lung parenchyma on the right. (**b**) High-magnification view of the relatively nonfibrotic lung parenchyma demonstrating the accumulation of pigmented macrophages (smoker's macrophages) within the alveolar spaces, closely mimicking the appearance of DIP

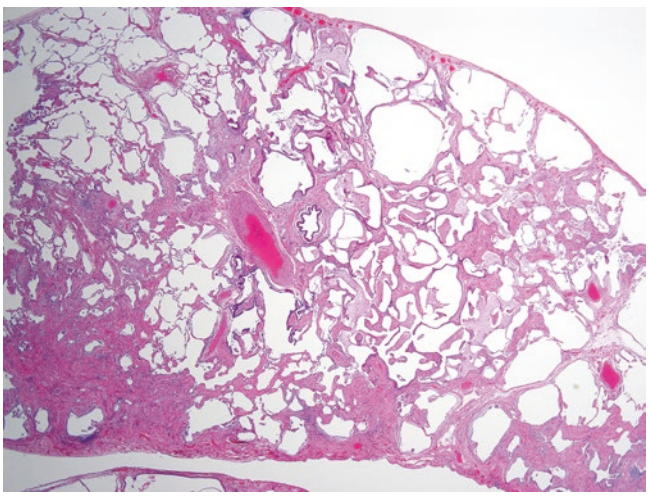

Fig. 6.73 UIP with coexisting emphysema. Low-magnification photomicrograph showing the patchwork fibrosis (lower left and lower right) and honeycomb change (upper middle and lower right) typical of UIP. The nonfibrotic lung parenchyma demonstrates emphysematous changes, including enlarged air spaces, and thinned, fragmented alveolar septa

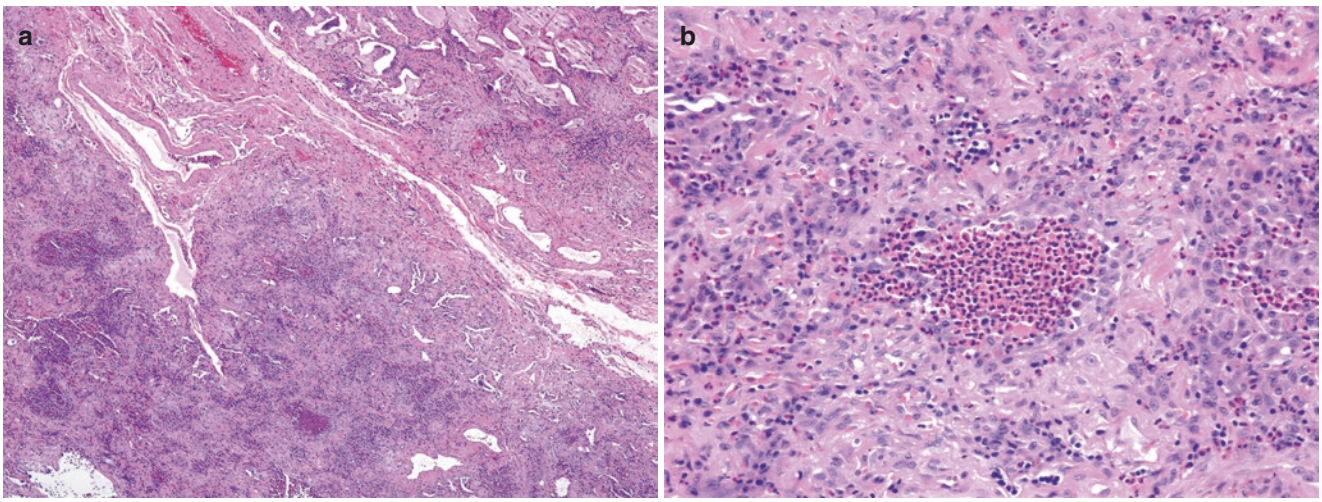

Fig. 6.74 UIP with coexisting eosinophilic pneumonia. (**a**) Low-magnification photomicrograph showing end-stage fibrosis and honeycomb change (upper right), typical of UIP. The residual air spaces are filled up with cellular infiltrates. (**b**) Higher-magnification view of the cellular air space infiltrates composed entirely of eosinophils

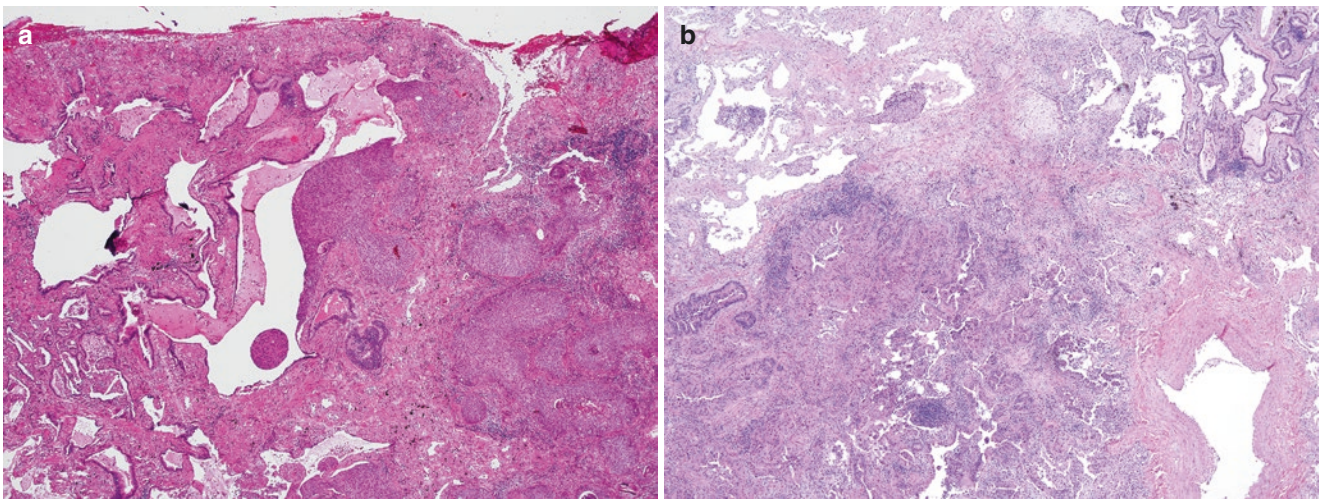

Fig. 6.75 UIP with coexisting carcinoma. (**a**) End-stage fibrotic lung with honeycomb change (left) and squamous cell carcinoma (right). (**b**) Honeycomb change and fibroblast foci typical of UIP (right upper) with coexisting adenocarcinoma in the lower left

Nonspecific Interstitial Pneumonia (NSIP)

NSIP (Figs. 6.76, 6.77, 6.78, 6.79, 6.79, 6.80 and 6.81) is the second most common form of idiopathic interstitial pneumonia. There are two histologic variants: cellular NSIP and fibrotic NSIP. The latter variant is more common and carries a worse prognosis. In addition to the clinical entity of idiopathic NSIP, the same histopathologic findings can occur focally (NSIP-like changes) in patients with other forms of diffuse lung disease, including most importantly patients with UIP. Furthermore, patients in whom NSIP represents the primary pathologic abnormality may have specific associated conditions or etiologies such as connective tissue disease, hypersensitivity pneumonia, or drug-induced lung disease. For these reasons a surgical lung biopsy diagnosis of NSIP is necessary but insufficient to establish a diagnosis of idiopathic NSIP, which is always a multidisciplinary process of exclusion requiring knowledge of clinical and radiologic findings. Patients with carefully defined idiopathic NSIP tend to be younger, more likely to be female, and less likely to have a smoking history compared to patients with UIP/IPF. They also have a more favorable prognosis and may respond favorably to immunosuppressive therapy.

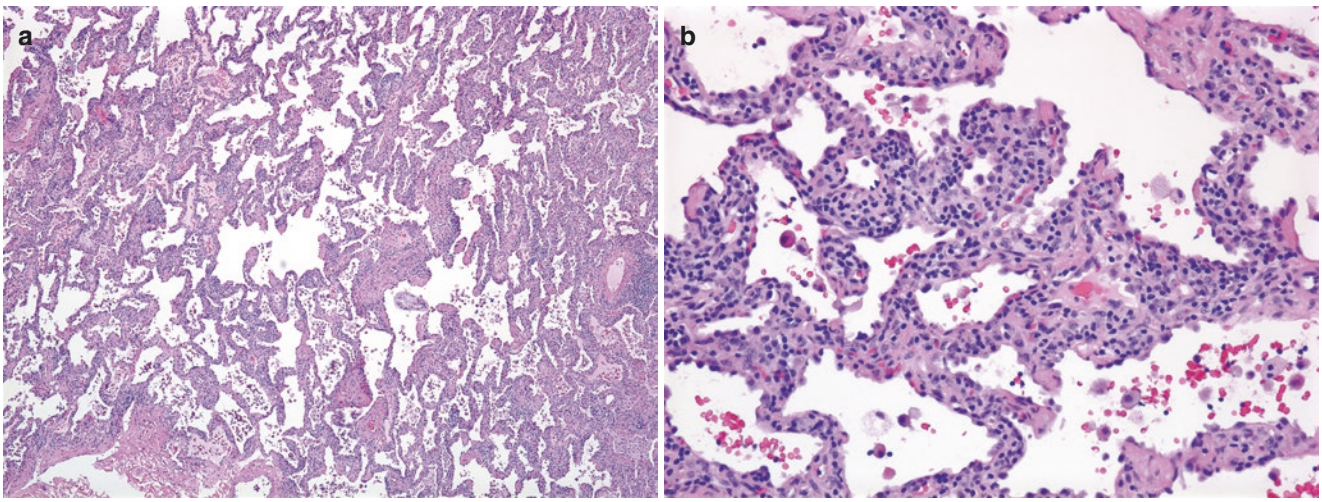

Fig. 6.76 NSIP. (**a**) Low-magnification photomicrograph showing uniform alveolar septal thickening by a cellular infiltrate. (**b**) At high magnification, the alveolar septa are thickened by a dense lymphoplasmacytic infiltrate. There is mild pneumocyte hyperplasia. No significant collagen deposition is present

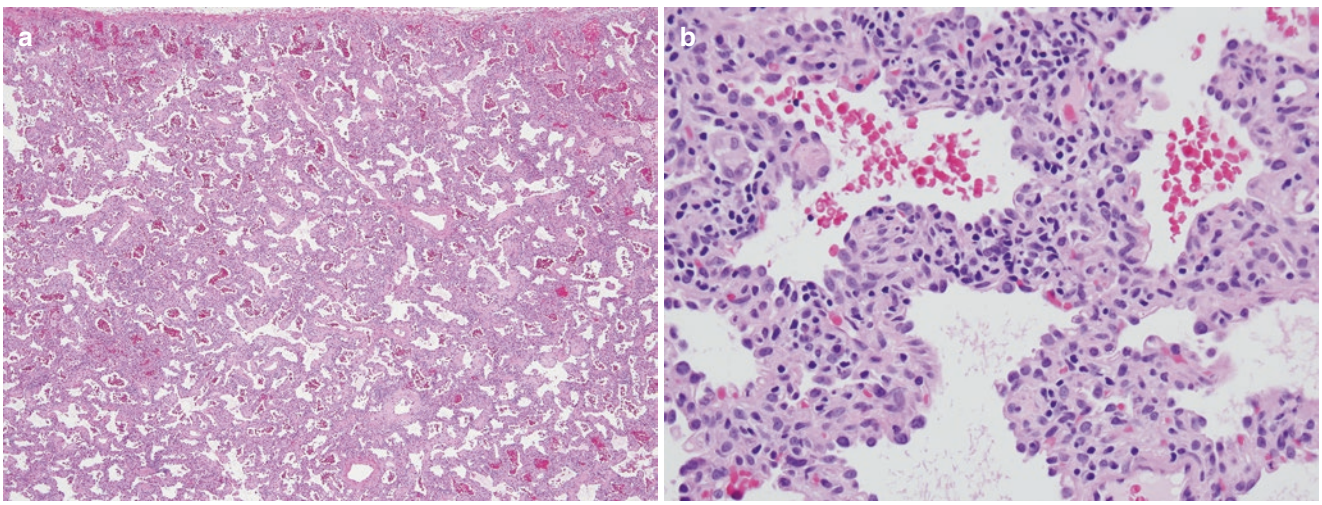

Fig. 6.77 Cellular NSIP. (**a**) At low magnification there is diffuse, uniform thickening of the alveolar septa. (**b**) In this example, the high-magnification view shows that the thickened alveolar septa contain lymphoplasmacytic infiltrates and minimal collagen deposition. Alveolar pneumocyte hyperplasia is also more prominent than the example in Fig. 6.76

Fig. 6.78 Fibrotic NSIP. Gross photograph of an explant lung with fibrotic NSIP. On a cut surface, the lung parenchyma is diffusely fibrotic, with no significant cystic or subpleural honeycomb change

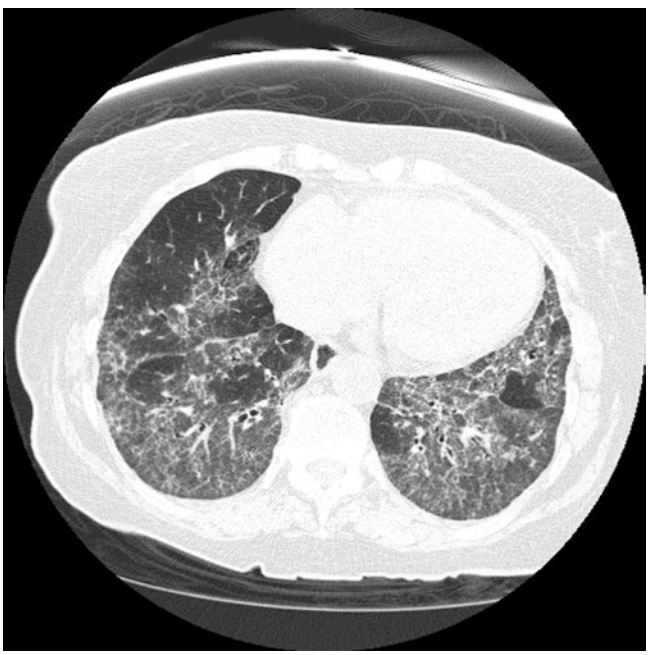

Fig. 6.79 Fibrotic NSIP. Chest CT scan of a patient with fibrotic NISP showing diffuse bilateral ground-glass opacities and interstitial reticular markings. No honeycomb change is present

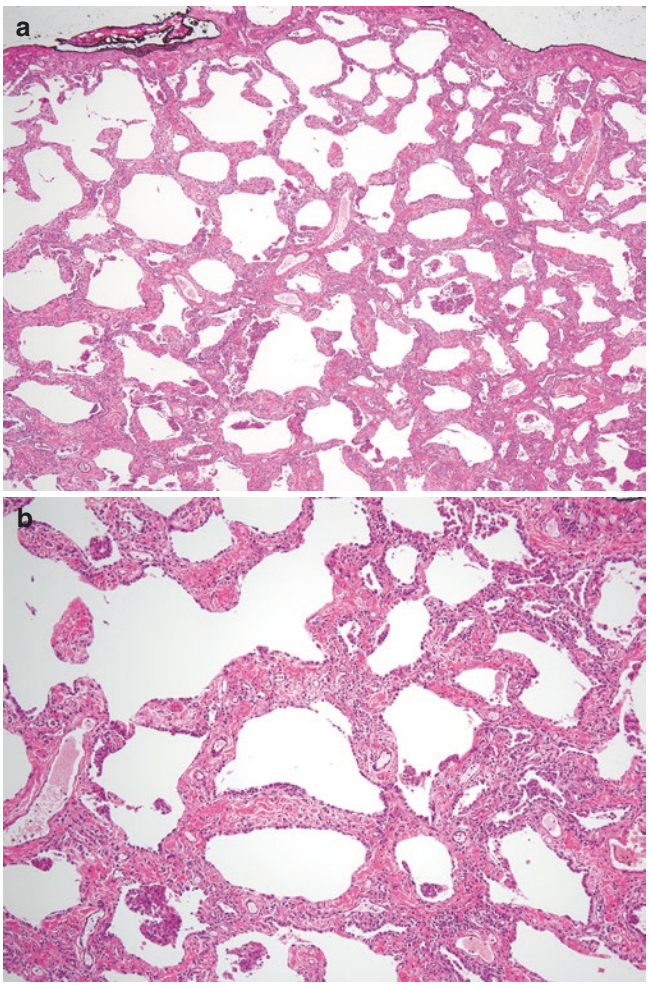

Fig. 6.80 Fibrotic NSIP. (**a**) At low magnification there is diffuse uniform thickening of alveolar septa by collagen fibrosis. The fibrosis does not cause significant architectural distortion in the form of honeycomb change or scars. (**b**) At high magnification the alveolar septa are thickened by collagen deposition and scant chronic inflammatory cells. There is also alveolar pneumocyte hyperplasia and focal intra-alveolar accumulation of macrophages. Fibroblast foci can be seen in NSIP (not shown in this image) but are generally scarce and are not a typical feature

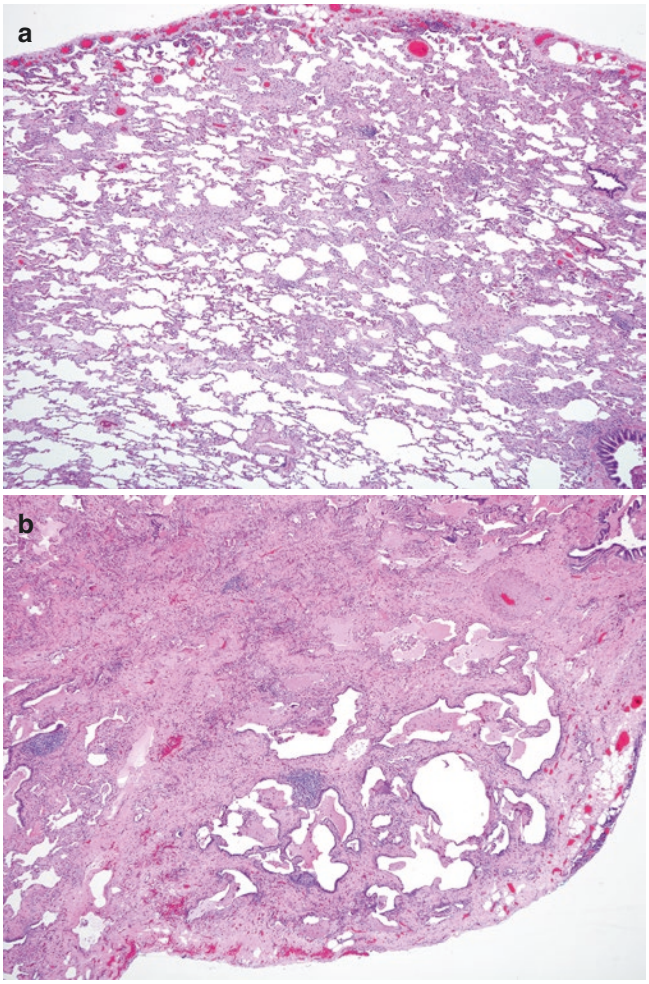

Fig. 6.81 NSIP-like area in UIP. (**a**) This area of uniform alveolar septal thickening by collagen fibrosis and mild chronic inflammation was taken from the upper lobe of an explanted lung with UIP. The features are consistent with fibrotic NSIP if the same changes were seen in the entire lung. (**b**) However, a section taken from the lower lobe lung demonstrated dense interstitial scars and honeycomb change typical of UIP. NSIP-like areas are actually common in otherwise typical UIP, which is why a pathologic diagnosis of NSIP requires correlation with the clinical and radiologic contexts to understand the significance of this finding

Connective Tissue Disease (CTD)-Associated Lung Diseases

Connective tissue disease (CTD)-associated lung diseases (Figs. 6.82, 6.83, 6.84 and 6.85). Pulmonary involvement is common in many systemic CTDs and is a major cause of morbidity and mortality in these patients. In addition to pleuritis and pleural effusions, the most common manifestations of thoracic involvement in almost all CTDs, interstitial lung diseases such as UIP or NSIP are also common findings in patients with CTD-associated lung disease. Some CTDs have uncommon but characteristic lesions that can be helpful in establishing the diagnosis (Table 6.1). In most the diagnosis hinges on the usual clinical and laboratory criteria, although certain histologic clues, such as prominent lymphoid hyperplasia, can be helpful in suggesting the possibility although with relatively low positive predictive values.

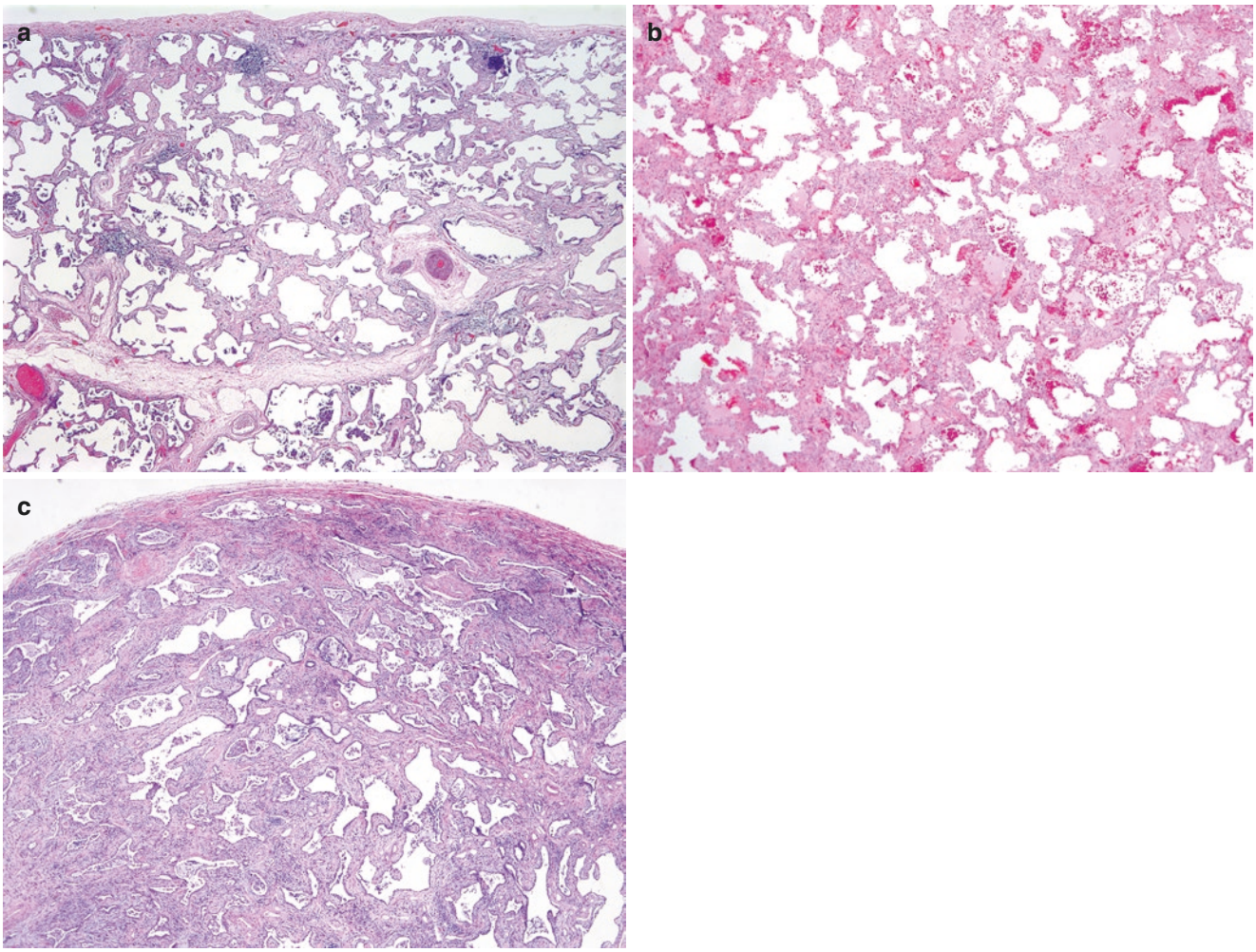

Fig. 6.82 CTD-associated fibrotic NSIP. The underlying CTDs are rheumatoid arthritis (**a**), scleroderma (**b**), and dermatomyositis (**c**). Both cellular and fibrotic variants of NSIP have been described in CTD-associated interstitial lung diseases. The histologic features are indistinguishable from those of idiopathic NSIP

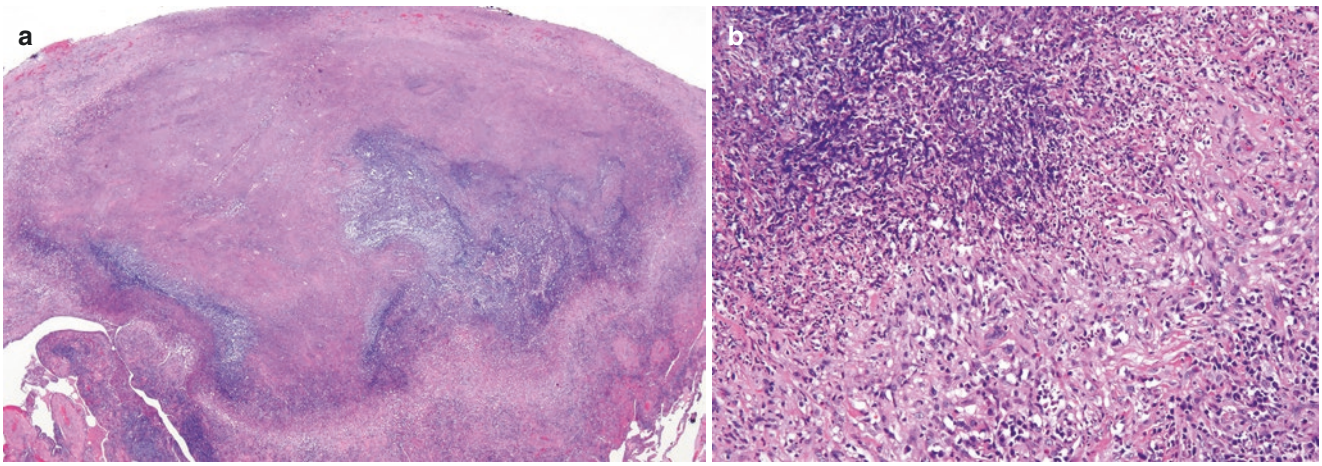

Fig. 6.83 Rheumatoid nodule. (**a**) Low-magnification photomicrograph showing a portion of lung parenchyma replaced by an irregularly shaped granuloma with a large geographic area of central necrosis. (**b**) At high magnification, the granuloma is characterized by central coagulative necrosis surrounded by peripheral palisading histiocytes admixed with acute and chronic inflammatory cells. No multinucleated giant cells are seen

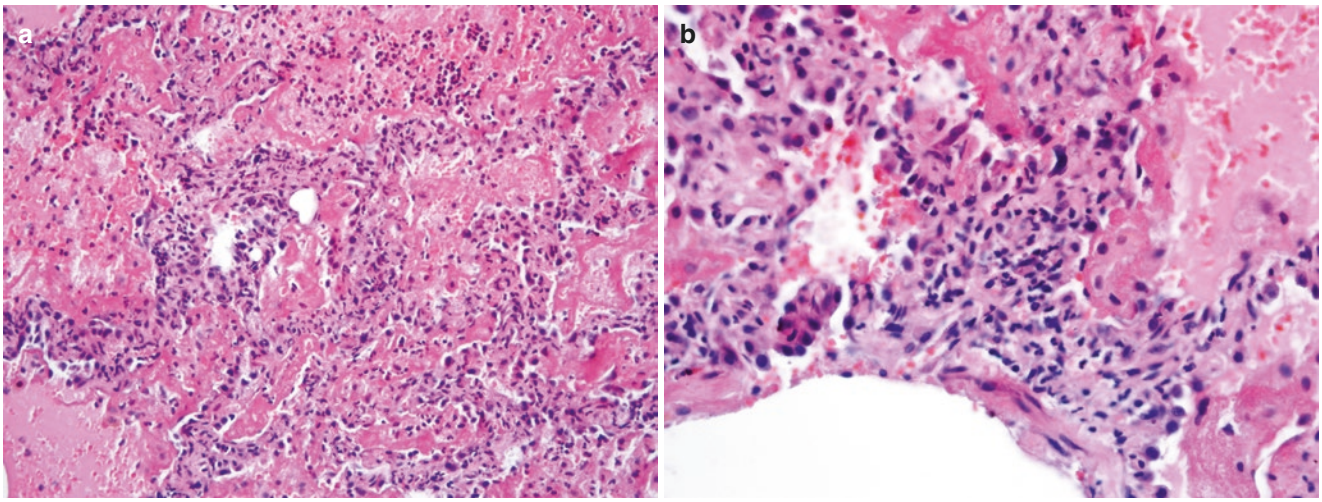

Fig. 6.84 Acute lupus pneumonitis. (**a**) Intermediate-magnification photomicrograph showing extensive intra-alveolar hemorrhage, reactive pneumocytes, and patchy acute inflammatory infiltrates centered on alveolar septa. (**b**) At high magnification, acute inflammatory cells with karyorrhexis are seen within alveolar septa, indicating necrotizing capillaritis

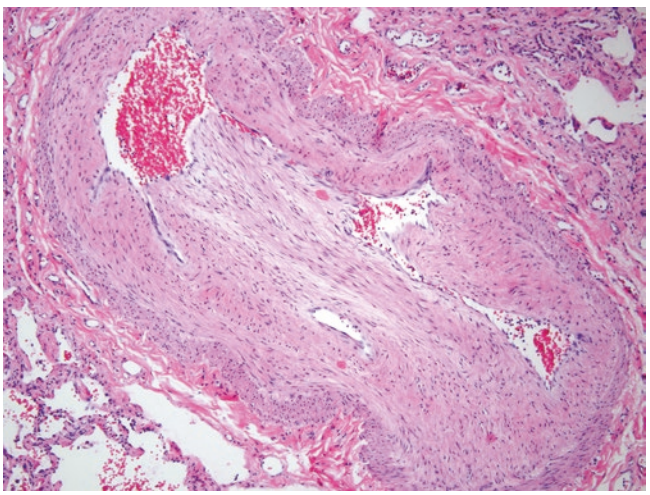

Fig. 6.85 Thromboembolic pulmonary hypertension in systemic lupus erythematosus. High-magnification view of an artery with eccentric intimal fibrosis and a recanalized lumen, indicating an organized thrombus

Table 6.1 The common manifestations of lung involvements associated with major connective tissue diseases

Diseases	Common interstitial disease patterns	Uncommon but characteristic lesions
Rheumatoid arthritis	UIP, NSIP	Rheumatoid nodule
Systemic lupus erythematosus	NSIP, UIP	Intralveolar hemorrhage and necrotizing capillaritis; pulmonary hypertension
Scleroderma	NSIP, UIP	Pulmonary hypertension
Polymyositis/ dermatomyositis	NSIP, occasionally UIP, DAD	Acute bronchopneumonia; occasionally hemorrhage and capillaritis

DAD diffuse alveolar damage, *NSIP* nonspecific interstitial pneumonia, *UIP* usual interstitial pneumonia

Lymphangioleiomyomatosis (LAM)

LAM (Figs. 6.86, 6.87, 6.88, 6.89, 6.90, 6.91, 6.92, 6.93 and 6.94) occurs almost exclusively in women of reproductive age; however, rare cases of LAM have been reported in men and postmenopausal women. Most cases are sporadic, while a small percentage are associated with tuberous sclerosis complex (TSC). Germline mutations in genes responsible for TSC, TSC1, and TSC2 are found in both sporadic and TSC-associated LAM. Patients with LAM usually present with breathlessness frequently attributable to recurrent spontaneous pneumothoraces. Some patients present with cough and hemoptysis. Serum VEGF-D is a useful diagnostic biomarker. Chest CT scans commonly show numerous thin-walled cysts and occasional nodules. The disease is usually slowly progressive and is variably responsive to hormonal therapy. More recently sirolimus has emerged as a potentially effective therapy that slows disease progression. End-stage disease may require lung transplantation.

Fig. 6.87 LAM. A high-resolution chest CT scan from the same patient whose surgical lung biopsy is illustrated in Fig. 6.86 shows a large right-sided pneumothorax with right upper lobe collapse. Numerous thin-walled cysts and some parenchymal nodules are seen in the non-collapsed lung

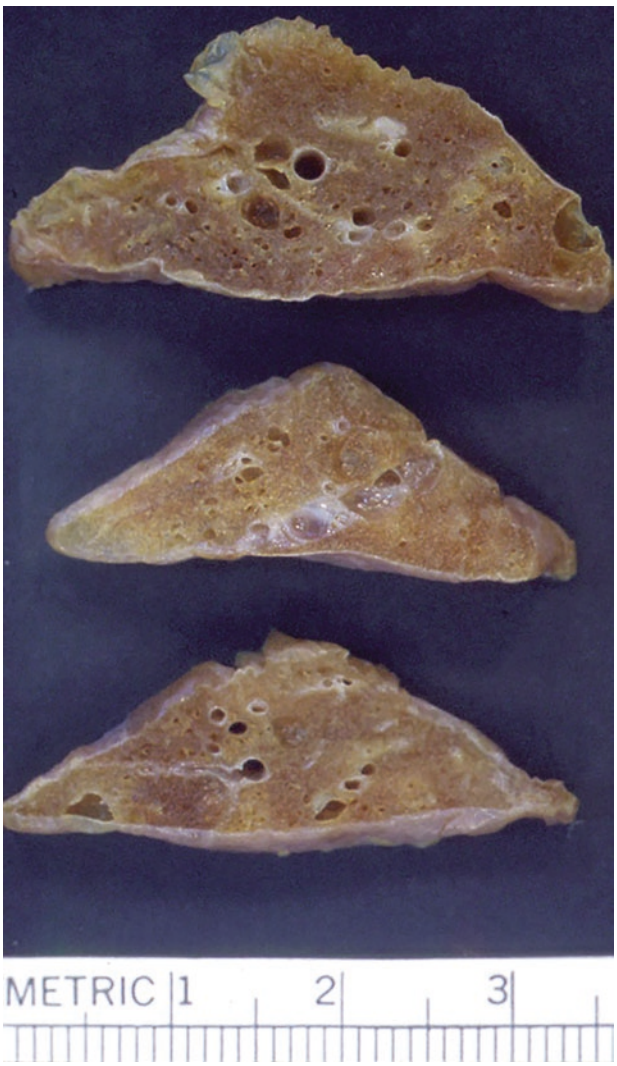

Fig. 6.86 LAM. Gross photograph of surgical lung biopsy from a 35-year-old woman with recurrent pneumothorax. The cut surface of the lung shows multiple variably sized thin-walled cysts. The intervening lung parenchyma is unremarkable, without significant fibrosis

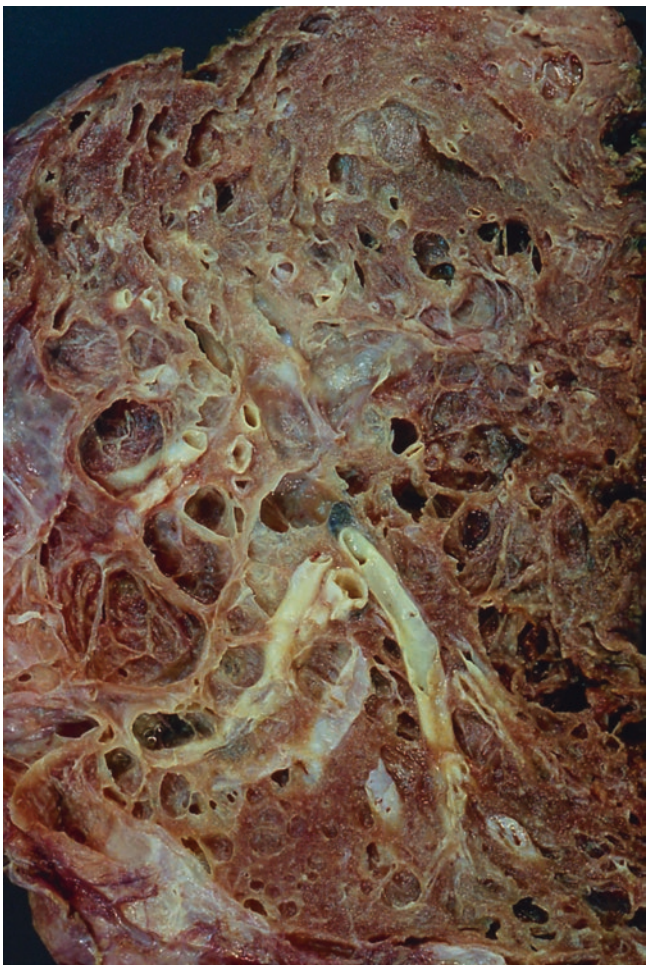

Fig. 6.88 LAM. Gross photograph of an explant lung from a patient with end-stage LAM. The lung is extensively involved with cystic lesions, with very few residual lung parenchyma

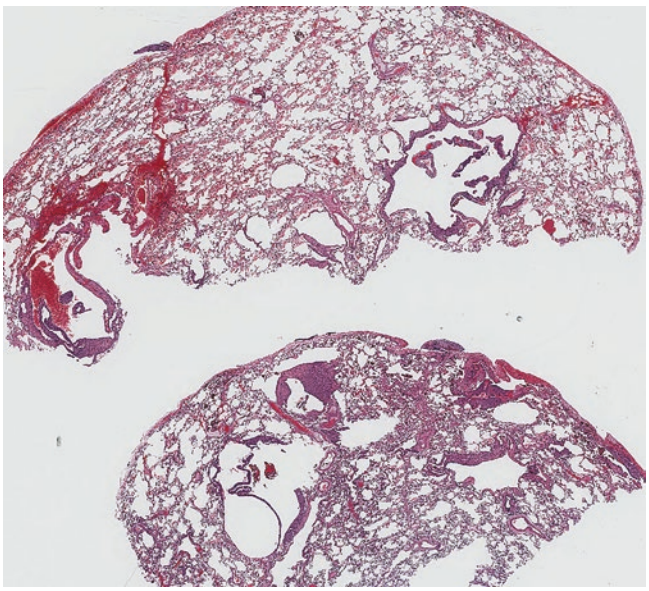

Fig. 6.89 LAM. Whole-mount section of a surgical lung biopsy showing multiple cystic lesions, some of which are surrounded by a variably thick and focally nodular wall. The two most nodular and cellular lesions are present in the lower piece of tissue

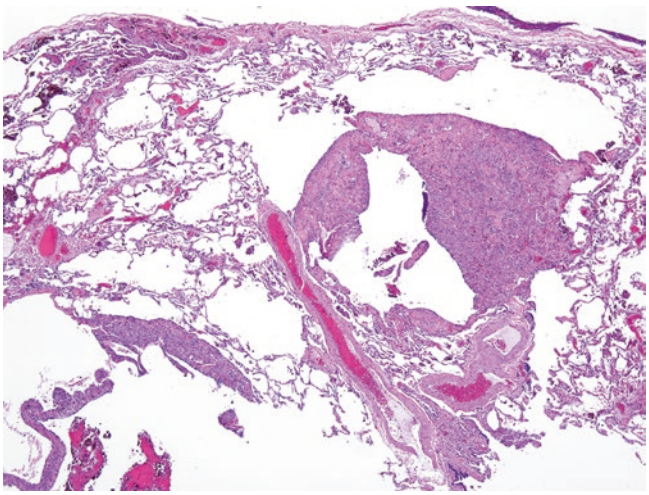

Fig. 6.90 LAM. Intermediate-magnification view of the lower piece of tissue illustrated in Fig. 6.89 showing nodular and cystic lesions. The thickened cyst walls comprise a proliferation of smooth muscle-like spindle cells. Some of the air spaces contain hemosiderin-laden macrophages, indicating old hemorrhage

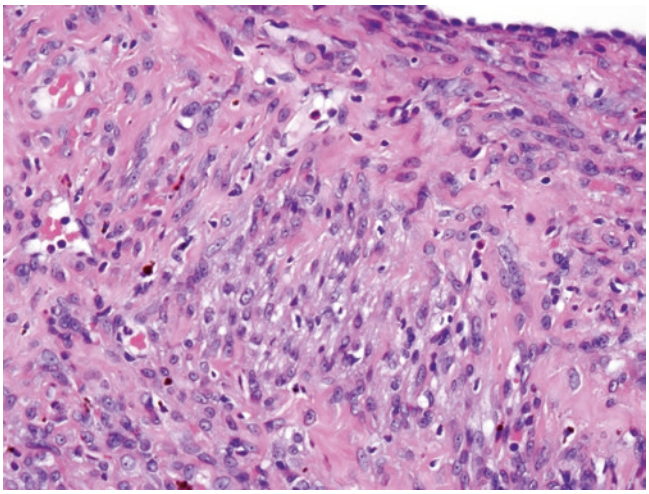

Fig. 6.91 LAM. High-magnification photomicrograph showing spindle and epithelioid LAM cells with bland, elongated nuclei and clear to eosinophilic cytoplasm. The cytoplasm is subtly vacuolated and slightly basophilic, resulting in tinctorial properties that differ from normal smooth muscle cells

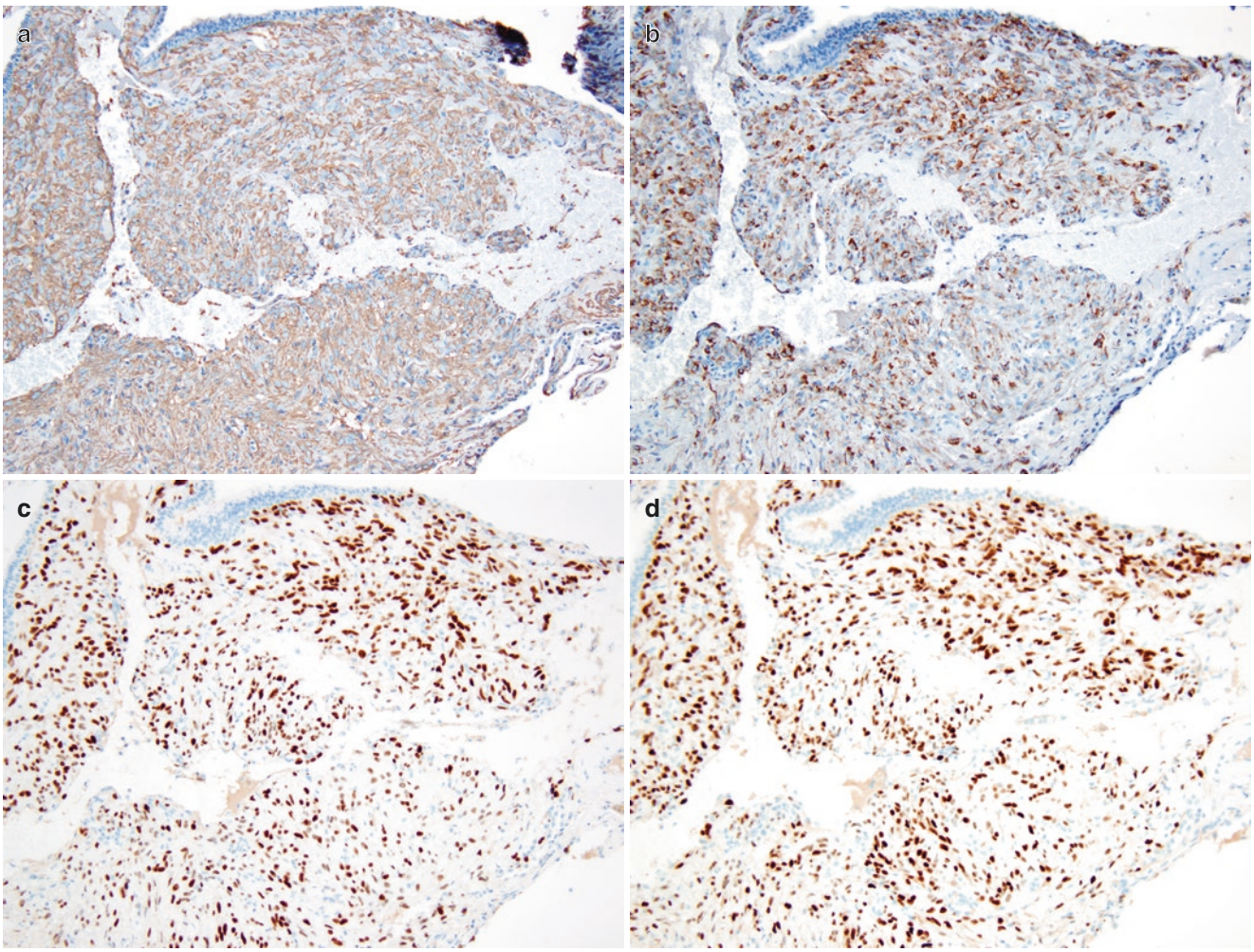

Fig. 6.92 LAM. The lesional cells are usually positive for smooth muscle actin (**a**), HMB-45 (**b**), estrogen receptor (**c**), and progesterone receptor (**d**). Staining for HMB-45 can be very patchy and therefore requires careful review of immunostained sections

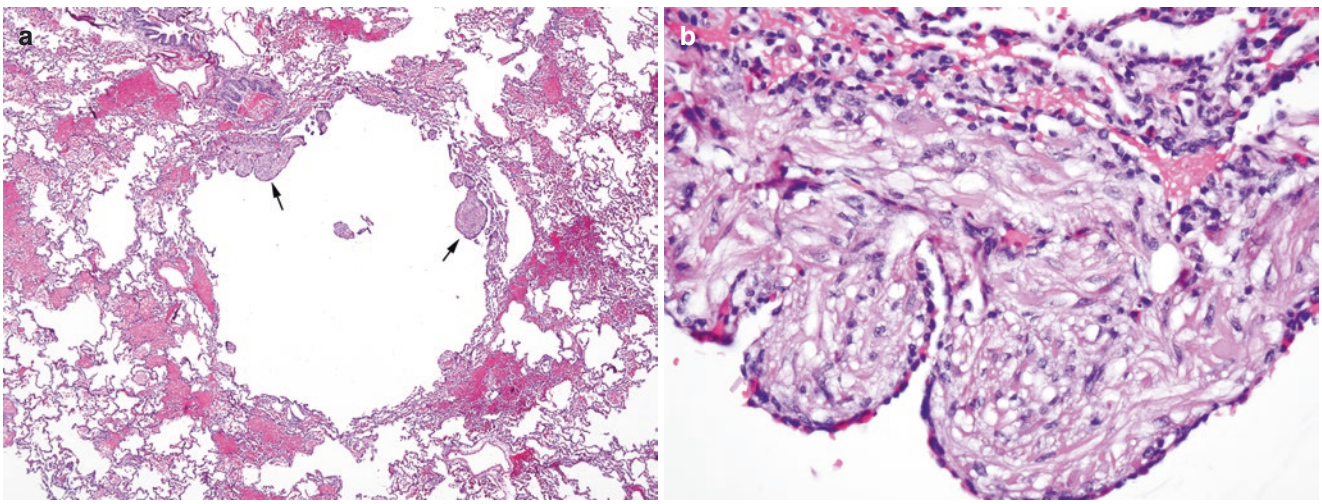

Fig. 6.93 LAM. (**a**) In this example, a thin-walled cyst is seen within the lung parenchyma, and the wall is focally thickened by bundles of smooth muscle-like LAM cells (arrows). (**b**) High-magnification view of the thickened area of the cyst wall showing bland-appearing spindle and epithelioid cells with overlying hyperplastic pneumocytes

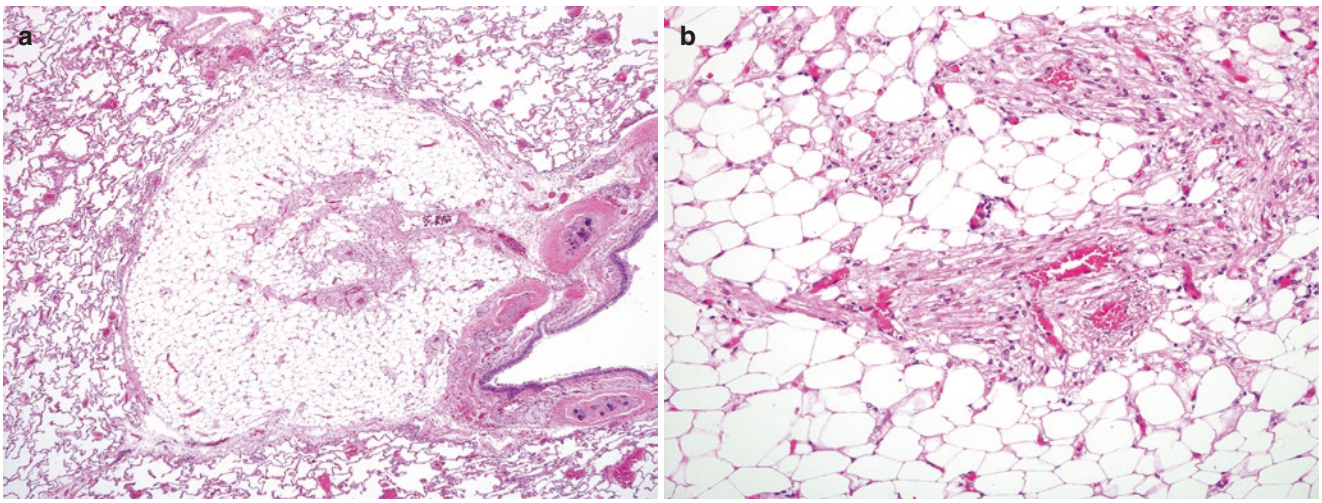

Fig. 6.94 Angiomyolipoma in the lung of a patient with tuberous sclerosis complex (TSC). (**a**) Low-magnification photomicrograph showing a well-demarcated lipomatous lesion next to a bronchus. (**b**) Higher-magnification photomicrograph from the center of the lesion shows features of angiomyolipoma: mature adipocytes, smooth muscle proliferation, and thick-walled blood vessels. Angiomyolipoma is more commonly seen in the kidneys of patients with TSC and has been reported in both sporadic and TSC-associated LAM

Suggested Reading

Beasley MB, Franks TJ, Galvin JR, Gochuico B, Travis WD. Acute fibrinous and organizing pneumonia: a histological pattern of lung injury and possible variant of diffuse alveolar damage. Arch Pathol Lab Med. 2002;126:1064–70.

Churg A, Muller NL, Silva CI, Wright JL. Acute exacerbation (acute lung injury of unknown cause) in UIP and other forms of fibrotic interstitial pneumonias. Am J Surg Pathol. 2007;31:277–84.

Force ADT, Ranieri VM, Rubenfeld GD, Thompson BT, Ferguson ND, Caldwell E, et al. Acute respiratory distress syndrome: the Berlin Definition. JAMA. 2012;307:2526–33.

Fraig M, Shreesha U, Savici D, Katzenstein AL. Respiratory bronchiolitis: a clinicopathologic study in current smokers, ex-smokers, and never-smokers. Am J Surg Pathol. 2002;26:647–53.

Heo JY, Song JY, Noh JY, Yong HS, Cheong HJ, Kim WJ. Acute fibrinous and organizing pneumonia in a patient with HIV infection and Pneumocystis jiroveci pneumonia. Respirology. 2010;15:1259–61.

Johnson SR, Cordier JF, Lazor R, Cottin V, Costabel U, Harari S, et al. Review panel of the European Respiratory Society guidelines for the diagnosis and management of lymphangioleiomyomatosis. Eur Respir J. 2010;35:14–26.

Katzenstein AL. Smoking-related interstitial fibrosis (SRIF): pathologic findings and distinction from other chronic fibrosing lung diseases. J Clin Pathol. 2013;66:882–7.

Katzenstein AL, Fiorelli RF. Nonspecific interstitial pneumonia/fibrosis. Histologic features and clinical significance. Am J Surg Pathol. 1994;18:136–47.

Katzenstein AL, Zisman DA, Litzky LA, Nguyen BT, Kotloff RM. Usual interstitial pneumonia: histologic study of biopsy and explant specimens. Am J Surg Pathol. 2002;26:1567–77.

Kitaichi M, Nishimura K, Itoh H, Izumi T. Pulmonary lymphangioleiomyomatosis: a report of 46 patients including a clinicopathologic study of prognostic factors. Am J Respir Crit Care Med. 1995;151(2 Pt 1):527–33.

Maldonado F, Daniels CE, Hoffman EA, Yi ES, Ryu JH. Focal organizing pneumonia on surgical lung biopsy: causes, clinicoradiologic features, and outcomes. Chest. 2007;132:1579–83.

Marchand E, Reynaud-Gaubert M, Lauque D, Durieu J, Tonnel AB, Cordier JF. Idiopathic chronic eosinophilic pneumonia. A clinical and follow-up study of 62 cases. The Groupe d'Etudes et de Recherche sur les maladies Orphelines Pulmonaires (GERMOP). Medicine (Baltimore). 1998;77:299–312.

Matsui K, Beasley MB, Nelson WK, Barnes PM, Bechtle J, Falk R, et al. Prognostic significance of pulmonary lymphangioleiomyomatosis histologic score. Am J Surg Pathol. 2001;25:479–84.

McCormack FX, Inoue Y, Moss J, Singer LG, Strange C, Nakata K, et al. National Institutes of Health Rare Lung Diseases and M. T. Group. Efficacy and safety of sirolimus in lymphangioleiomyomatosis. N Engl J Med. 2011;364:1595–606.

Mukhopadhyay S, Katzenstein AL. Pulmonary disease due to aspiration of food and other particulate matter: a clinicopathologic study of 59 cases diagnosed on biopsy or resection specimens. Am J Surg Pathol. 2007;31:752–9.

Myers JL, Katzenstein AL. Beyond a consensus classification for idiopathic interstitial pneumonias: progress and controversies. Histopathology. 2009;54:90–103.

Nishino M, Mathai SK, Schoenfeld D, Digumarthy SR, Kradin RL. Clinicopathologic features associated with relapse in cryptogenic organizing pneumonia. Hum Pathol. 2014;45:342–51.

Omote N, Taniguchi H, Kondoh Y, Watanabe N, Sakamoto K, Kimura T, et al. Lung-dominant connective tissue disease: clinical, radiologic, and histologic features. Chest. 2015;148:1438–46.

Parambil JG, Myers JL, Ryu JH. Histopathologic features and outcome of patients with acute exacerbation of idiopathic pulmonary fibrosis undergoing surgical lung biopsy. Chest. 2005;128:3310–5.

Patel SR, Karmpaliotis D, Ayas NT, Mark EJ, Wain J, Thompson BT, Malhotra A. The role of open-lung biopsy in ARDS. Chest. 2004;125:197–202.

Philit F, Etienne-Mastroianni B, Parrot A, Guerin C, Robert D, Cordier JF. Idiopathic acute eosinophilic pneumonia: a study of 22 patients. Am J Respir Crit Care Med. 2002;166:1235–9.

Raghu G, Rochwerg B, Zhang Y, Garcia CA, Azuma A, Behr J, et al., American Thoracic Society, European Respiratory, S. Japanese Respiratory and A. Latin American Thoracic. An Official ATS/ERS/JRS/ALAT Clinical Practice Guideline: Treatment of idiopathic pulmonary fibrosis. An Update of the 2011 Clinical Practice Guideline. Am J Respir Crit Care Med. 2015;192:e3–19.

Seymour JF, Presneill JJ. Pulmonary alveolar proteinosis: progress in the first 44 years. Am J Respir Crit Care Med. 2002;166: 215–35.

Song JW, Do KH, Kim MY, Jang SJ, Colby TV, Kim DS. Pathologic and radiologic differences between idiopathic and collagen vascular disease-related usual interstitial pneumonia. Chest. 2009;136:23–30.

Tansey D, Wells AU, Colby TV, Ip S, Nikolakoupolou A, du Bois RM, et al. Variations in histological patterns of interstitial pneumonia between connective tissue disorders and their relationship to prognosis. Histopathology. 2004;44:585–96.

Thille AW, Esteban A, Fernandez-Segoviano P, Rodriguez JM, Aramburu JA, Penuelas O, et al. Comparison of the Berlin definition for acute respiratory distress syndrome with autopsy. Am J Respir Crit Care Med. 2013;187:761–7.

Tomashefski JF. Pulmonary pathology of acute respiratory distress syndrome. Clin Chest Med. 2000;21:435–66.

Travis WD, Borok Z, Roum JH, Zhang J, Feuerstein I, Ferrans VJ, Crystal RG. Pulmonary Langerhans cell granulomatosis (histiocytosis X). A clinicopathologic study of 48 cases. Am J Surg Pathol. 1993;17:971–86.

Travis WD, Costabel U, Hansell DM, King TE, Lynch DA, Nicholson AG, et al. American Thoracic Society/European Respiratory Society statement: update of the international multidisciplinary classification of the idiopathic interstitial pneumonias. Am J Respir Crit Care Med. 2013;188:733–48.

Travis WD, Hunninghake G, King TE, Lynch DA, Colby TV, Galvin JR, et al. Idiopathic nonspecific interstitial pneumonia: report of an American Thoracic Society project. Am J Respir Crit Care Med. 2008;177:1338–47.

Uner AH, Rozum-Slota B, Katzenstein LA. Bronchiolitis obliterans-organizing pneumonia (BOOP)-like variant of Wegener's granulomatosis. A clinicopathologic study of 16 cases. Am J Surg Pathol. 1996;20:794–801.

Villar J, Sulemanji D, Kacmarek RM. The acute respiratory distress syndrome: incidence and mortality, has it changed? Curr Opin Crit Care. 2014;20:3–9.

Wang CW, Colby TV. Histiocytic lesions and proliferations in the lung. Semin Diagn Pathol. 2007;24:162–82.

Wang T, Lazar CA, Fishbein MC, Lynch JP. Pulmonary alveolar proteinosis. Semin Respir Crit Care Med. 2012;33:498–508.

Yousem SA, Lohr RY, Colby TV. Idiopathic bronchiolitis obliterans organizing pneumonia/cryptogenic organizing pneumonia with unfavorable outcome: pathologic predictors. Mod Pathol. 1997;10:864–71.